EXPERIMENTAL AND COMPUTATIONAL INVESTIGATIONS OF THERAPEUTIC DRUG RELEASE FROM BIODEGRADABLE POLY(LACTIDE-CO-GLYCOLIDE) (PLG) MICROSPHERES

A Dissertation

by

NADER SAMIR BERCHANE

Submitted to the Office of Graduate Studies of
Texas A&M University
in partial fulfillment of the requirements for the degree of

DOCTOR OF PHILOSOPHY

December 2007

Major Subject: Mechanical Engineering

EXPERIMENTAL AND COMPUTATIONAL INVESTIGATIONS OF THERAPEUTIC DRUG RELEASE FROM BIODEGRADABLE POLY(LACTIDE-CO-GLYCOLIDE) (PLG) MICROSPHERES

A Dissertation

by

NADER SAMIR BERCHANE

Submitted to the Office of Graduate Studies of
Texas A&M University
in partial fulfillment of the requirements for the degree of

DOCTOR OF PHILOSOPHY

Approved by:

Co-Chairs of Committee,	Malcolm J. Andrews
	Allison C. Rice-Ficht
Committee Members,	Obdulia Ley
	Christian Schwartz
Head of Department,	Dennis O'Neal

December 2007

Major Subject: Mechanical Engineering

ABSTRACT

Experimental and Computational Investigations of Therapeutic Drug Release from Biodegradable Poly(lactide-co-glycolide) (PLG) Microspheres. (December 2007)

Nader Samir Berchane, B.E., American University of Beirut;

M.S., Texas A&M University

Co-Chairs of Advisory Committee: Dr. Malcolm J. Andrews
Dr. Allison C. Rice-Ficht

The need to tailor release-rate profiles from polymeric microspheres remains one of the leading challenges in controlled drug delivery. Microsphere size, which has a significant effect on drug release rate, can potentially be varied to design a controlled drug delivery system with desired release profile. In addition, drug release rate from polymeric microspheres is dependent on material properties such as polymer molecular weight. Mathematical modeling provides insight into the fundamental processes that govern the release, and once validated with experimental results, it can be used to tailor a desired controlled drug delivery system.

To these ends, PLG microspheres were fabricated using the oil-in-water emulsion technique. A quantitative study that describes the size distribution of poly(lactide-co-glycolide) (PLG) microspheres is presented. A fluid mechanics-based correlation that predicts the mean microsphere diameter is formulated based on the theory of emulsification in turbulent flow. The effects of microspheres' mean diameter, polydispersity, and polymer molecular weight on therapeutic drug release rate from

poly(lactide-co-glycolide) (PLG) microspheres were investigated experimentally. Based on the experimental results, a suitable mathematical theory has been developed that incorporates the effect of microsphere size distribution and polymer degradation on drug release. In addition, a numerical optimization technique, based on the least squares method, was developed to achieve desired therapeutic drug release profiles by combining individual microsphere populations.

The fluid mechanics-based mathematical correlation that predicts microsphere mean diameter provided a close fit to the experimental results. We show from *in vitro* release experiments that microsphere size has a significant effect on drug release rate. The initial release rate decreased with an increase in microsphere size. In addition, the release profile changed from first order to concave-upward (sigmoidal) as the microsphere size was increased. The mathematical model gave a good fit to the experimental release data. Using the numerical optimization technique, it was possible to achieve desired release profiles, in particular zero-order and pulsatile release, by combining individual microsphere populations at the appropriate proportions.

Overall, this work shows that engineering polymeric microsphere populations having predetermined characteristics is an effective means to obtain desired therapeutic drug release patterns, relevant for controlled drug delivery.

DEDICATION

To my parents,

Samir and Nadia Berchane

ACKNOWLEDGMENTS

I would like to express my gratitude to my advisor and committee chair, Dr. Malcolm J. Andrews, for his support and guidance throughout the course of this research. Thanks to my committee members, Dr. Allison C. Rice Ficht, Dr. Obdulia Ley, and Dr. Cris Schwartz for their helpful input and patience. I also thank Dr. Harry Hogan and Dr. Ali Beskok for their time and assistance.

Thanks to my colleagues at the Advanced Mixing Laboratory, my friends, and the departmental faculty and staff for their support. Thanks also to Dr. Kenneth Carson at the Department of Molecular and Cellular Medicine for his help in preparing polymeric microspheres. Thanks to Mr. Thomas Stephens and Mr. Michael Pendleton of the Microscopy and Imaging Center at Texas A&M University for their help in SEM imaging.

This work was supported by the Texas Institute for Intelligent Bio-Nano Materials and Structures for Aerospace Vehicles (TiiMS), a NASA URETI under NASA Cooperative Agreement No. NCC-1-02038. The FE-SEM acquisition was supported by the National Science Foundation under Grant No. DBI-0116835.

TABLE OF CONTENTS

Page

ABSTRACT iii

DEDICATION v

ACKNOWLEDGMENTS vi

TABLE OF CONTENTS vii

LIST OF FIGURES x

LIST OF TABLES xiii

1. INTRODUCTION 1

1.1. Controlled Drug Delivery 1
1.2. Classification of Controlled Drug Delivery Systems 4
1.3. Biodegradable Polymers 7
1.4. Microspheres as Drug Delivery Devices 9
1.4.1. Fabrication Techniques 10
1.5. Desired Drug Release Patterns 13
1.6. Commercially Available Controlled Drug Release Formulations 15
1.7. Motivation and Organization 15

2. MEAN DIAMETER AND SIZE DISTRIBUTION OF PLG MICROSPHERES 18

2.1. Background 18
2.2. Materials and Methods 20
2.2.1. Materials 20
2.2.2. Microsphere Preparation 20
2.2.3. Microsphere Characterization 22
2.3. Theory of Droplet Formation 23
2.4. Results and Discussion 29
2.4.1. Microsphere Size Distributions 29
2.4.2. Mathematical Distribution Function 30

Page

2.4.3. Microsphere Mean Diameters 36
2.5. Conclusions 36

3. EFFECT OF MICROSPHERE SIZE ON DRUG RELEASE 39

3.1. Background 39
3.2. Materials and Methods 40
3.2.1. Materials 40
3.2.2. Microsphere Preparation 41
3.2.3. Determination of Piroxicam Loading 42
3.2.4. *In Vitro* Release 42
3.2.5. Microsphere Characterization 43
3.3. Mathematical Model 45
3.3.1. Modeling Size Distribution 50
3.3.2. Numerical Solution of Model Equations 52
3.4. Results and Discussion 55
3.4.1. Microsphere Fabrication and Characterization 55
3.4.2. *In Vitro* Drug Release Kinetics 66
3.4.3. Model Results 72
3.5. Conclusions 79

4. DESIGNING DRUG RELEASE PROFILES 81

4.1. Background 81
4.2. Materials and Methods 83
4.2.1. Materials 83
4.2.2. Microsphere Preparation 83
4.2.3. Determination of Piroxicam Loading 84
4.2.4. *In Vitro* Release 84
4.2.5. Microsphere Characterization 86
4.3. Mathematical Model 86
4.4. Numerical Optimization Technique 88
4.4.1. Steepest Descent Method 89
4.5. Results and Discussion 90
4.5.1. *In Vitro* Drug Release Kinetics 90
4.5.2. Model Results 92
4.5.3. Release from Mixtures of Individual Microsphere Populations 96
4.6. Conclusions 108

5. CONCLUSIONS AND RECOMMENDATIONS 110

Page

REFERENCES 114

APPENDIX A 127

VITA 129

LIST OF FIGURES

FIGURE Page

1.1 Concentration profiles for conventional and controlled release formulations. 3

1.2 Two main types of diffusion controlled systems: reservoir and monolithic. 6

1.3 Chemical structure of (a) poly(lactide), (b) poly(glycolide), and (c) poly(lactide-co-glycolide). 8

1.4 Basics of the single emulsion solvent extraction/evaporation microsphere preparation technique.....12

1.5 Schematic of ideal desired release profiles for controlled drug delivery: (a) pulsatile release, and (b) constant release. 14

2.1 Schematic of PLG microsphere preparation procedure. 21

2.2 SEM micrographs of PLG microspheres prepared at (a) N = 300 rpm, (b) N = 600 rpm, (c) N = 900 rpm, and (d) N = 1200 rpm. 31

2.3 Cumulative volume distribution at different impeller speeds, (a) 300 rpm, (b) 600 rpm, (c) 900 rpm, and (d) 1200 rpm. 32

2.4 Volume moment mean diameter (d_{43}) of PLG microspheres as a function of We_m on logarithmic scale; error bars represent interval estimate of population mean diameter with 99% level of confidence. 37

3.1 Maximum error in approximating the infinite series by its fist J terms. 54

3.2 SEM micrographs of sieved piroxicam loaded PLG microspheres: (a) > 90 μm, (b) 63 – 90 μm, (c) 40 – 63 μm, (d) 20 – 40 μm, and (e) 0.2 – 20 μm. 57

FIGURE Page

3.3 SEM micrographs of raw piroxicam loaded PLG microspheres: (a) N = 140 rpm, (b) N = 300 rpm, and (c) N = 900 rpm. 58

3.4 Volume fraction distributions of sieved piroxicam loaded PLG microspheres: (a) 63 – 90 μm, (b) 40 – 63 μm, (c) 20 – 40 μm, and (d) 0.2 – 20 μm. 59

3.5 Volume fraction distributions of raw piroxicam loaded PLG microspheres: (a) N = 140 rpm, (b) N = 300 rpm, and (c) N = 900 rpm. 61

3.6 Cumulative volume fraction distributions of (a) sieved and (b) raw, piroxicam loaded PLG microspheres. 64

3.7 Experimental drug release profile of sieved PLG microspheres: (a) > 90 μm, (b) 63 – 90 μm, (c) 40 – 63 μm, (d) 20 – 40 μm, and (e) 0.2 – 20 μm. 67

3.8 Effect of microsphere size on piroxicam release for raw microspheres....71

3.9 Comparison of model profiles to experimental results of sieved piroxicam loaded PLG microspheres: (a) 63 – 90 μm, (b) 40 – 63 μm, (c) 20 – 40 μm, and (d) 0.2 – 20 μm. 74

3.10 Comparison of model profiles to experimental results of raw piroxicam loaded PLG microspheres: (a) N = 140 rpm, (b) N = 300 rpm, and (c) N = 900 rpm. 76

4.1 Effect of microsphere size and polymer molecular weight on piroxicam release from PLG microspheres. 91

FIGURE Page

4.2 Comparison of model profiles to experimental results of piroxicam loaded PLG microspheres: (a) 55 kDa, 63 – 90 μm; (b) 55 kDa, 20 – 40 μm; (c) 55 kDa, 0.2 – 20 μm; (d) 18 kDa, 63 – 90 μm; (e) 18 kDa, 20 – 40 μm; and (f) 18 kDa, 0.2-20 μm. 93

4.3 Combining appropriate proportions of two individual PLG microsphere populations to achieve desired drug release profiles: a) pulasatile, b) zero-order, c) near zero-order, and d) near zero-order. 98

4.4 Combining appropriate proportions of multiple individual PLG microsphere populations to achieve desired drug release profiles: a) pulasatile, b) zero-order, c) near zero-order, and d) near zero-order. 104

LIST OF TABLES

TABLE Page

1.1 List of FDA approved drug delivery products using PL and PLG polymers.....16

2.1 Measured volume moment mean diameter of PLG microspheres at different We_m 24

2.2 Coefficients of Rosin-Rammler mathematical function obtained through least squares fit to the volume fraction data at different We_m 35

3.1 Characterization of sieved and raw piroxicam loaded PLG microspheres 44

4.1 Characterization of piroxicam-loaded PLG microspheres 85

1. INTRODUCTION

Humans have always attempted to improve their health by administrating therapeutic drugs. Modern science has produced numerous active agents that manipulate the biological environment within us; however, the effectiveness of these agents has been limited due to the inability to deliver these agents at the right time and in the right amounts. In recent years, increasing attention has been given to methods by which active agents are administered giving rise to the field of controlled release drug delivery which offers temporal and/or spatial control over the release of therapeutic drugs.

1.1. Controlled Drug Delivery

Controlled drug delivery offers several advantages compared with conventional drug release formulations, in particular: reduced toxicity, improved patient compliance and convenience, and site directed drug delivery [1].

Controlled drug delivery promises an increase for the shelf life of a drug, and offers the flexibility of controlled release kinetics for the administered drug. An ideal drug delivery system is one which provides the therapeutic drug at the desired site of action and in the minimum concentration required to produce the desired therapeutic effects. However, as a drug is administered through conventional release formulations, the drug concentration first rises rapidly to a maximum, and then slowly falls as the drug gets metabolized, excreted or degraded (Figure 1.1). Two critical drug concentration levels

---

This dissertation follows the style of Journal of Controlled Release.

are the minimum effective concentration (MEC) and the maximum safe concentration (MSC), as depicted in Figure 1.1. With conventional release formulations, it is difficult to maintain the drug concentration between the minimum effective and toxic levels because this type of formulation tends to first overdose and then underdose the site of application. Controlled release systems can be designed to overcome this limitation by balancing the rate of drug delivery to the rate of drug removal from the site of application. It is evident from Figure 1.1 that a controlled release formulation maintains an effective drug concentration for prolonged periods, and thus fewer applications of the active agent are required. Reduced frequency of administration significantly improves patient compliance and convenience with a consequent improvement in the efficacy of the treatment. In addition to the temporal control over the therapeutic drug release, controlled release formulations enable the local delivery of the drug and its containment at the site of action. This produces high and effective drug concentrations locally but avoids systematic side effects as the therapeutic drug is metabolized locally and does not enter the system's circulation.

Drug delivery patterns from a controlled release system can vary over a wide range, but it is important to introduce two main categories of release profiles [1]. In the first category, the drug release remains constant with time until the drug is completely released. The release rate can then be mathematically expressed as:

$$\frac{dM}{dt} = k \tag{1.1}$$

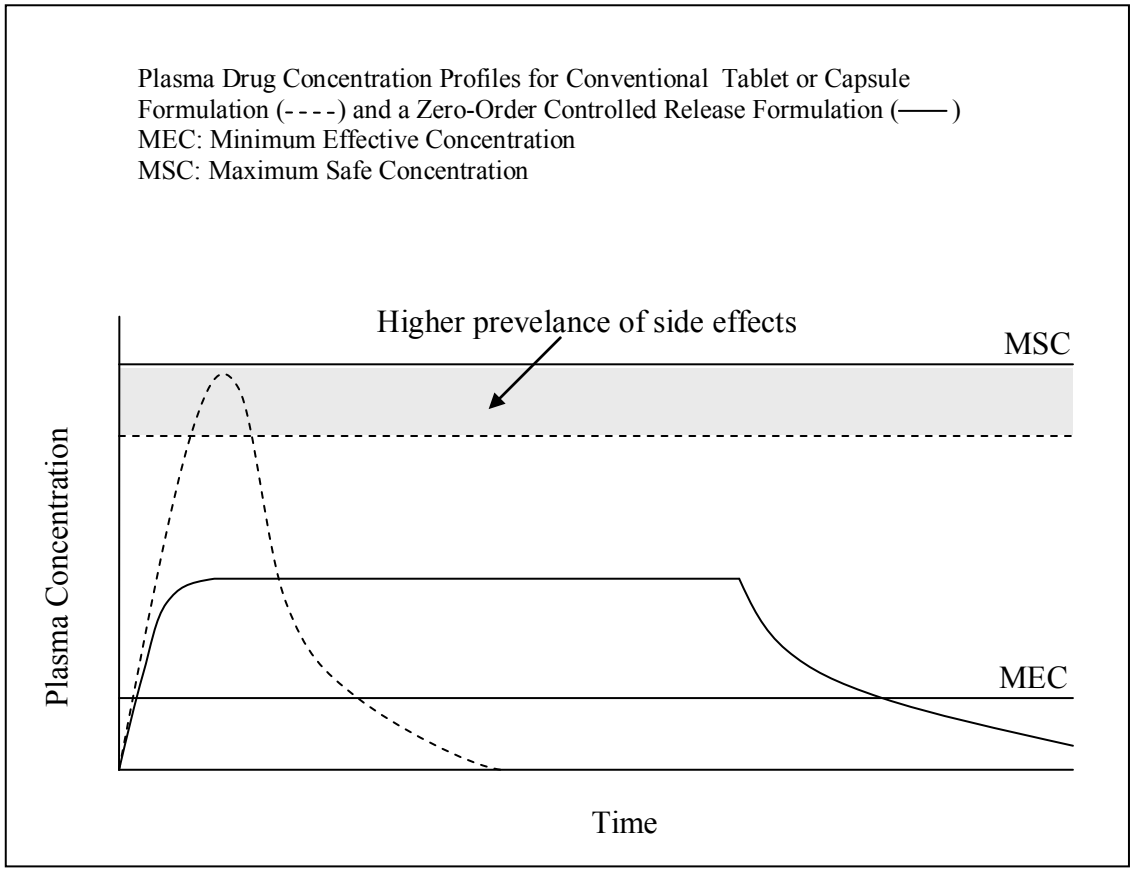

Figure 1.1 Concentration profiles for conventional and controlled release formulations.

where M is mass of drug released, t is time, and k is a constant. This pattern of release is called zero-order release. The second common type of release profile is the first-order release, where the release rate is proportional to the mass of drug contained within the device. The release rate can then be mathematically expressed as:

$$\frac{dM}{dt} = k(M_0 - M) \tag{1.2}$$

where M_0 is mass of drug contained within the device at t_0. In this type of release profile, the release rate declines exponentially with time until the device is exhausted of the drug:

$$\frac{dM}{dt} = kM_0 \exp(-kt) \tag{1.3}$$

1.2. Classification of Controlled Drug Delivery Systems

There are five major types of controlled release systems [1,2]:

- Diffusional systems (reservoir and monolithic)
- Chemically controlled systems (biodegradable systems)
- Combination of diffusional and biodegradable systems
- Osmotic systems
- Mechanical pumps

In diffusion controlled drug release systems, a substance is released from a device by permeation from its interior to the surrounding. There are two main types of diffusion controlled systems, the reservoir system and the monolithic system. As depicted in Figure 1.2, in the diffusion controlled reservoir system the active agent is enclosed by an inert outer membrane. As a consequence, the drug release rate from this type of system is dependent on the thickness, and the material properties of the membrane. Thin spots or pinholes could lead to catastrophic failure in this type of system, and quality control requirements make fabrication of a reservoir system usually more expensive and difficult than of a monolithic system because the membrane properties must be controlled carefully [1,2]. In a monolithic system, the drug is homogenously dissolved or dispersed through-out the rate controlling polymer matrix, as depicted in Figure 1.2. If the active agent is dissolved in the polymer matrix, then the device is called monolithic solution, while if the drug is dispersed as a solid, the system is called monolithic dispersion [1]. The release pattern from diffusion controlled systems depends on the geometry of the system, and the identity and nature of the carrier material.

In a chemically controlled system, the release of the active agent occurs by either gradual bioerosion of the drug containing polymer matrix, or by cleavage of unstable bonds by which the drug is coupled to the polymer matrix [2]. As a consequence, the drug release rate from a purely chemically controlled system is governed by the biodegradation process. Alternatively, a biodegradable polymer can be utilized to prepare

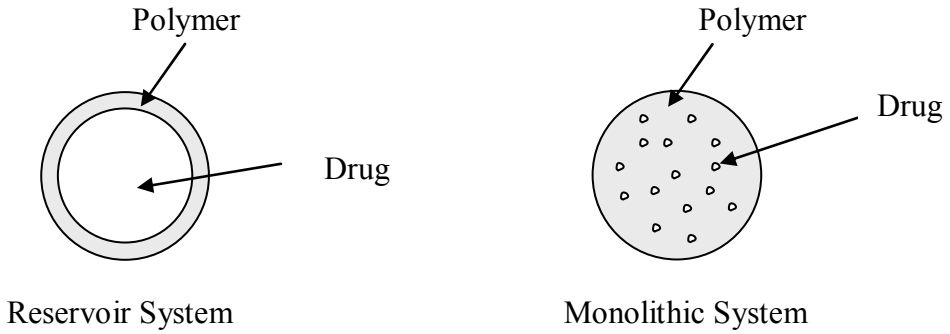

Figure 1.2 Two main types of diffusion controlled systems: reservoir and monolithic.

a diffusion based drug delivery device. If polymer degradation occurs while the active agent is being released, then the release is determined by both the diffusion and the biodegradation process. In contrast, devices can be designed to biodegrade long after the drug is exhausted which eliminates the need for their surgical removal.

Mechanical pumps [3] were among the first reliable controlled release delivery systems. More recent pumps have been small enough to be made implantable [1]. In contrast, the development of osmotic pumps [3] is more recent. Osmotic systems utilize osmotic effects to control the release of the active agent. The osmotic pressure developed by diffusion of water across a semi permeable membrane into a salt solution pushes a solution of the active agent from the device. These devices have been used as implantable systems and in simple oral tablet formulations [1,4].

1.3. Biodegradable Polymers

Biodegradable polymers have been used to prepare a number of devices for controlled release, such as implants (microchips [5], disks [6-8]), and micro and nanospheres [9]. The linear polyesters are the most widely investigated type of biodegradable polymers. The most important of these esters are poly(lactide) (PL), poly(glycolide) (PG) and their copolymer poly(lactide-co-glycolide) (PLG) (Figure 1.3). PLG based drug delivery devices are attractive because of their biocompatibility, biodegradability, and non-toxicity. In addition, drug release from these synthetic polymers is dependent on properties such as polymer molecular weight and lactide:glycolide ratio [10]. By selection of an appropriate polymer composition with a

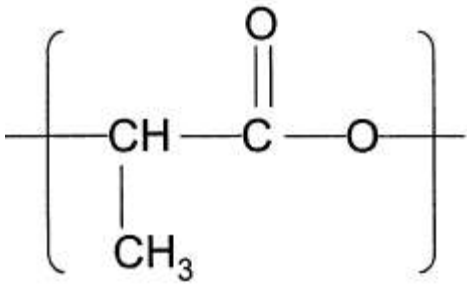

(a)

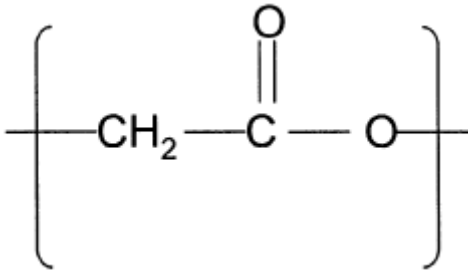

(b)

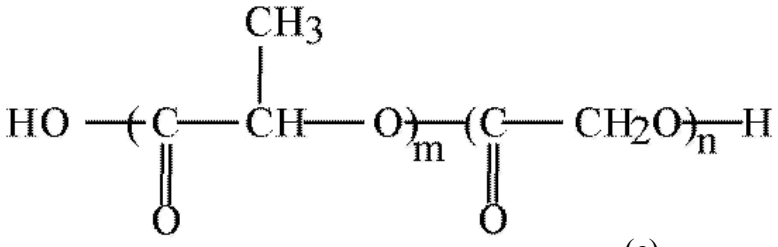

(c)

Figure 1.3 Chemical structure of (a) poly(lactide), (b) poly(glycolide), and (c) poly(lactide-co-glycolide).

known rate of degradation, such polymers can be exploited to produce a drug delivery system that releases active agents at predetermined rates.

The hydrolysis of aliphatic polyesters starts with water uptake followed by random hydrolytic splitting of the ester bonds which yields a carboxyl end group and a hydroxyl one. The thus formed carboxyl end groups are capable of catalyzing hydrolysis of other ester bonds, in a phenomenon called autocatalysis [11-14]. This hydrolytic degradation process occurs in the bulk of the polymer and is thus macroscopically homogeneous (bulk degradation). As a consequence of the polymer degradation process, the average molar mass decreases significantly before any weight loss takes place [11-13, 15]. This weight loss occurs at a molecular weight of 5000 – 10000 Da, when oligomers are produced that can dissolve in the diffused solvent. [11-13].

1.4. Microspheres as Drug Delivery Devices

Most traditional biodegradable drug delivery systems involve either entrapping a drug into biodegradable polymer matrices and surgically implanting it into the body [5-8], or entrapping the drug into polymeric nano and micro spheres [9]. Microspheres (and nanospheres) are very versatile drug delivery vehicles, and can be administered through a variety of routes such as inhalation [16,17], oral [18], and parenteral routes [16]. The parenteral route includes subcutaneous [19], intravenous [20], and intramuscular [21] injection. This variety in the administration routes coupled with the ability to tailor the size of the microspheres enables site directed drug delivery. Also the first pass effect inherent in the oral route can be eliminated. Microspheres can be easily prepared from

biodegradable polymers and do not require implantation or explantation. In addition, various factors, such as size, polymer composition and molecular weight, can be used to tailor the drug release profiles from these devices [10,22-24]. Due to these attractive properties, microspheres occupy a unique position in drug delivery technology, and have shown to control release profiles for drugs having a wide range of molecular weights (small molecules [25-29], steroids [30], and proteins [31-37]).

1.4.1. Fabrication Techniques

Biodegradable polymeric microspheres encapsulating a therapeutic agent are often prepared by coacervation, spray drying, or solvent evaporation/extraction techniques [1,38-40]:

Coacervation [41] was the first microencapsulation technique used to prepare microspheres, and usually involves 4 steps. Initially the active agent is dissolved or dispersed in an organic polymer solution. The polymer is then forced to slowly phase separate which yields two liquid phases, the polymer containing coacervate phase and the supernatant phase depleted in polymer. The coacervate phase then gets adsorbed around the drug particles to form very soft coacervate droplets which entrap the drug. In the final stage of this process the microdroplets are dehydrated and hardened to form the final microspheres [1,38,39,41].

As previously mentioned, the spray drying method is also used to prepare polymeric microspheres [31, 42]. In this technique, a solution of the polymer, the drug and the organic solvent is prepared and then atomized, and air is usually used as the drying agent

to dry the particles. A major problem encountered while using this technique is the formation of polymer fibers due to insufficient breaking force applied by the nozzle [31,39,42].

The most common technique currently used to prepare polymeric microspheres for controlled drug delivery is the solvent evaporation/extraction technique [30,40,43-48]. This technique can be divided into the single emulsion process used to entrap water-insoluble drugs, and the double emulsion process used to entrap water-soluble drugs. In the single emulsion process, the polymer and the drug to be encapsulated are dissolved or dispersed in an organic solvent to form an organic solution. This organic solution is then added to a large-volume aqueous solution which results in an oil-in-water (o-w) emulsion (Figure 1.4). The emulsion is then stirred at high speeds to form fine droplets. The aqueous solution usually contains a polymer to prevent droplet aggregation. The organic solvent is then removed either by slowly evaporating under reduced pressure (solvent evaporation) or by quick extraction through addition of large volumes of de-ionized water (solvent extraction) [1,30,38,39,43,44]. In the double emulsion process, the water-soluble drug is dissolved in an aqueous solvent, while the polymer is dissolved in an organic solvent. The aqueous solution is then emulsified in the organic solution with vigorous stirring to form the first water-in-oil emulsion (w-o). This emulsion is then added to a large-volume of aqueous solution to form a water-in-oil-in-water (w-o-w) emulsion. This emulsion is then subjected to solvent removal by either evaporation or extraction as in the single emulsion process [1,38,39,45-48].

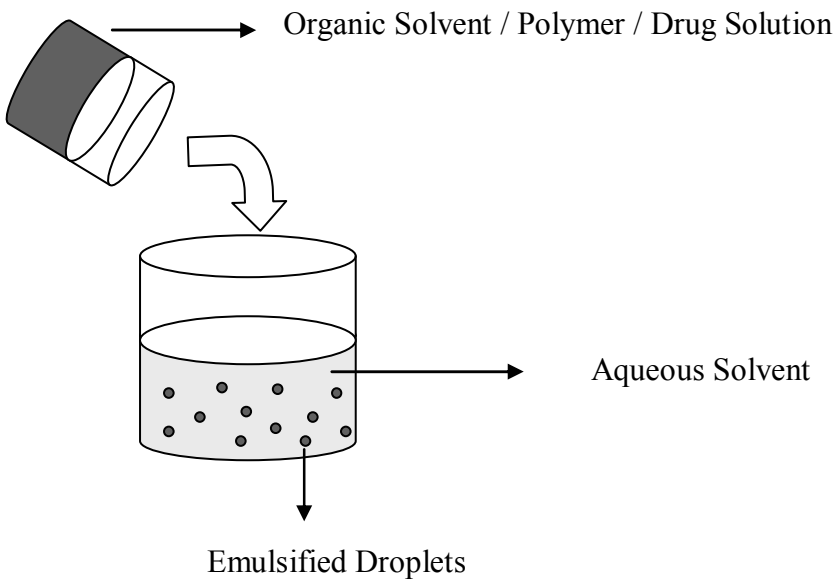

Figure 1.4 Basics of the single emulsion solvent extraction/evaporation microsphere preparation technique.

1.5. Desired Drug Release Patterns

Controlled drug release formulations should be designed to achieve drug release patterns that produce the optimal therapeutic response. Some therapeutics requires a constant release for a wide range of durations (days to months) [49-51], while for other therapeutics, sustained or continuous release is not optimal [5, 51-54]. In addition to the traditional zero-order release kinetics, pulsatile release (or pulsed release) is also of interest to the pharmaceutical industry (Figure 1.5). For example, in antigen delivery, pulsatile release is often more effective than sustained release profile [51], and a vaccine preparation could be designed to deliver two timed-release pulses of antigen from a single injection which would eliminate the need for a "booster" vaccination. Through this immunization formulation, an initial burst release of antigen in the first several days will induce the primary immune response, and after a period of weeks, during which little antigen is released, the system will deliver a second pulse of antigen release. Thus, the release pattern will mimic the release obtained from two different administrations [51]. Other examples include the release of insulin and hormones of the anterior pituitary gland such as growth hormone and the gonadotropin-releasing hormone (GnRH). These molecules are secreted by the human body in a pulsatile manner [53,54], and a delivery system that mimics the natural pulsatile release profile is desirable.

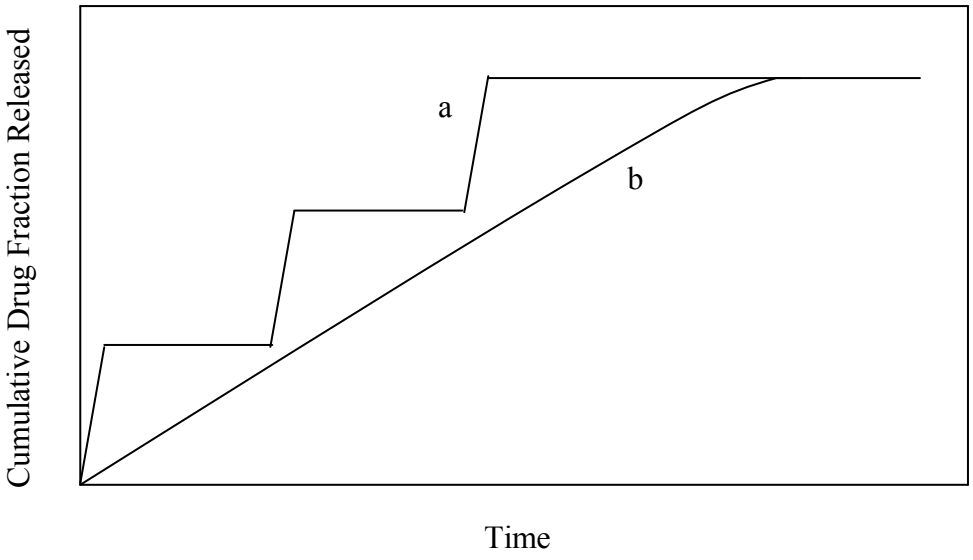

Figure 1.5 Schematic of ideal desired release profiles for controlled drug delivery: (a) pulsatile release, and (b) constant release.

1.6. Commercially Available Controlled Drug Release Formulations

A considerable number of controlled release formulations are becoming commercially available, and Table 1.1 includes a list of currently marketed poly(lactide) and poly(lactide-co-glycolide) microsphere formulations. [55-62]. As depicted in Table 1.1, polymeric microsphere formulations are versatile and have been used to entrap a wide range of drugs (small molecules, peptides, and proteins), having a wide range of molecular weight (410 Da – 22,000 Da). These drugs are used to treat a variety of indications which include periodontal diseases, prostate cancer, endometriosis, growth deficiency, acromegaly, and schizophrenia. In addition, these formulations have successfully achieved sustained drug release for time periods that range from days to months [57-62].

1.7. Motivation and Organization

Difficulty achieving desired release rates remains to be one of the main challenges in controlled drug delivery. The aim of this work is to investigate different methodologies that can be utilized to design a delivery system with desired release kinetics. This is done by preparing polymeric microspheres of specified mean diameter and size distribution and examining the effect of microsphere size and polymer molecular weight on *in vitro* release. A mathematical model is then developed which can be a useful tool to predict drug release from polymeric microspheres. In addition to modulating release kinetics by controlling microsphere size and polymer molecular weight, a numerical optimization

Table 1.1 List of FDA approved drug delivery products using PL and PLG polymers

Product	Pharmaceutical/ M_w (Da)	Indication for use	Duration of action
Atridox	Doxycycline/444	Periodontal disease	1 week
Lupron Depot	Leuprolide/1209	Prostate cancer, endometriosis	1,3,4 months
Trelsar Depot	Triptorelin/1311	Prostate cancer	1 month
Suprecur MP	Buserelin/1299	Endometriosis	1 month
Nutropin	Human Growth Hormone/22000	Growth deficiency	2 weeks,1 month
Sandostatin LAR	Octreotide/1019	Acromegaly	1 month
Somatuline	Lanreotide	Acromegaly	1 month
Arestin	Minocycline/457	Periodontitis	2 weeks
Risperdal Consta	Risperidone/(410)	Schizophrenia	2 weeks
Zoladex	Goserelin acetate/(1269)	Prostate cancer, endometriosis	1,3 months

technique is developed to achieve desired drug release profiles by mixing appropriate proportions of individual microsphere preparations.

Section 2 of this dissertation investigates the mean diameter and size distribution of PLG microspheres prepared using the oil-in-water emulsion technique. Section 3 covers computational and experimental work done to investigate the effect of mean diameter and polydispersity of PLG microspheres on drug release. Section 4 covers work done to design desired drug release profiles by combining microsphere populations having different microsphere size and polymer molecular weight.

2. MEAN DIAMETER AND SIZE DISTRIBUTION OF PLG MICROSPHERES*

2.1. Background

Controlled drug delivery offers numerous advantages compared with conventional free dosage forms, in particular: improved efficacy, reduced toxicity, and improved patient compliance and convenience. Consequently there is considerable interest from the pharmaceutical industry about the encapsulation of vaccines and drugs in biodegradable proteinaceous or polymeric micro- and nano-spheres. Microencapsulation promises an increase for the shelf life of a vaccine, and offers the flexibility of controlled release kinetics for the administered drug [9].

Commonly used microspheres in drug delivery include: polylactide (PL), polyglycolide (PG), poly(lactide-co-glycolide) (PLG), albumin, and alginate [9, 63-65]. PLG based microspheres are attractive macromolecular (drugs/vaccines) carriers because of their biocompatibility, biodegradability and non-toxicity. In addition, these synthetic polymers degrade at a rate that is dependent on properties such as polymer molecular weight and lactide:glycolide ratio [10]. By selection of an appropriate polymer composition with a known rate of degradation, such polymers can be exploited to produce a drug delivery system that releases active agents at predetermined rates. In

*Part of the data reported in this section is reprinted with permission from N.S. Berchane, F.F. Jebrail, K.H. Carson, A.C. Rice-Ficht, and M.J. Andrews, About mean diameter and size distributions of poly(lactide-co-glycolide) (PLG) microspheres, Journal of Microencapsul. 23 (2006) 539-552, Taylor and Francis.

addition, PLG microspheres are versatile, and can be prepared using the oil-in-water (o/w) emulsion solvent evaporation technique which was shown to successfully entrap hydrophobic materials [30, 43, 44]. Alternatively, PLG microspheres can be prepared through the (water-in-oil)-in-water (w-o-w) solvent evaporation technique that has been shown to be efficient in entrapping water soluble material [45-48].

Drug release kinetics primarily depends on microsphere size and composition. In addition, microsphere size plays a crucial role when targeting a particular site in the body. For example, bioadherent microspheres of size less than 10 μm are absorbed by the intestinal lining in Peyer's patches, while larger microspheres pass through without being affected. Despite the importance of microsphere size, little work has been done to quantitatively predict the distribution of microspheres from manufacturing techniques. Jeffery et al. [44] investigated the effect of various process parameters on microsphere size. Jeffery found that an increase in the rate of agitation resulted in a reduction in droplet size. In addition, it was also found that the choice of stabilizer significantly affects droplet size. However, it appears that no effort was made to relate these parameters to the physics of droplet formation [44]. Giletto [66] performed a study to determine PLG microsphere size and surface morphology, and scanning electron micrographs qualitatively showed that polymer molecular weight played a significant role in controlling microsphere size [66]. Berkland et al. [67] developed a method to produce microspheres of a monodisperse size distribution by spraying a polymer-containing solution through a nozzle. The nozzle was equipped with acoustic excitation and a non-solvent carrier stream to produce uniform droplets [67]. Bahukudumbi et al.

[68] employed the turbulent dispersion theory to develop a mathematical correlation for the average diameter of bovine serum albumin (BSA) microspheres.

In this Section we describe work to prepare PLG microspheres using the oil-in-water (o/w) emulsion solvent extraction technique. Microsphere diameter has been related to the size of the stable droplets formed in the emulsion. Turbulent dispersion theory is used to consider the different working parameters, and construct a correlation that predicts the final mean droplet size of the PLG emulsion.

2.2. Materials and Methods

2.2.1. Materials

The poly(D,L-lactide-co-glycolide) used had a copolymer composition of 50:50, and a Mw of 50 – 75 kDa. The Poly (vinyl-alcohol) (PVA) was 87%-89% hydrolyzed, with a Mw of 13-23 kDa, and the Dichloromethane used had a molecular weight of 84.93 Da. All these chemicals and other miscellaneous items were purchased from Sigma (St. Louis, MO, USA).

2.2.2. Microsphere Preparation

PLG microspheres were prepared by the oil-in-water (o/w) emulsion solvent extraction technique described next, and depicted in Figure 2.1. The protocol is detailed in the literature [30,43,44]. PLG was dissolved in dichloromethane (DCM) to yield a 10% (w/v) PLG solution. PVA solution (8% w/v) was stirred at the desired stirring speed

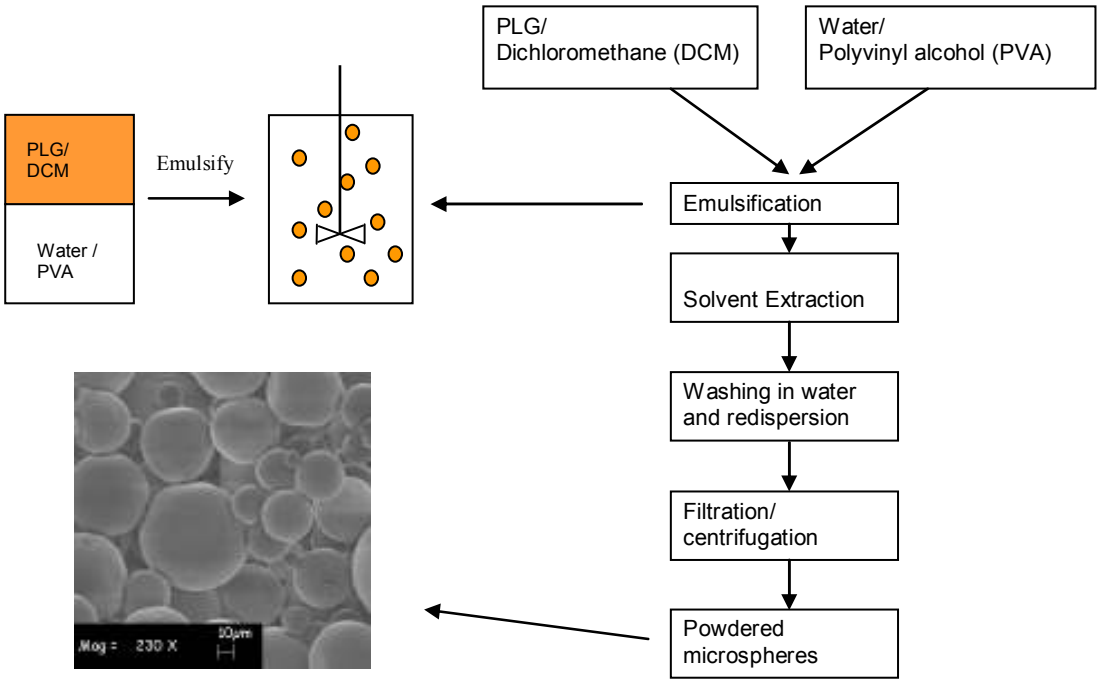

Figure 2.1 Schematic of PLG microsphere preparation procedure.

for 5 minutes in a 400 ml Pyrex beaker with a Caframo ultra high torque stirrer (model BDC1850) having a speed range of 0 -1800 rpm. The PLG solution was slowly added to the beaker and stirring was continued for 60 minutes. Afterwards, the resulting emulsion was added to 1L of double distilled water, and stirring was continued for an additional 90 minutes at a speed of 1200 rpm. Microspheres were then collected by filtration, where the filter size used was 0.2 μm to prevent any loss of microspheres.

Like others [44], we were not able to produce PLG microspheres without a stabilizer. Typical stabilizers used at the DCM/water interface include: Poly (vinyl alcohol) (PVA), sodium dodecyl sulphate (SDS), cetyltrimethyl ammonium bromide (CTAB), and methylcellulose. PVA was used in this research because it gave the smallest microspheres [44].

2.2.3. Microsphere Characterization

Imaging of microspheres was performed with a LEO-VP1530 field emission scanning electron microscope at the Microscopy and Imaging Center (MIC) at Texas A&M University. Samples of the spheres were mounted on aluminum stubs using double adhesive tape. The stubs were then left overnight in a desiccator to dry. The samples were sputter-coated with 4 nm of platinum-palladium in an atmosphere of argon. Scanning was then performed at ambient temperature and vacuum pressure. The mean microsphere diameter was quantitatively determined by measuring ~550 microspheres from the SEM micrographs using the Scion Image Analysis software. The pixel to distance ratio for each micrograph was entered into the software, and the edges of the

spheres were specified by hand. The number of microspheres (~550) measured for each stirring speed was sufficient to provide an accurate average (Table 2.1).

2.3. Theory of Droplet Formation

The following briefly reviews the basic principles of emulsification and droplet formation. A substantial literature of experimental, theoretical, and numerical work that discusses the mechanism of droplet breakdown is available [69,70]. Addition of Dichloromethane/PLG solution to the PVA solution forms an emulsion in which PLG is the dispersed phase and PVA is the continuous phase. Emulsion coalescence occurs when dispersed droplets collide with each other. Because the volume fraction of the dispersed PLG solution is low (Φ = 0.05), the analysis here is limited to the case of emulsion dispersion in turbulent flow under non-coalescing conditions.

We next consider an isolated droplet and analyze the forces that lead to its breakup. As agitation is started, an external inertial stress (τ) acts on the droplet to cause its deformation. The inertial stress results from a dynamic pressure associated with the surrounding continuous phase. As the droplet starts to deform, internal restoring forces (viscous or surface tension) resist the deformation. The interfacial tension stress has magnitude σ/d where σ is the interfacial tension and d is the droplet diameter. Viscous stresses within the droplet are of the order of magnitude: $\frac{\mu_d}{d}\sqrt{\frac{\tau}{\rho_d}}$, where μ_d and ρ_d are the viscosity and density of the droplet respectively. A stable droplet is formed when a

Table 2.1 Measured volume moment mean diameter of PLG microspheres at different We_m

Speed (rpm)	Mixing Tank Weber Number (We_m)	Mean Diameter [a] d_{43} (μm)
300	76949	52.64 ± 0.8
600	307796	24.83 ± 0.4
900	692541	16.20 ± 0.2
1200	1231185	13.30 ± 0.2

[a] Mean diameter ± standard error

balance between these three forces, dynamic pressure, internal viscous stress and surface tension, is reached [69].

Accordingly, two independent non-dimensional numbers can be obtained from dimensional analysis. The first non-dimensional number is a viscosity group that accounts for the effect of the viscosity of the fluid in the droplet:

$$N_{Vi} = \frac{\mu_d}{\sqrt{\rho_d \sigma d}} \tag{2.1}$$

Here we consider the case of a non-viscous dispersed phase where the viscous stress within the droplet is negligible compared with the interfacial tension at the droplet-water interface (i.e. $N_{Vi} \rightarrow 0$) [69].

The second non-dimensional number is the ratio of the dynamic pressure to the interfacial stress which results in the non-dimensional Weber number:

$$N_{We} = \tau d / \sigma \tag{2.2}$$

As the ratio of the inertial stresses (dynamic pressure) to the interfacial tension force increases (an increase in Weber number), the deformation of the droplet increases to a point when a critical Weber number $(N_{We})_{crit}$ is reached and breakup occurs. If the flow pattern is the same throughout the entire flow region, all droplets having a Weber number greater than $(N_{We})_{crit}$ will be subject to break up.

Of significance here is the smallest eddy length scale (η), commonly referred to as the Kolmogorovs' length scale ($\eta = (\frac{\nu^3}{\varepsilon})^{1/4}$, where ε is the rate of energy dissipation and ν is the kinematic viscosity), and the largest eddy scale L. For drop breakup in the inertial sub-range ($\eta << d << L$), the external viscous shear stresses are generally assumed negligible relative to the turbulent dynamic pressure forces [69]. Dynamic pressure forces are associated with changes in velocity over distances equal to the diameter of the droplet. Thus the turbulent stresses (τ) across a droplet can be expressed as $\rho_c \overline{v^2}$, where $\overline{v^2}$ is the average value across the whole flow field of the square of the velocity difference across the droplet [69,70]. As a consequence, the critical Weber number can be expressed as:

$$(N_{We})_{crit} = \frac{\rho_c \overline{v^2} d_{\max}}{\sigma} \qquad \textbf{(2.3)}$$

where d_{max} is the diameter of the largest droplet that can resist breakup. For the case of isotropic turbulence [69,71]:

$$\overline{v^2} = c(\varepsilon d_{\max})^{2/3} \qquad \textbf{(2.4)}$$

Thus

$$(N_{We})_{crit} = \frac{c\rho_c \varepsilon^{2/3} d_{\max}^{5/3}}{\sigma} \qquad \textbf{(2.5)}$$

Assuming that v (velocity difference across the droplet) is proportional to ND (where N is the stirring speed in radians per second, and D is the impeller diameter in meters) and the turbulence in the tank to be isotropic and fully developed, the turbulence energy dissipation, ε, can be shown to be proportional to N^3D^2 [70,72]:

$$\frac{d_{\max}}{D} = c_1\left(\frac{\rho_c N^2 D^3}{\sigma}\right)^{-3/5} = c_1 We_m^{-3/5} \tag{2.6}$$

where We_m is called the Weber number of the mixing tank, and c_1 is a constant to be uniquely determined for different emulsions [69,70].

The next step is to relate the maximum droplet diameter (d_{max}) to the mean droplet diameter. The general expression for mean diameters is:

$$d_{gh} = \left[\frac{\sum n_i d_i^{\,g}}{\sum n_i d_i^{\,h}}\right]^{1/(g-h)} \tag{2.7}$$

where g and h take values that correspond to the phenomena being investigated, n_i is the number of droplets in size range i, and d_i is the diameter at the center of size range i. The Sauter mean diameter (d_{32}) is the diameter of a drop whose ratio of volume to surface area is the same as that of the entire population:

$$d_{32} = \frac{\sum n_i d_i^{\,3}}{\sum n_i d_i^{\,2}} \tag{2.8}$$

Alternatively, the volume moment mean diameter (d_{43}), which is of interest for controlled drug delivery, is the center of gravity of the volume fraction size distribution:

$$d_{43} = \frac{\sum n_i d_i^{\,4}}{\sum n_i d_i^{\,3}} \tag{2.9}$$

The Sauter mean diameter (d_{32}) has generally been assumed to be proportional to the maximum sphere diameter (d_{max}) [70]. However, the generality of this assumption has been questioned in recent work by Pacek et al. [73]. Since the drop size distribution is universal, all representative diameters are uniquely related, so d_{43} is also taken to be proportional to d_{max}:

$$\frac{d_{43}}{D} = c_2 We_m^{\,-3/5} \tag{2.10}$$

The main objective here is to evaluate c_2 for PLG microspheres, and investigate how closely the correlation (2.10) predicts PLG microsphere mean diameter at different operating parameters.

2.4. Results and Discussion

2.4.1. Microsphere Size Distributions

To validate the theory presented in the previous Section, several batches of PLG microspheres were prepared over a wide range of stirring speeds. PLG microspheres were prepared according to the protocol described above, and a Caframo stirring paddle with a pitched–blade impeller was used with an impeller blade diameter of 5.8 cm. For consistency, the impeller was positioned in the center of the Pyrex beaker, half-way between the top surface of the PVA continuous phase and the bottom of the flask. In our experiment, the PLG/dichloromethane solution is the dispersed phase while the PVA solution is the continuous phase. As the stirring speed increased, more air was entrained and foam was formed. To avoid excessive foaming, antifoam of silicone and non-silicon constituents was used (0.1% v/v) that served to increase the rate at which air bubbles were dissipated. An aluminum foil lid was also used to seal the top of the beaker to reduce air entrainment. This was necessary as the entrained bubbles can damp turbulence intensity and affect the size of the microspheres [70].

To study the effect of We_m on the mean diameter of the microspheres formed, PLG microspheres were prepared at different stirring speeds (300-1200 rpm). For microspheres prepared at each stirring speed, the mean diameter was quantitatively determined by measuring the size of ~ 550 microspheres giving a small error for the mean diameter (Table 2.1).

Figure 2.2 shows SEM micrographs of PLG microspheres prepared at: (a) N = 300 rpm, (b) N = 600 rpm, (c) N = 900 rpm, and (d) N = 1200 rpm. Figure 2.3 shows the

corresponding cumulative volume fraction distributions, plotted against the diameter of PLG microspheres. When characterizing microspheres, the volume fraction of a specified range is significant because it indicates the mass distribution of microspheres at different diameters. This is required for calculating release kinetics for a population of microspheres. From inspection of the micrographs, it is apparent that the microspheres appear rigid and nicely spherical (Figure 2.2). It is also evident from the micrographs and the size distributions (Figure 2.3) that the microspheres are polydisperse, in some cases having microsphere diameters ranging from 6 to 92 μm (Figure 2.3 (a)). As expected from turbulent dispersion theory, Figure 2.2 and Figure 2.3 show a decrease in microsphere diameter with an increase in stirring speed. At 300 rpm (Figure 2.3 (a)), the microspheres span a wide range of diameters from 6 to 92 μm, this is also apparent in Figure 2.2 (a). As the stirring speed is increased to 600 rpm, the range of microsphere diameters is reduced to 7 to 43 μm (Figure 2.3 (b)). A further increase in the stirring speed to 900 rpm results in the microsphere diameter range being distributed from 4 to 22 μm (Figure 2.3 (c)). Further increase in impeller speed to 1200 rpm has a weak effect on the distribution as can be seen in Figure 2.3 (d) where the majority of the spheres have a diameter that ranges from 3 to 20 μm.

2.4.2. Mathematical Distribution Function

A number of functions have been proposed, based on either probability or empirical considerations, that allow the mathematical representation of measured microsphere size

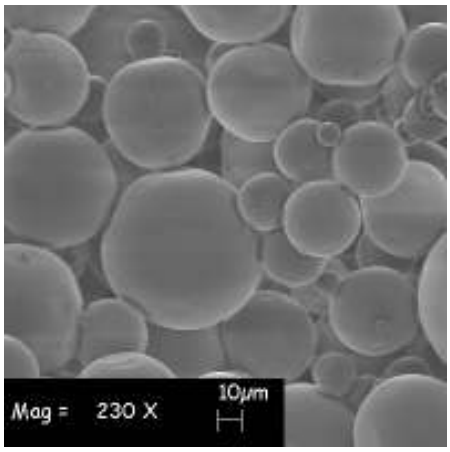

(a) N = 300 rpm

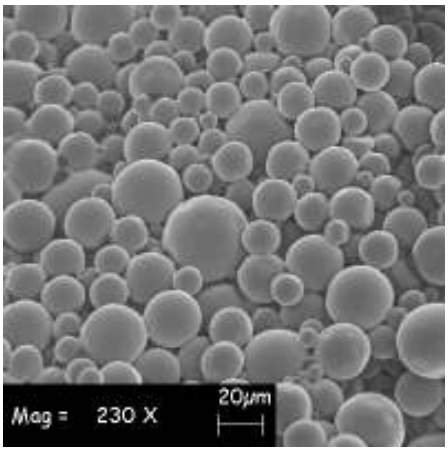

(b) N = 600 rpm

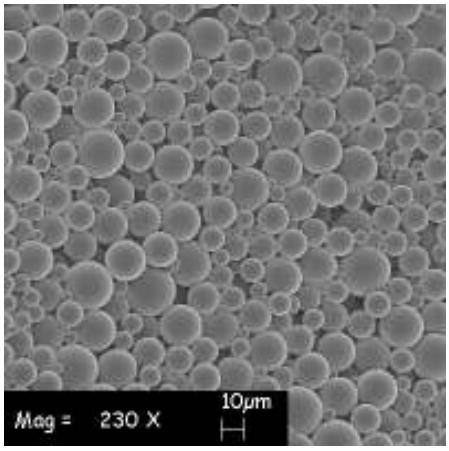

(c) N = 900 rpm

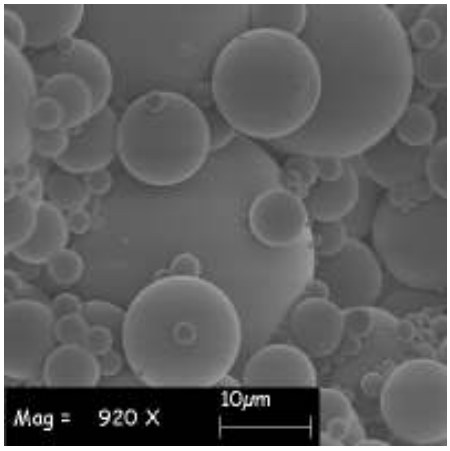

(d) N = 1200 rpm

Figure 2.2 SEM micrographs of PLG microspheres prepared at (a) N = 300 rpm, (b) N = 600 rpm, (c) N = 900 rpm, and (d) N = 1200 rpm.

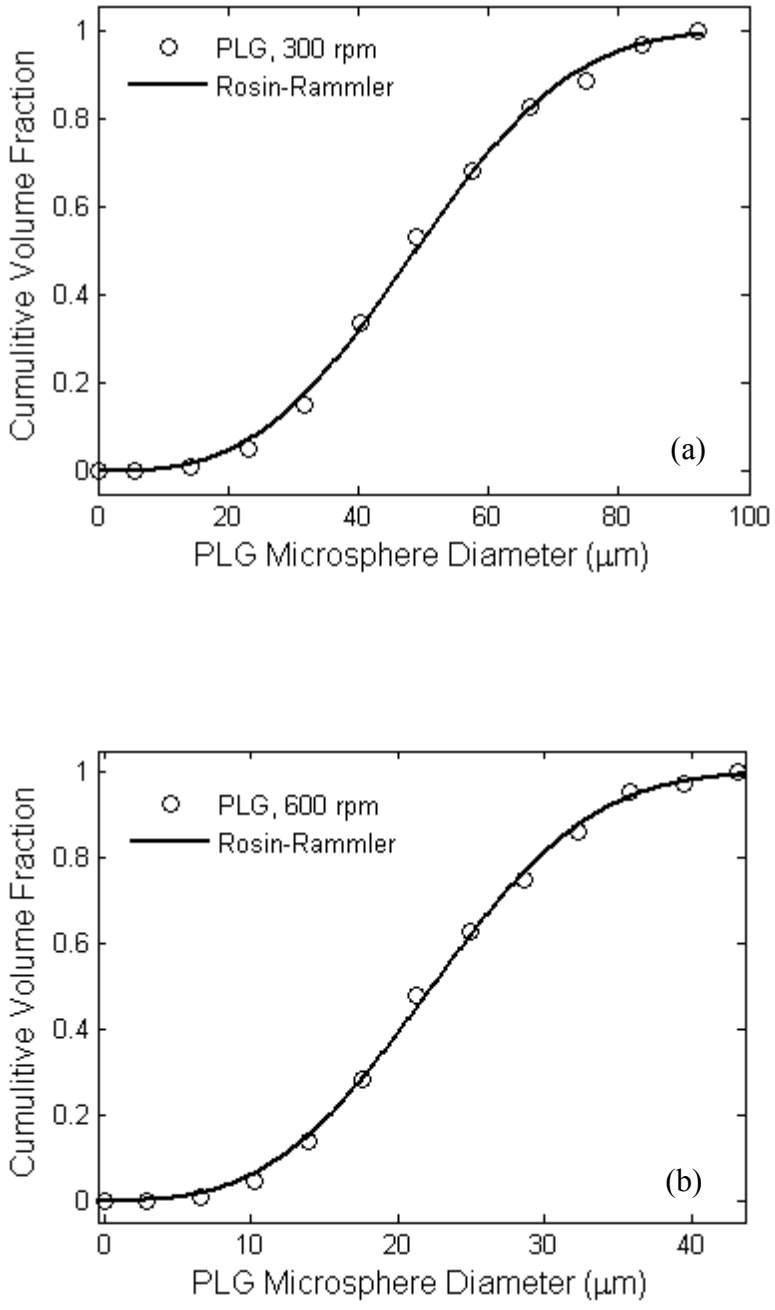

Figure 2.3 Cumulative volume distribution at different impeller speeds, (a) 300 rpm, (b) 600 rpm, (c) 900 rpm, and (d) 1200 rpm.

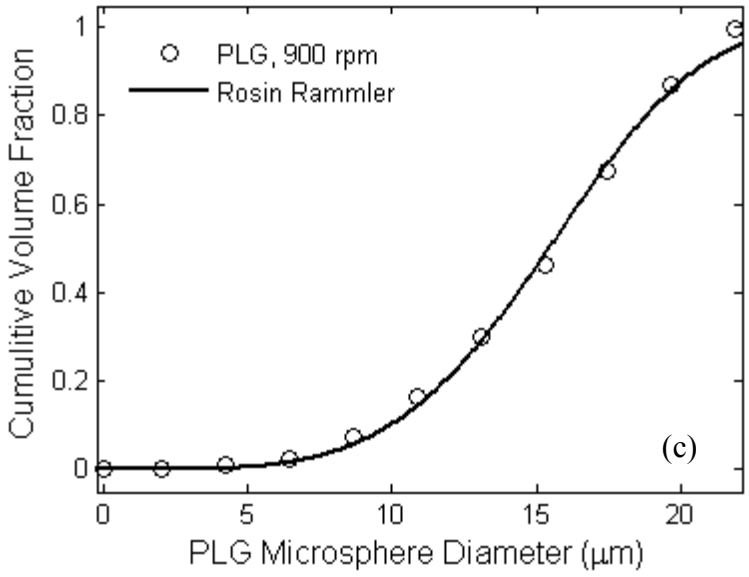

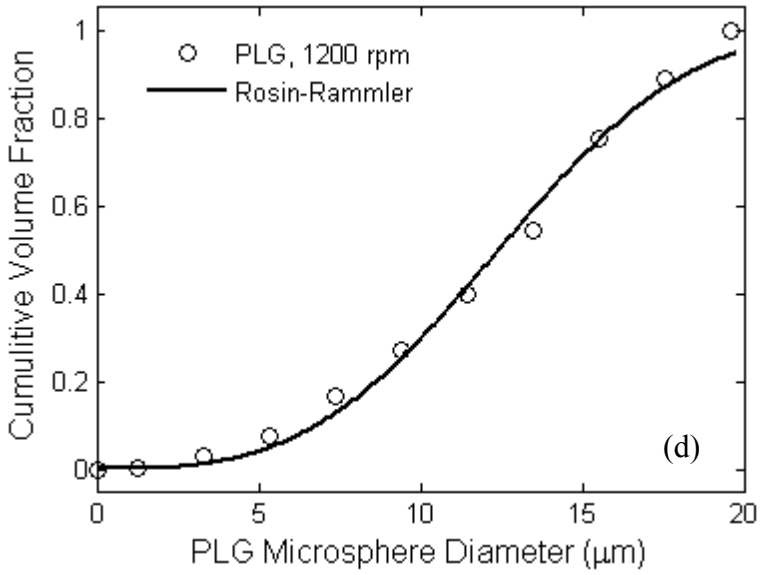

Figure 2.3 Continued

distributions. Those used include: normal, log-normal, Nukiyama-Tanasawa, and Rosin Rammler distributions [74]. After some trial and error the Rosin-Rammler distribution function provided the best representation of our experimental data. The volume fraction distribution function can be expressed in the following form:

$$(\frac{1}{V_{tot}})\frac{dV}{dd} = f_V(d) = \frac{b}{a}(\frac{d}{a})^{(b-1)} \exp(-(\frac{d}{a})^b) \quad \textbf{(2.11)}$$

where V_{tot} is the total volume of the microsphere population, d is the droplet diameter, and a and b are constants to be obtained from a least squares fit to the volume fraction data. The Rosin-Rammler relationship describes drop size distribution in terms of the parameters a and b. For most distributions, b lies between 1.5 and 4. Integration of the volume fraction distribution function (Equation 2.11) yields the cumulative volume distribution function expressed as:

$$\frac{V}{V_{tot}} = F_V(d) = 1 - \exp(-(\frac{d}{a})^b) \quad \textbf{(2.12)}$$

where V is the total volume contained in drops of diameter less than d. As depicted in Figure 2.3, the cumulative Rosin-Rammler distribution function provides a good fit to the cumulative volume fraction distributions of PLG microspheres prepared using our experimental set-up. Corresponding values of a and b are given in Table 2.2.

Table 2.2 Coefficients of Rosin-Rammler mathematical function obtained through least squares fit to the volume fraction data at different We_m

Speed (rpm)	Mixing tank Weber number (We_m)	a	b
300	76949.1	58.15	3.15
600	307796.2	26.54	3.21
900	692541.5	18.65	4.52
1200	1231184.8	16.13	3.42

2.4.3. Microsphere Mean Diameters

The correlation of Equation (2.10) predicts the mean diameter of microspheres formed as a function of We_m and D. In this Section the validity of this correlation is tested by comparing analytical predictions with experimentally obtained mean microsphere diameters at four different stirring speeds. We_m is calculated from Equation (2.6), using the density of PVA, impeller diameter, stirring speed in rpm, and interfacial tension at the water/dichloromethane interface [75-77].

Measured volume moment mean diameter (d_{43}) of PLG microspheres prepared at different Weber numbers are given in Table 2.1, and Figure 2.4 shows a comparison between these measured mean diameters and the predicted mean diameters (given by Equation (2.10)) on logarithmic scale. The value of the coefficient c_2 = 0.88, was obtained from a least squares fit to the experimental data. It is evident from Figure 2.4 that the developed mathematical correlation provides a close fit to the experimental mean diameters over a wide range of Weber numbers.

2.5. Conclusions

PLG microspheres have been prepared using an emulsion technique, and a quantitative study has been performed on the resultant microsphere size distributions. A fluid mechanics based mathematical correlation for the mean microsphere diameter was developed based on the turbulent dispersion theory. The correlation, is given in Equation (2.10) with c_2 = 0.88, and was validated by comparisons with experimental results for a

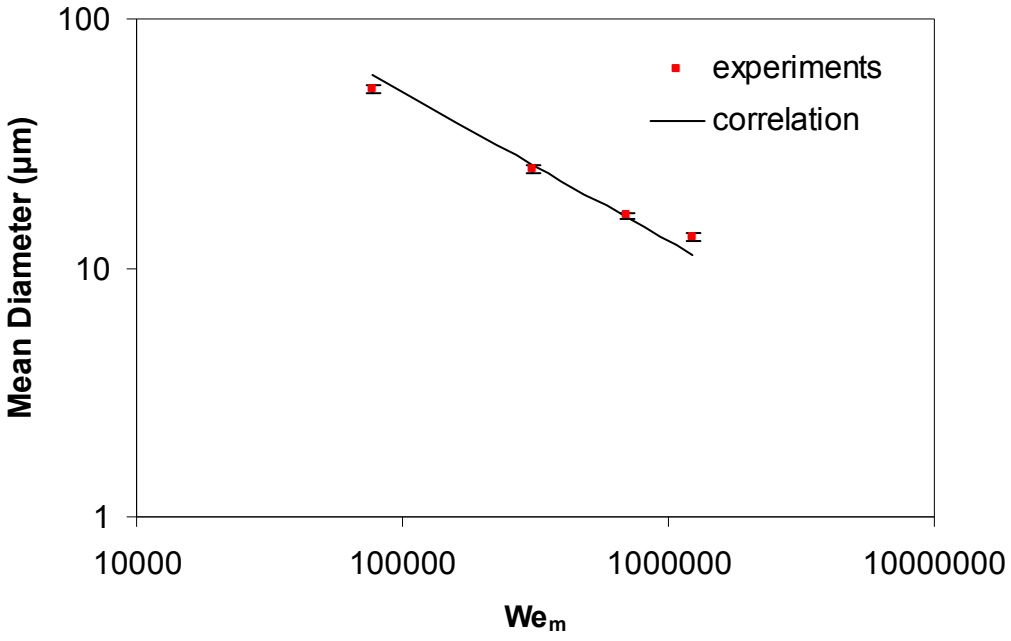

Figure 2.4 Volume moment mean diameter (d_{43}) of PLG microspheres as a function of We_m on logarithmic scale; error bars represent interval estimate of population mean diameter with 99% level of confidence.

wide range of We_m. This correlation is valid for non-coalescing dispersions, with the dispersed phase having low viscosity, and volume fraction. The size distribution of PLG microspheres was described by a Rosin-Rammler distribution function that provided a close fit to the experimental data. This quantitative study makes possible an estimate of the mean size and size distribution of PLG microspheres prepared using the emulsion technique. In particular, the known size distribution is suitable for design of controlled release drug delivery systems.

3. EFFECT OF MICROSPHERE SIZE ON DRUG RELEASE*

3.1. Background

Difficulty achieving desired release rates is an important limitation in controlled drug delivery. Microsphere size, which has a significant effect on drug release rate, can potentially be varied to design a controlled drug delivery system with desired release profile. Mathematical modeling provides insight into the fundamental processes that govern the release, and once validated with experimental results, it can be used to tailor a controlled drug delivery system with specified drug release profile. Even though the majority of the conventional manufacturing techniques used for controlled drug delivery result in polydisperse microspheres, the mean diameter is used to represent the size of the microspheres when modeling drug release. As a consequence, the model does not account for the effect of population polydispersity which is believed to be one of the main causes for the initial drug "burst" release [78].

To minimize the polydispersity effect on release kinetics, some investigators used manufacturing techniques that result in monodisperse populations, while others used sieves to fractionate the microspheres into more uniform size distributions. Berkland et al. [67] developed a method to produce microspheres of a monodisperse size distribution by spraying a polymer-containing solution through a nozzle. The nozzle was equipped with acoustic excitation and a non-solvent carrier stream to produce uniform droplets.

*Part of the data reported in this section is published in Int. J. Pharmaceut., doi:10.1016/j.ijpharm.2006.12.037, N.S. Berchane, K.H. Carson, A.C. Rice-Ficht, and M.J. Andrews, Effect of mean diameter and polydispersity of PLG microspheres on drug release: experiment and theory. Copyright Elsevier (2007).

This technology was later used to produce monodisperse PLG microspheres to investigate the effect of microsphere size and polymer molecular weight on drug release [23,79]. Siepmann et al. [24] investigated the effect of the size of biodegradable microparticles on release rate of dispersed drug (monolithic dispersions). The manufacturing technique resulted in microspheres with a wide size distribution, and five different size fractions were then obtained by sieving [24]. Alternatively, Bezemer et al. [22] studied the release of protein from amphilic multiblock copolymers, based on hydrophilic poly(ethylene glycol) (PEG) blocks and hydrophobic poly(butylenes terephthalate) (PBT) blocks. Despite the wide microsphere size distribution, the effect of microsphere size was only represented in terms of the mean diameter [22].

In this Section the effects of microspheres mean diameter, polydispersity, and polymer degradation on drug release rate from poly(lactide-co-glycolide) (PLG) microspheres are investigated experimentally. Based on the experimental results, a mathematical model is proposed that accounts for the effects of diffusion, polymer degradation, and microsphere size distribution to predict drug release kinetics from polydisperse PLG microsphere populations.

3.2. Materials and Methods

3.2.1. Materials

The poly(D,L-lactide-co-glycolide) used had a copolymer composition of 50:50, a Mw of ~ 40 kDa, and is a product of Sigma. The Poly (vinyl-alcohol) (PVA) was 87%-

89% hydrolyzed, with a Mw of 13 – 23 kDa. In addition to these chemicals, Piroxicam (Mw 331.3), and HPLC grade Dichloromethane (DCM) were purchased from Sigma. Sodium hydroxide was purchased from EM Science. All chemicals were used as provided.

3.2.2. Microsphere Preparation

PLG microspheres were prepared using the oil-in-water (o-w) emulsion solvent extraction technique described previously (Section 2.2.2, Figure 2.1). Briefly, Piroxicam was co-dissolved with PLG (10% w/v) in dichloromethane (DCM) at 20% of the PLG mass (20% theoretical loading (w/w)). PVA solution (8% w/v) was stirred at the desired stirring speed for 5 minutes in a 400 ml Pyrex beaker with a Caframo ultra high torque stirrer (model BDC1850) having a speed range of 0 -1800 rpm. The PLG solution was slowly added to the beaker and stirring was continued for 60 minutes. Afterwards, the resulting emulsion was added to 1L of double distilled water, and stirring was continued for an additional 90 minutes at a speed of 1200 rpm. Microspheres were then collected by filtration, where the filter size used was 0.2 μm to prevent any loss of microspheres.

Three batches of microspheres were prepared at three different impeller speeds (140, 300 and 900 rpm) to produce microspheres having a wide size distribution (0.2 - 140 μm). The correlation developed by Berchane et al. [80], which relates PLG microsphere population mean diameter to impeller speed, was utilized to determine the impeller speeds that would result in the desired microsphere sizes. A portion of the microspheres, prepared at different impeller speeds, was stored for drug release investigations from raw

batches, while the rest of the microspheres were combined and sieved to obtain five different size fractions: 0.2 - 20, 20 - 40, 40 - 63, 63 - 90, and > 90 μm (average pore sizes of the sieves: 20, 40, 63, and 90 μm; Keison Products, United Kingdom). Once sieved, the microspheres were lyophilized and stored at -20˚C.

3.2.3. Determination of Piroxicam Loading

The experimental loading of piroxicam was determined by dissolving 2 mg of microspheres in 1 ml of 0.25 M sodium hydroxide at 37 ºC for 48 hours. Piroxicam has been shown to be stable in sodium hydroxide solution [81], and is thus believed to be stable under extraction. Piroxicam free microspheres of the same molecular weight were treated similarly. Drug concentration was determined by measuring the absorbance of the piroxicam containing solution in a quartz cuvette at 276 nm (Gilford Response Spectrophotometer) and subtracting the absorbance of the piroxicam free solution. The experiments were done in triplicate.

3.2.4. *In Vitro* Release

Drug release was determined by suspending 5 mg of piroxicam loaded microspheres in 1.3 ml of phosphate buffered saline (PBS, pH 7.4). Piroxicam maintains an unchanged structure in buffer media [82], and is thus believed to be stable under the *in vitro* release conditions. The suspension was continuously agitated by shaking (Glas-Col, Terre Haute, USA) at 100 strokes per minute in a 37 ºC incubator. At predetermined intervals,

the samples were centrifuged, and 1 ml of the supernatant was extracted, and replaced by fresh buffer. The microspheres were then vortexed and put back into the incubator. Resuspending the microspheres in fresh buffer after centrifugation (by vortexing), and continuous agitation of the suspension throughout the release experiment prohibited microsphere aggregation and sedimentation. The piroxicam concentration in the supernatant was determined by measuring the absorbance at 276 nm in a spectrophotometer (Gilford Response Spectrophotometer). Drug concentration was less than 10% of the saturation solubility in the release medium at 37 ºC, which conforms to sink conditions [83]. Piroxicam-free microspheres were treated similarly, and the absorbance from their supernatant was subtracted from all measurements. The experiments were done in triplicate.

3.2.5. Microsphere Characterization

Imaging of microspheres was performed with a LEO-VP1530 field emission scanning electron microscope as described in Section 2.2.3. The mean diameter was quantitatively determined by measuring ~1000 microspheres from the SEM micrographs using the Scion Image Analysis software. The pixel to distance ratio for each micrograph was entered into the software, and the edges of the spheres were specified by hand. The number of microspheres (~1000) measured for each population was sufficient to provide an accurate mean diameter (Table 3.1).

Table 3.1 Characterization of sieved and raw piroxicam loaded PLG microspheres

Microsphere population	Mean diameter[a] d_{43} (μm)	*a*	*b*	Theoretical drug loading (% w/w)	Experimental drug loading (% w/w)	Encapsulation efficiency (%)
> 93 μm	-	-	-	20	5.94	29.7
63 – 90 μm	81.2 ± 0.4	80.5	9.7	20	5.33	26.65
40 – 63 μm	51.0 ± 0.4	50.9	5.4	20	5.2	26
20 – 40 μm	29.6 ± 0.3	29.6	6.0	20	4.7	23.5
0.2 – 20 μm	13.9 ± 0.2	13.8	3.17	20	5.38	26.9
140 rpm	76.0 ± 0.9	75.3	3.78	20	6.05	30.25
300 rpm	33.5 ± 0.4	33.1	3.1	20	5.23	26.15
900 rpm	13.5 ± 0.2	13.3	2.7	20	5.65	28.25

[a] Mean diameter ± standard error

3.3. Mathematical Model

In diffusion-controlled drug release systems, a substance is released from a device by permeation from its interior to the surrounding. There are two main types of diffusion controlled systems, the reservoir system and the monolithic system [1]. In a reservoir system the active agent is enclosed by an inert outer membrane, while in monolithic systems the drug is dispersed uniformly through-out the rate controlling polymer matrix (Figure 1.2). If the active agent is dissolved in the polymer matrix, the device is called monolithic solution, while if the drug is dispersed as a solid, the system is called a monolithic dispersion [1]. In this work the microspheres were prepared by co-dissolving the polymer and the drug in DCM which results in a monolithic solution.

Diffusion is the process by which matter is transported from one part of a system to another as a result of random molecular motions. The motion of a single molecule can be described in terms of the "random walk" in which no molecule has a preferred direction of motion. Although it is not possible to know in which direction any individual molecule will move in a given interval of time, there is a net transfer of molecules from regions of high concentration to regions of low concentration as a result of the random molecular motions [84]. Transfer of heat by conduction is also due to random molecular motions, and there is an analogy between the two processes. This was recognized by Fick [85] who adopted the mathematical equation of heat conduction derived by Fourier [86] to develop the mathematical theory of diffusion. The diffusion theory is based on the hypothesis that the rate of transfer of diffusing substance through unit area of a

Section is proportional to the concentration gradient measured normal to the Section [85]:

$$F = -D\frac{\partial C}{\partial x} \tag{3.1}$$

where F is the diffusion flux in dimensions of [amount of substance length^{-2} time^{-1}], example (gm/m^{2}s), C is the concentration of the diffusing substance in dimensions of [amount of substance length^{-3}], example (gm/m^3), x is the space coordinate measured normal to the Section in dimensions of [length], example (m), and D is the diffusion coefficient in dimensions of [length^2 time^{-1}], example (m^2/s) . The negative sign in Equation (3.1) arises because diffusion occurs in the direction opposite to that of increasing concentration [85].

The fundamental differential equation of diffusion can be derived by considering an element volume in the form of a rectangle whose sides are parallel to the axes of the coordinates. By evaluating the rate at which diffusing substance enters the element volume through its faces, and the rate at which the amount of diffusing substance in the element increases, Fick [85] obtained the following expression for the diffusion equation:

$$\frac{\partial C}{\partial t} = D\left(\frac{\partial^2 C}{\partial x^2} + \frac{\partial^2 C}{\partial y^2} + \frac{\partial^2 C}{\partial z^2}\right) \tag{3.2}$$

where t is time. Expressions (3.1) and (3.2) are usually referred to as Fick's first and second laws of diffusion respectively, since they were first formulated by Fick [85] through direct analogy with the equations of heat conduction. If the diffusion coefficient (*D)* is time dependent, then on introducing a new time-scale T such that [84]:

$$dT = D(t)dt \tag{3.3}$$

the diffusion equation becomes:

$$\frac{\partial C}{\partial T} = \frac{\partial^2 C}{\partial x^2} + \frac{\partial^2 C}{\partial y^2} + \frac{\partial^2 C}{\partial z^2} \tag{3.4}$$

For diffusion in a sphere, Equation (3.4) can be expressed in spherical polar coordinates as [84]:

$$\frac{\partial C}{\partial T} = \frac{1}{r^2}\{\frac{\partial}{\partial r}(r^2 \frac{\partial C}{\partial r}) + \frac{1}{\sin\theta}\frac{\partial}{\partial \theta}(\sin\theta \frac{\partial C}{\partial \theta}) + \frac{1}{\sin^2\theta}\frac{\partial^2 C}{\partial \phi^2}\} \tag{3.5}$$

The simplified form of Equation (3.5) for purely radial diffusion in a spherically symmetrical system can be expressed as:

$$\frac{\partial C}{\partial T} = \frac{1}{r^2}\left\{\frac{\partial}{\partial r}(r^2 \frac{\partial C}{\partial r})\right\} \tag{3.6}$$

Solving the above equation for a sphere of specified diameter d_m and radius R having a surface concentration maintained at zero (sink condition), and an initial uniform concentration, C_1 [84]:

$$C(r = R, t > 0) = 0 \; ; \; C(r, t = 0) = C_1$$

results in the following solution [84]:

$$\frac{C_1 - C}{C_1} = 1 + \frac{2R}{\pi r} \sum_{j=1}^{\infty} \frac{(-1)^j}{j} \sin \frac{j \pi r}{R} e^{-j^2 \pi^2 T / R^2} \qquad \textbf{(3.7)}$$

The total amount of drug released from the sphere per unit time can be determined by evaluating Fick's first law of diffusion (Equation (3.1) in polar coordinates) at the surface of the sphere ($r = R$), using equation 3.7. After integration and further mathematical manipulation, the following equation is obtained for the total amount of diffusing drug leaving a sphere of diameter d_m [84]:

$$\left(\frac{M_t}{M_\infty}\right)_{d_m} = \left(1 - \frac{6}{\pi^2} \sum_{j=1}^{\infty} \frac{1}{j^2} e^{-j^2 \pi^2 T / \left(\frac{d_m}{2}\right)^2}\right) \qquad \textbf{(3.8)}$$

$$T = \int_0^t D(t) dt$$

where $(\frac{M_t}{M_\infty})_{d_m}$ is the cumulative fraction of drug released from a sphere of diameter d_m, at time t.

The drug diffusion coefficient is time dependent due to bulk degradation of the polymer matrix. As the polymer molecular weight (M_w) decreases, the drug has more available space to diffuse through the polymer chains, and so the diffusion coefficient increases. The dependence of diffusion coefficient of piroxicam on PLG molecular weight was investigated by Raman et al. [79], and an empirical mathematical equation was obtained to represent this dependence:

$$\ln(D) = -0.347x^3 + 10.394x^2 - 104.95x + 316.95 \quad \textbf{(3.9)}$$

where $x = ln(M_w)$. Initial drug burst release is well documented in the literature, and has been attributed to a variety of physical, chemical, and processing parameters, but for the most part, the underlying mechanism is not clearly understood [87]. To account for this initial burst release, an initial diffusivity (D_0) is used as a fitting parameter. D_0 is used until the time dependent diffusivity $D(M_w)$ is larger than D_0.

Hydrolysis, which causes bulk degradation of PLG polymer, starts with water uptake. The first stage of the process is confined to a decrease in the molecular weight caused by random hydrolytic ester cleavage, while the second stage is characterized by the onset of weight loss. The first stage of the degradation process is expressed as [13]:

$$M_w(t) = M_w(0) \cdot \exp(-k_{\deg} t) \quad \textbf{(3.10)}$$

where $Mw(t)$ is the molecular weight of the polymer at time t, $Mw(0)$ is the molecular weight of the polymer at time $t = 0$, and k_{deg} is the polymer degradation constant. The rate of polymer degradation, represented by the degradation constant (k_{deg}), is dependent on the hydrolysis mechanism taking place. PLG degradation has been widely investigated [24,79,88-91], and values for k_{deg} reported in the literature range from 0.0638 d^{-1} to 0.104 d^{-1}. Other degradation studies performed on PLG microspheres have shown dependence of polymer degradation constant (k_{deg}) on microsphere diameter [78]. It is believed that large microspheres degrade more quickly than small microspheres because of an increased buildup of the acidic byproducts of polymer hydrolysis in large microspheres [78]. In addition, drug release can occur by diffusion through pores formed as a result of polymer erosion which results in higher effective diffusivities than those predicted solely by polymer bulk degradation. In this work the degradation constant, k_{deg}, is used as a fitting parameter, and the obtained values are compared with the reported data in the literature.

3.3.1. Modeling Size Distribution

This work considers the release from a microsphere population of non-uniform size distribution. The non-dimensional cumulative mass release equation for a polydisperse microsphere population can be expressed as:

$$\frac{M_t}{M_\infty} = \int_{d_{\min}}^{d_{\max}} g(d_m)(\frac{M_t}{M_\infty})_{d_m} dd_m \quad \textbf{(3.11)}$$

where $\frac{M_t}{M_\infty}$ is the cumulative fraction of drug released from the population at time *t*, d_{min} and d_{max} are the diameters of the smallest and largest microspheres in the population respectively, $g(d_m)$ represents the size distribution of the population, and $(\frac{M_t}{M_\infty})_{d_m}$ is the cumulative fraction of drug released from a sphere of diameter d_m, at time t, evaluated using Equation (3.8). When characterizing microspheres for drug release studies, the mass fraction size distribution is used which represents the mass of microspheres in a specific size interval divided by the total mass of the population and the length of the size interval. Since the density of the microspheres is not a function of microsphere size, the mass fraction size distribution and the volume fraction size distribution are equivalent, and are thus used interchangeably. It was shown in previous work by Berchane et al. [80] that the Rosin-Rammler mathematical distribution function provides an accurate representation of the size distributions of PLG microspheres prepared using our experimental set-up. For constant drug loading throughout the entire population (Table 3.1), the Rosin-Rammler function also represents the drug mass distribution for the population. The Rosin-Rammler distribution function can be expressed in the following form [74,80]:

$$\left(\frac{1}{M_\infty}\frac{dM}{dd_m}\right) = g(d_m) = \frac{b}{a}\left(\frac{d_m}{a}\right)^{b-1}\exp\left(-\left(\frac{d_m}{a}\right)^b\right) \quad \textbf{(3.12)}$$

where d_m is the microsphere diameter, a and b are constants to be obtained from a least squares fit to the experimentally measured size distributions of PLG microspheres.

Alternatively, the microsphere population size distribution can be accounted for in the mathematical model using the representative mean diameter, and then Equation (3.11) is reduced to Equation (3.8). In this work the mean diameter calculated is the mass/volume moment mean diameter (d_{43}), also known as De Brouckere mean diameter, which is the center of gravity of the mass/volume fraction size distribution.

3.3.2. Numerical Solution of Model Equations

A Matlab program was written to implement the mathematical theory developed in this Section. To determine the accuracy in approximating the infinite series in Equation (3.8), we use the concept of remainder [92]:

$$S = S_J + R_J \quad \textbf{(3.13 a)}$$

$$S = \sum_{j=1}^{j=\infty} a_j \quad \textbf{(3.13 b)}$$

$$S_J = \sum_{j=1}^{j=J} a_j \quad \textbf{(3.13 c)}$$

$$R_J = \sum_{j=J}^{j=\infty} a_j \quad \textbf{(3.13 d)}$$

$$a_j = \frac{6}{\pi^2}\frac{1}{j^2}e^{(-j^2\pi^2 T/(\frac{d_m}{2})^2)} \qquad \textbf{(3.13 e)}$$

where a_j represent the terms of the infinite series, S is the exact value of the series, S_J is the approximate value of the series using its first J terms, and R_J is the remainder. Inspection of Equation (3.13 e) reveals that the terms of the infinite series have the largest values at $T = 0$ when the decaying exponential term is equal to unity. As a consequence, the largest value of R_J occurs at $T = 0$:

$$R_J < R_J\big|_{T=0} = \frac{6}{\pi^2}\sum_{j=J}^{\infty}\frac{1}{j^2} \qquad \textbf{(3.14)}$$

A series of the form $\sum_{j=1}^{j=\infty}\frac{1}{j^p}$ is called a p-series and has a remainder $R_J < \frac{J^{1-p}}{p-1}$, which reduces to $R_J < \frac{1}{J}$ for $p = 2$ [92]. Then the infinite series in Equation (3.13) has a remainder $R_J < \frac{6}{\pi^2 J}$, and Figure 3.1 plots the maximum value of R_J as a function of J. Here we use the hundredth partial sum to approximate the infinite series which results in $R_J < 0.006$.

The integral in Equation (3.8) was evaluated numerically over the interval [0,t]. This is achieved by dividing the interval [0,t] into n uniformly spaced subintervals of length h ($h = t/n$), and then sampling with a set of discrete points $\{t_0, t_1, \ldots, t_n\}$ where $t_0 = 0$, and

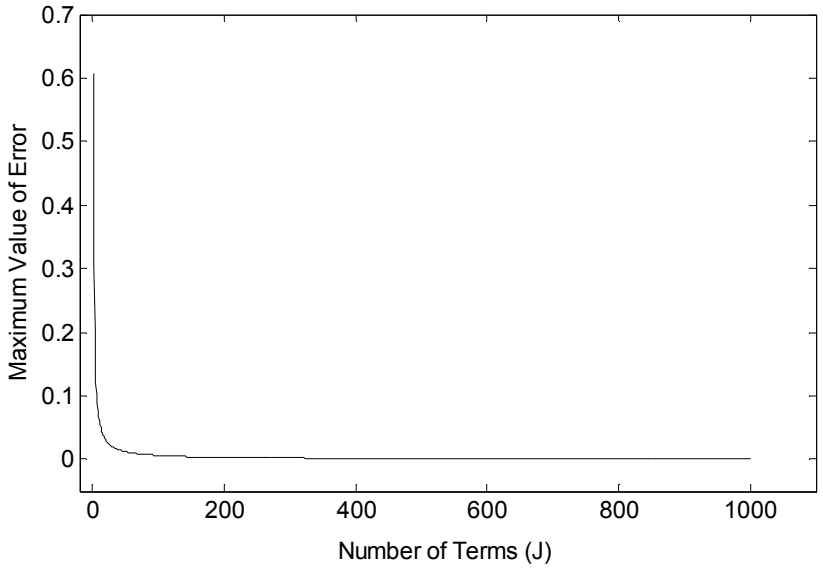

Figure 3.1 Maximum error in approximating the infinite series by its fist *J* terms.

$t_n = t$. The trapezoid rule was then used, which estimates the area beneath the curve using trapezoids [93]:

$$T(t) = \frac{h}{2}(D(t_0) + 2D(t_1) + ... + 2D(t_{n-1}) + D(t_n)) \quad \textbf{(3.15)}$$

Since the trapezoids only approximate the integrand $D(t)$, there is a truncation error which decreases as the step length (h) decreases [93]:

$$Error = \frac{1}{12} t h^2 \overline{D''} \quad \textbf{(3.16)}$$

where t is time, h is the step length, and $\overline{D''}$ represents the average value of the second derivative of $D(t)$ over the n intervals. The largest error in approximating the integral occurs at late time when the value of $\overline{D''}$ exhibits a sharp increase. In this work a step length of 1 hr was used for evaluating the integral in Equation (3.8), which results in a maximum error < 1% when determining $T(t)$.

3.4. Results and Discussion

3.4.1. Microsphere Fabrication and Characterization

To investigate the effect of microsphere size on drug release rate, three batches of PLG microspheres were prepared at different impeller speeds (140, 300, and 900 rpm).

A portion of the microspheres was removed from each batch, and then the different portions were added together and sieved which resulted in five different size fractions (0.2 – 20; 20 – 40; 40 – 63; 63 – 90; and >90 μm). SEM micrographs of the sieved and raw microspheres are shown in Figure 3.2 and Figure 3.3 respectively. The volume fraction size distribution is used when characterizing microspheres for drug release studies. This size distribution represents the mass of microspheres in a specific size interval divided by the total mass of the population and the length of the size interval. Figure 3.4 and Figure 3.5 show the corresponding volume fraction distributions, plotted against the diameter of PLG microspheres. From inspection of the micrographs in Figure 3.2 and Figure 3.3, it is apparent that the microspheres appear rigid and nicely spherical with a smooth surface. It is also evident from the micrographs and the size distributions that the majority of the fractionated microspheres lie within the mean pore diameter of the sieves used, except for some very small microspheres trapped with the large microspheres (Figure 3.2, and Figure 3.4). Although these small microspheres are large in number (as can be seen from the micrographs), the size distributions show that their volume fraction is negligible and as a result does not have an effect on the release profile.

The Rosin-Rammler Distribution function was shown by Berchane et al. [80] to give the best representation of the volume fraction experimental data. This function is expressed in the following form [74]:

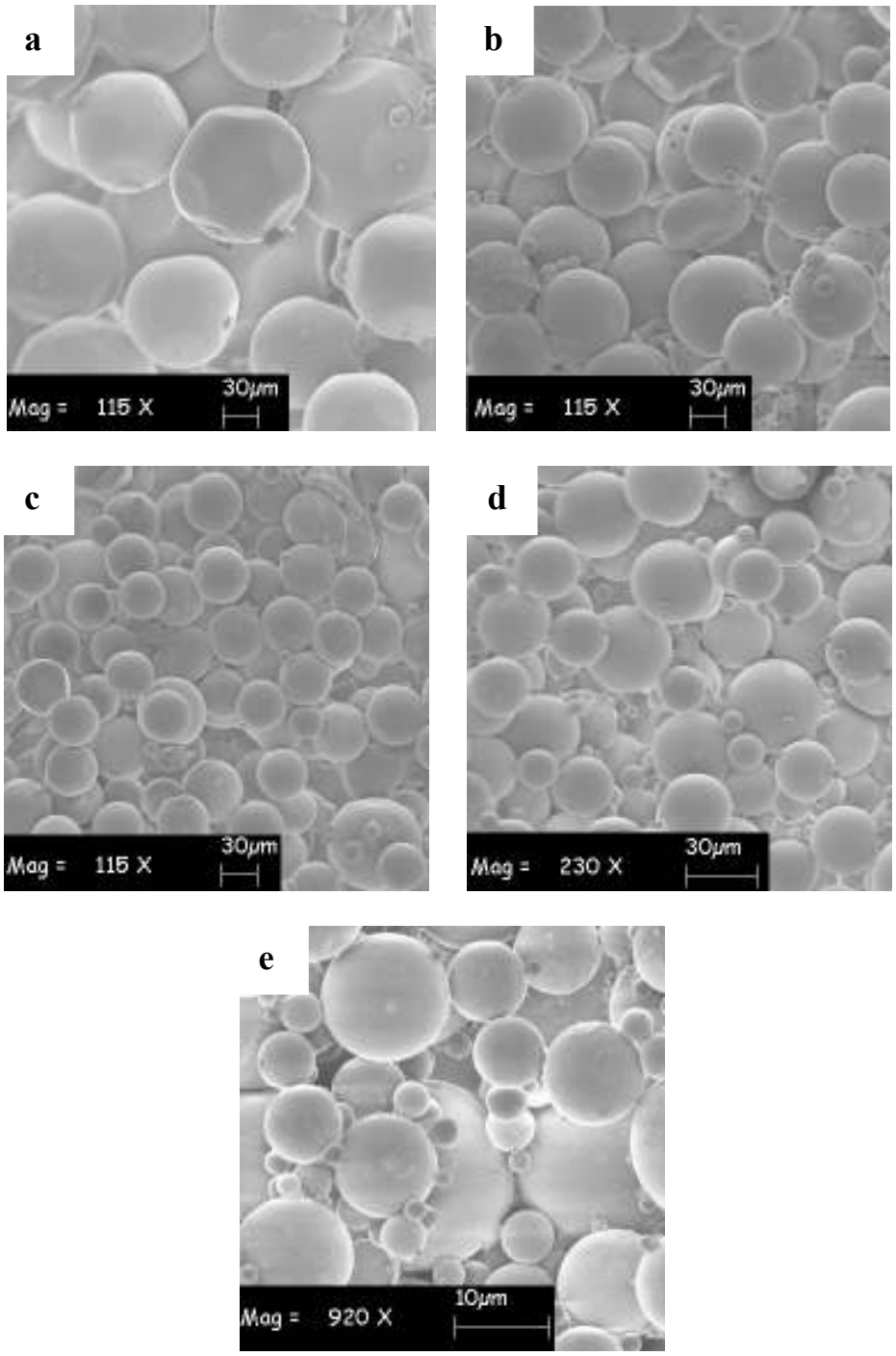

Figure 3.2 SEM micrographs of sieved piroxicam loaded PLG microspheres: (a) > 90 µm, (b) 63 – 90 µm, (c) 40 – 63 µm, (d) 20 – 40 µm, and (e) 0.2 – 20 µm.

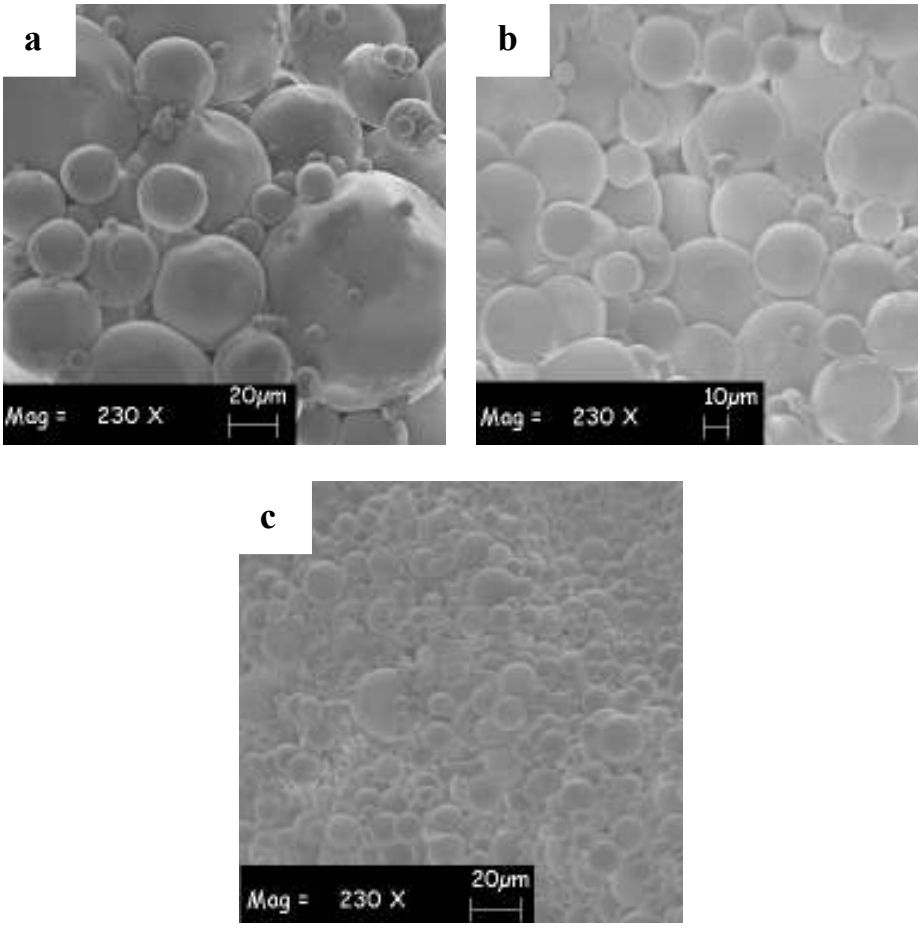

Figure 3.3 SEM micrographs of raw piroxicam loaded PLG microspheres: (a) *N* = 140 rpm, (b) *N* = 300 rpm, and (c) *N* = 900 rpm.

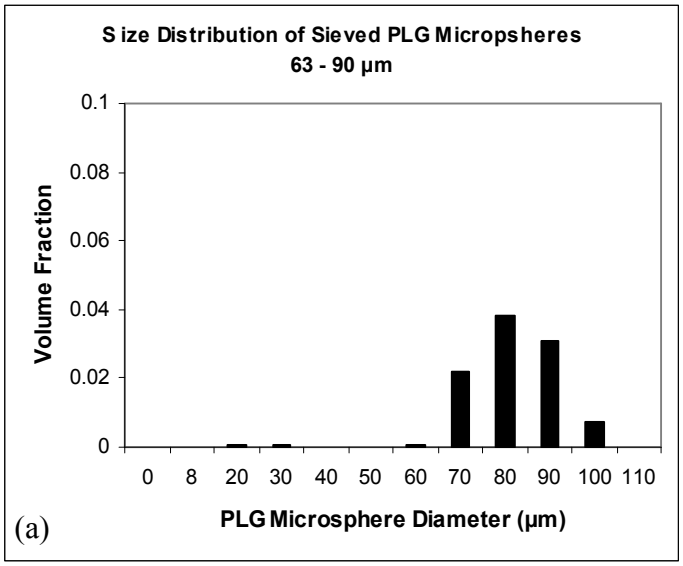

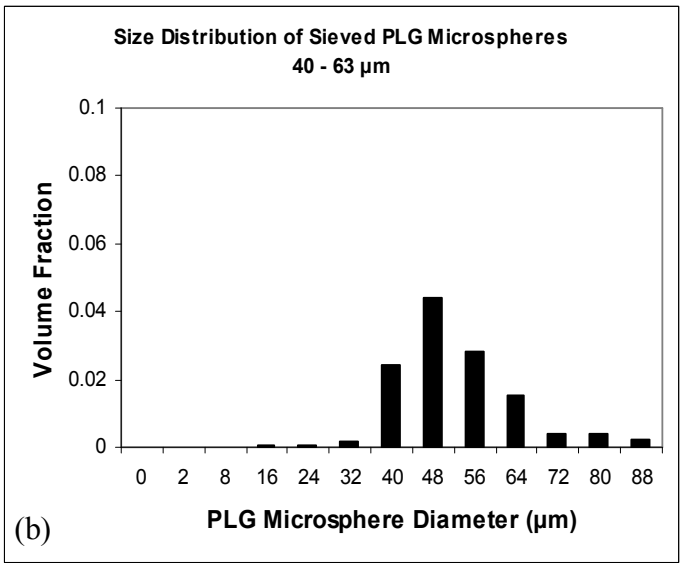

Figure 3.4 Volume fraction distributions of sieved piroxicam loaded PLG microspheres: (a) 63 – 90 µm, (b) 40 – 63 µm, (c) 20 – 40 µm, and (d) 0.2 – 20 µm.

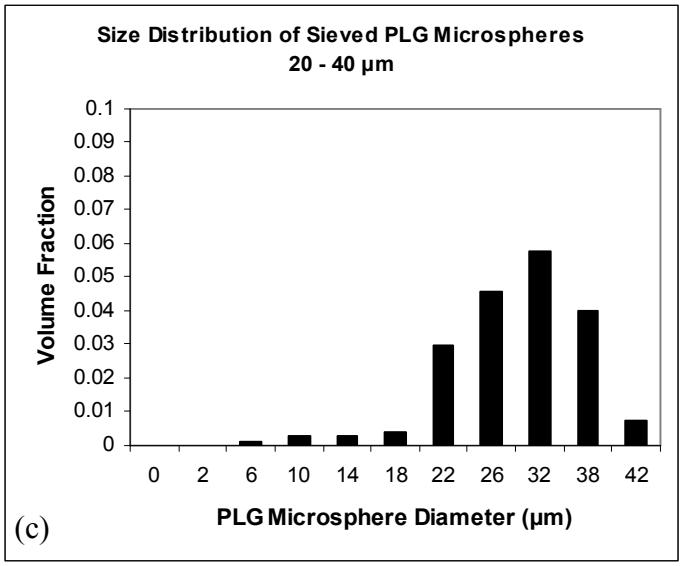

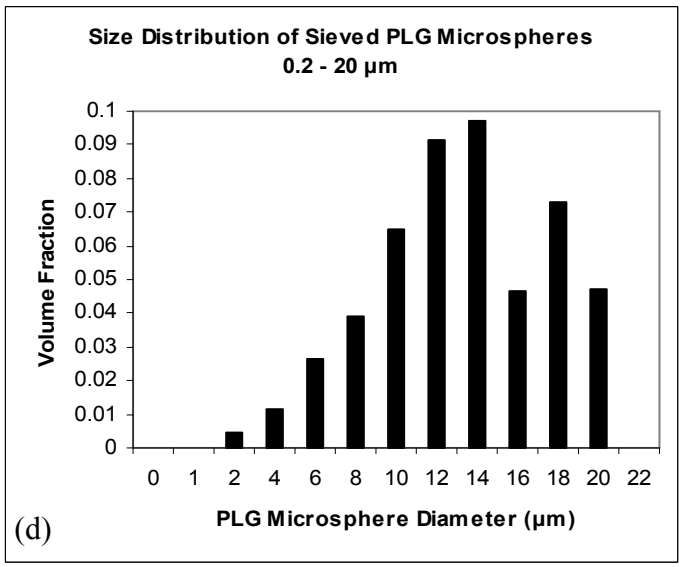

Figure 3.4 Continued

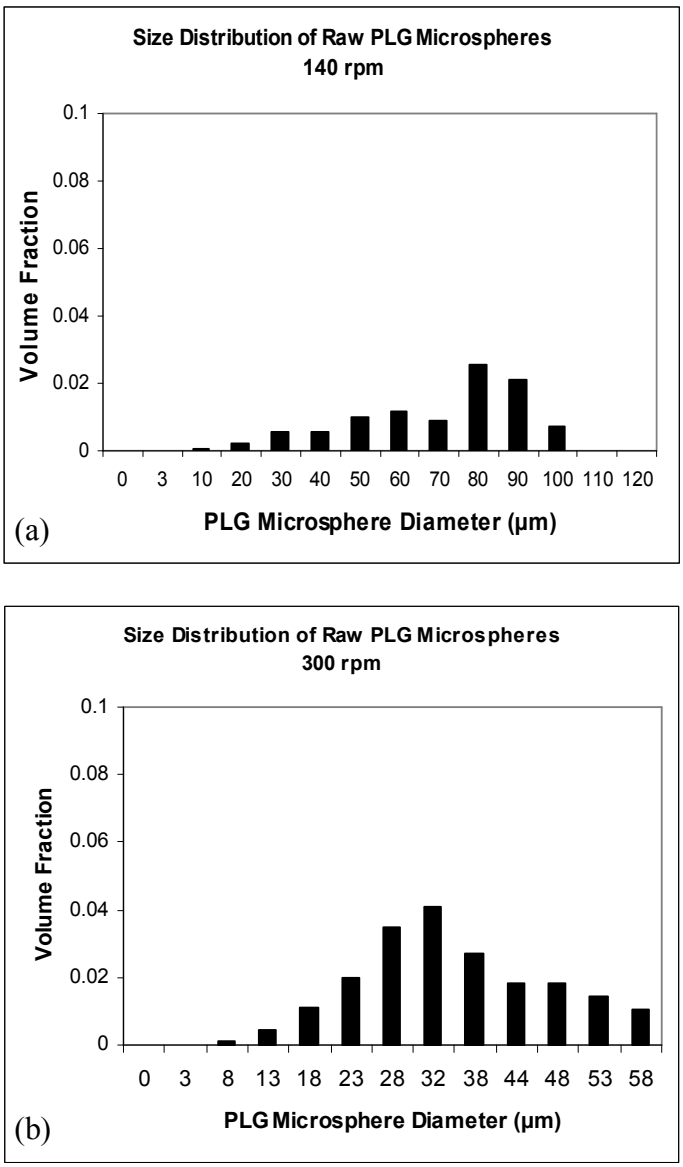

Figure 3.5 Volume fraction distributions of raw piroxicam loaded PLG microspheres: (a) N = 140 rpm, (b) N = 300 rpm, and (c) N = 900 rpm.

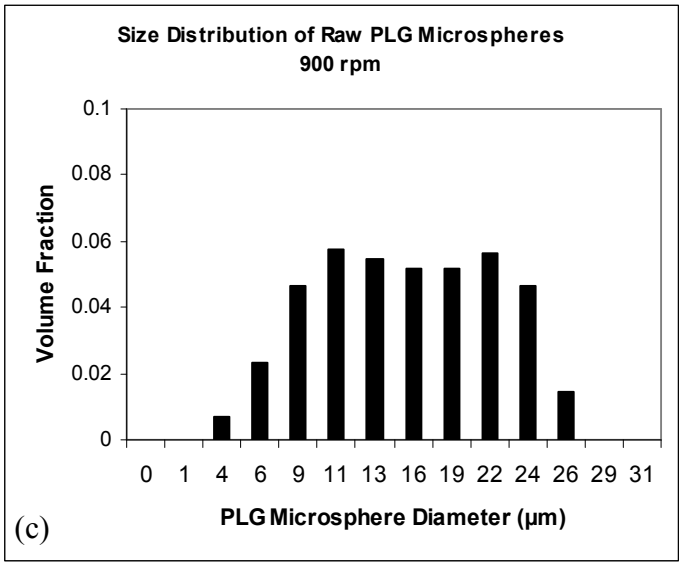

Figure 3.5 Continued

$$(\frac{1}{V_{tot}})\frac{dV}{dd_m} = f_V(d_m) = \frac{b}{a}(\frac{d_m}{a})^{(b-1)}\exp(-(\frac{d_m}{a})^b) \quad \textbf{(3.17)}$$

where V_{tot} is the total volume of the microsphere population, d_m is the microsphere diameter. The Rosin-Rammler relationship describes microsphere size distribution in terms of the parameters a and b, where a provides a measure of the distribution mean diameter, while b provides a measure of the spread of the microsphere sizes. If b is infinite, the microspheres are all of the same size, and as the value of b decreases, the spread of the microspheres increases [74]. Integration of the volume fraction distribution function (Equation (3.17)) yields the cumulative volume distribution function expressed as:

$$\frac{V}{V_{tot}} = F_V(d_m) = 1 - \exp(-(\frac{d_m}{a})^b) \quad \textbf{(3.18)}$$

where V is total volume contained in microspheres of diameter less than d_m. The parameters a and b are obtained from a least squares fit of the Rosin-Rammler cumulative volume distribution function (Equation (3.18)) to the experimental cumulative volume fraction distributions (Figure 3.6). The values for a and b are given in Table 3.1. The parameter b, which provides a measure of polydispersity, ranges from 2.7 to 3.78 for raw populations and from 3.17 to 9.7 for sieved populations (Table 3.1).

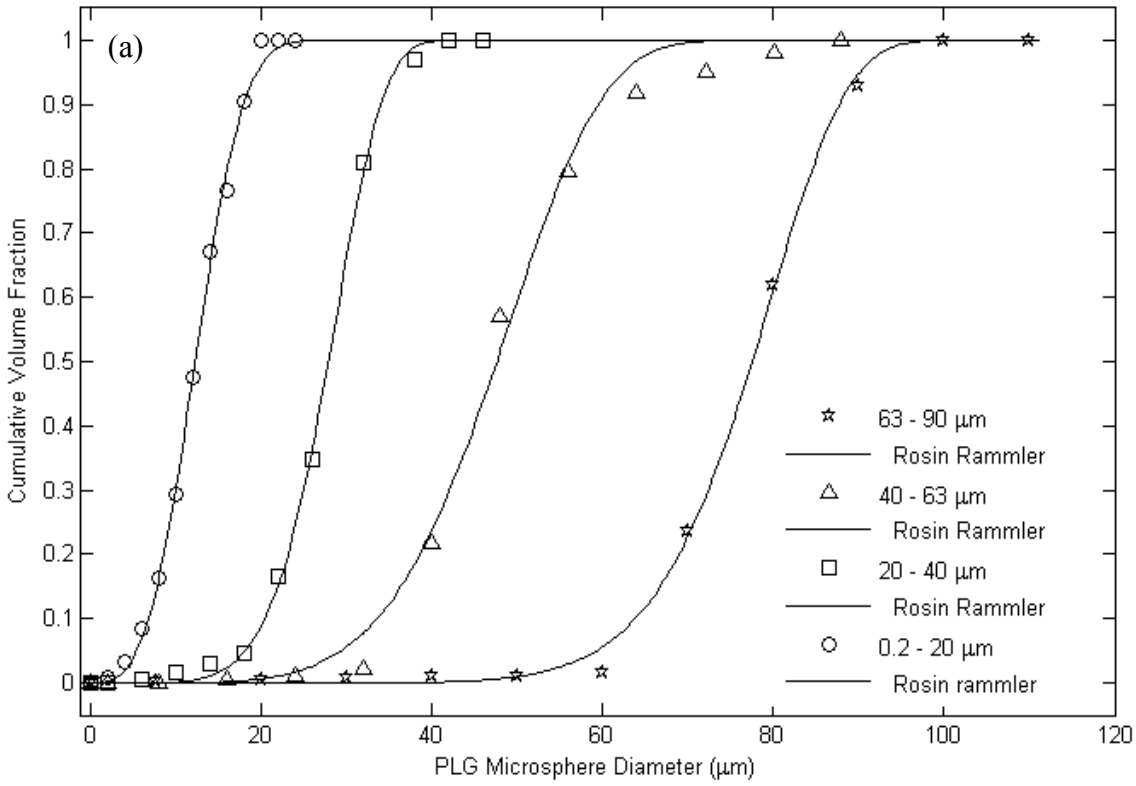

Figure 3.6 Cumulative volume fraction distributions of (a) sieved and (b) raw, piroxicam loaded PLG microspheres.

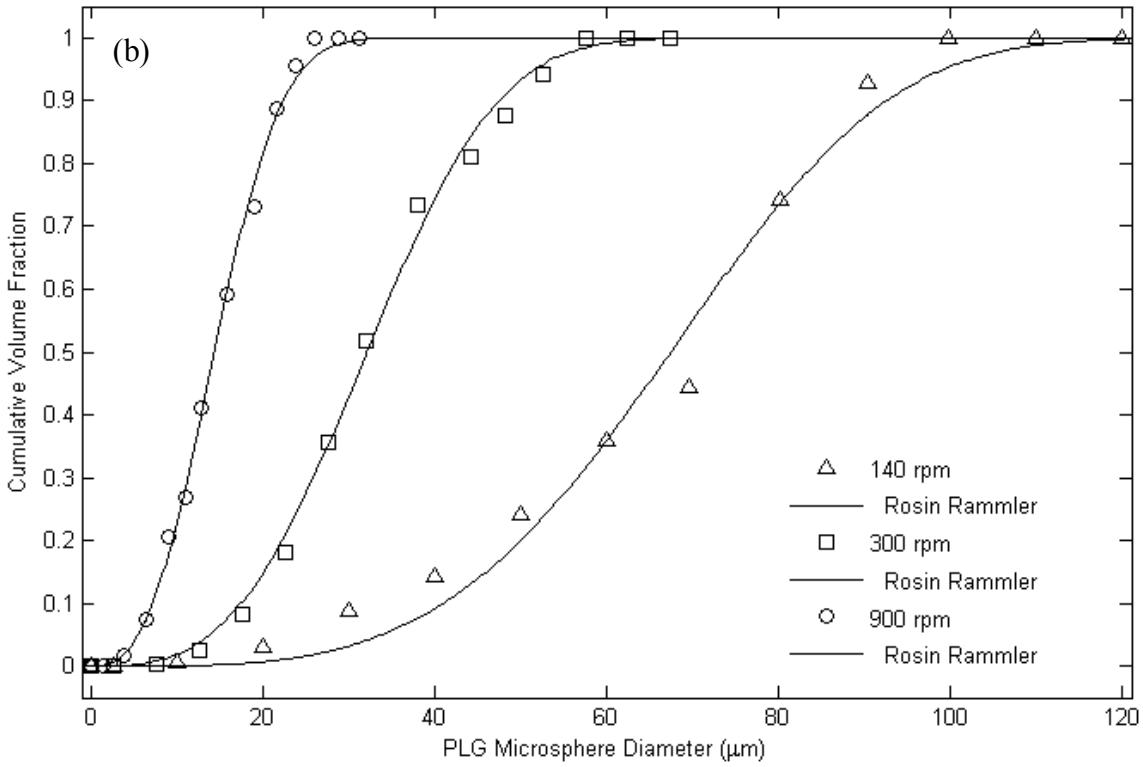

Figure 3.6 Continued

This shows that sieving was effective in reducing the polydispersity of the microsphere populations, and is important because one of the objectives of this work was to fabricate microsphere populations of varying polydispersity to investigate the effect of polydispersity on drug release rate.

3.4.2. *In Vitro* Drug Release Kinetics

Figure 3.7 shows experimentally measured *in vitro* release of sieved piroxicam loaded PLG microspheres having different size fractions. The release profiles shown in the figures are normalized to the total amount of drug released at the end of the study, which was within 10% of the experimental loading shown in Table 3.1. The mean diameters (d_{43}) of the microspheres range from 13.9 to 81.2 μm (Table 3.1). Inspection of Figure 3.7 reveals that size is a major determinant of the release profile, and drug initial release rate decreased with increasing microsphere size. This is consistent with Fick's law of diffusion which attributes this decrease in drug release rate to an increase of diffusion pathways (reduced surface area to volume ratio for large spheres). In addition, microsphere populations having a mean diameter of 29.6 μm and above exhibit concave-upward (i.e sigmoidal) profile, with a high initial rate of drug release ("burst release") which then slows down before it progresses again into a more rapid release phase before leveling off. This sigmoidal profile is most obvious for populations with large mean diameters (d_{43} > 51.0, Figure 3.7 (a)-(c)), and to a lesser extent in the 29.6 μm mean diameter population (Figure 3.7 (d)), which exhibits a near constant release

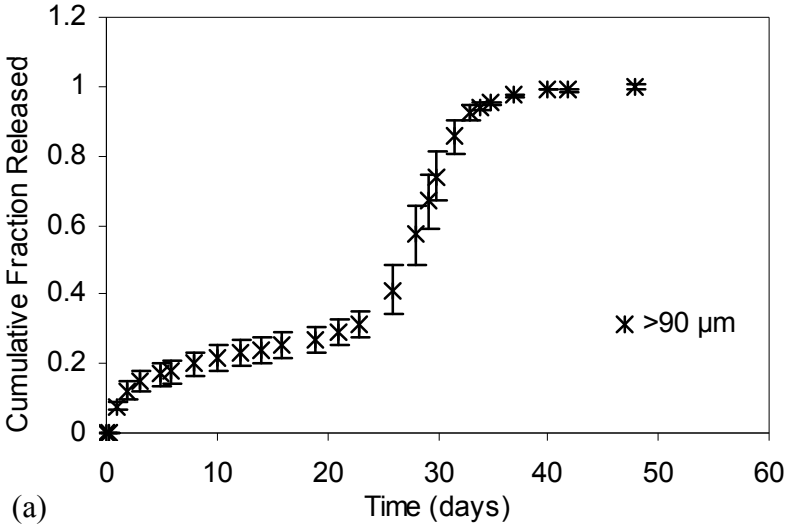

(a)

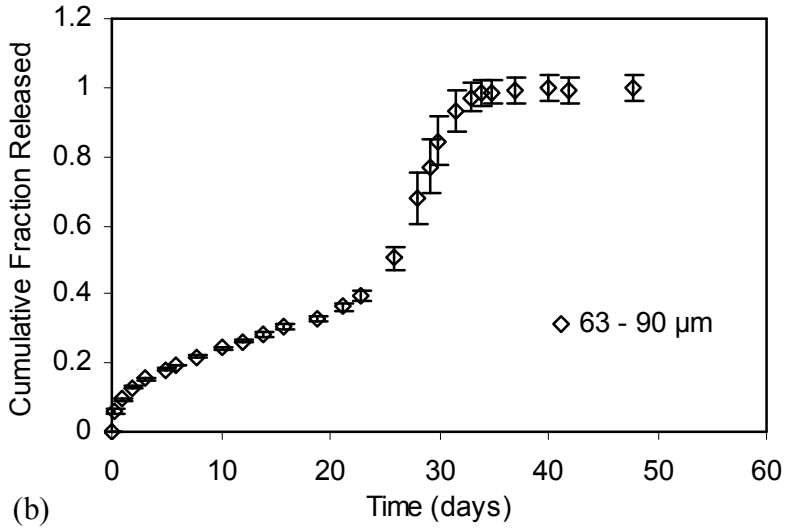

(b)

Figure 3.7 Experimental drug release profile of sieved PLG microspheres: (a) > 90 µm, (b) 63 – 90 µm, (c) 40 – 63 µm, (d) 20 – 40 µm, and (e) 0.2 – 20 µm.

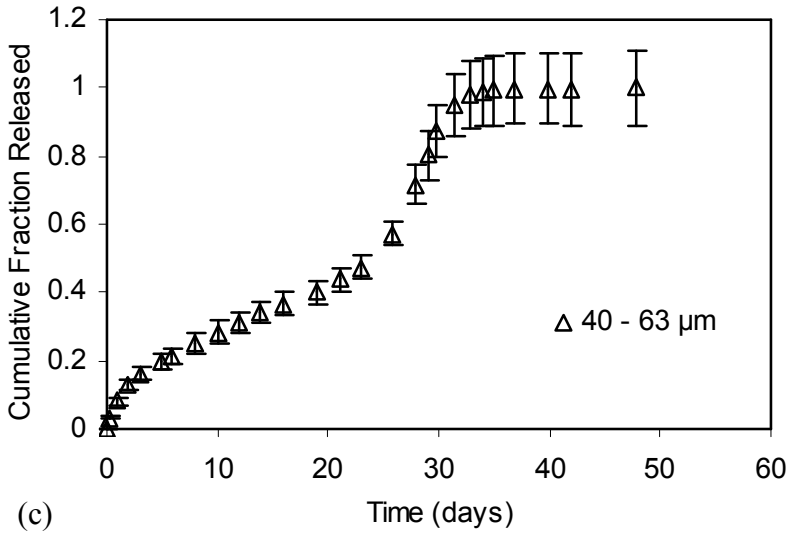

(c)

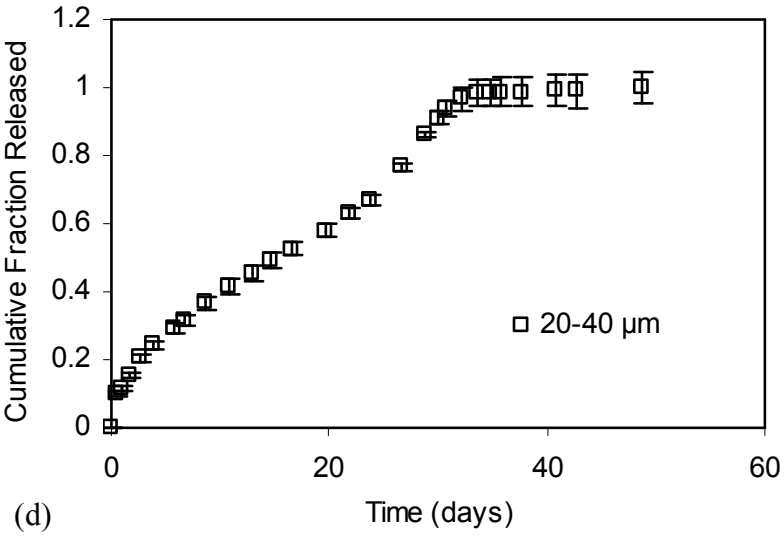

(d)

Figure 3.7 Continued

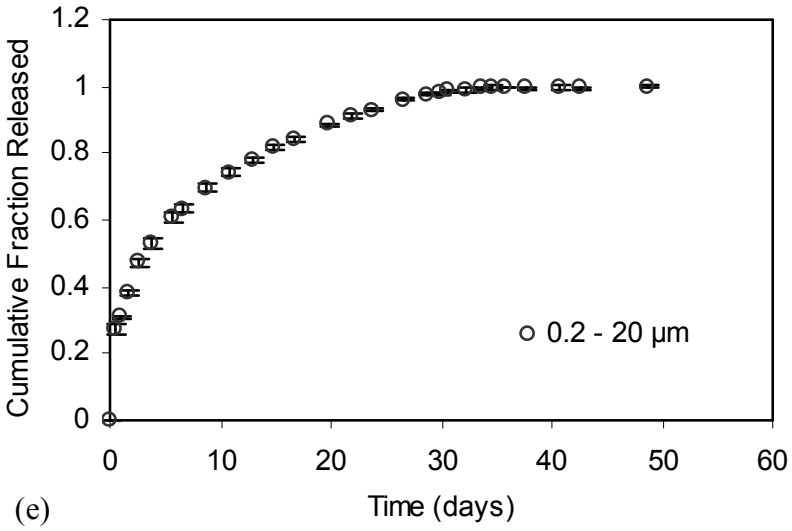

(e)

Figure 3.7 Continued

(near zero-order profile). Although the initial burst release has been reported in numerous publications in our field, knowledge about the underlying mechanism is limited. One potential explanation for this burst release is that some drug becomes trapped on the surface of the polymer matrix during the manufacturing process [87]. The sigmoidal shape is believed to be a result of polymer degradation. As the polymer degrades, its molecular weight decreases, which causes an increase of the diffusion coefficient of the drug through the polymer matrix. This is translated into an increase in the drug release rate which gives rise to the sigmoidal profile. The 13.9 μm population (our smallest), and contrary to the other populations, exhibits first order release (Figure 3.7 (e)). It is believed that this is a result of the rapid initial rate of release with ~ 50% of encapsulated drug released within the first 3 days, during which polymer degradation effects are still negligible. In addition, polymer degradation proceeds at a slower rate for smaller microspheres [78].

Figure 3.8 shows the release from raw microsphere populations prepared at 3 different speeds (140, 300, 900 rpm). The mean diameters of the microspheres range from 13.5 to 76 μm (Table 3.1). The drug release profiles from raw populations exhibit the same behavior as those from sieved populations having comparable mean diameters. Microspheres prepared at 140, and 300 rpm (having mean diameters of 76.0 and 33.5 μm respectively) have concave- upward (i.e. sigmoidal) profile, while microspheres prepared at 900 rpm (13.5 μm mean diameter) exhibit first order release.

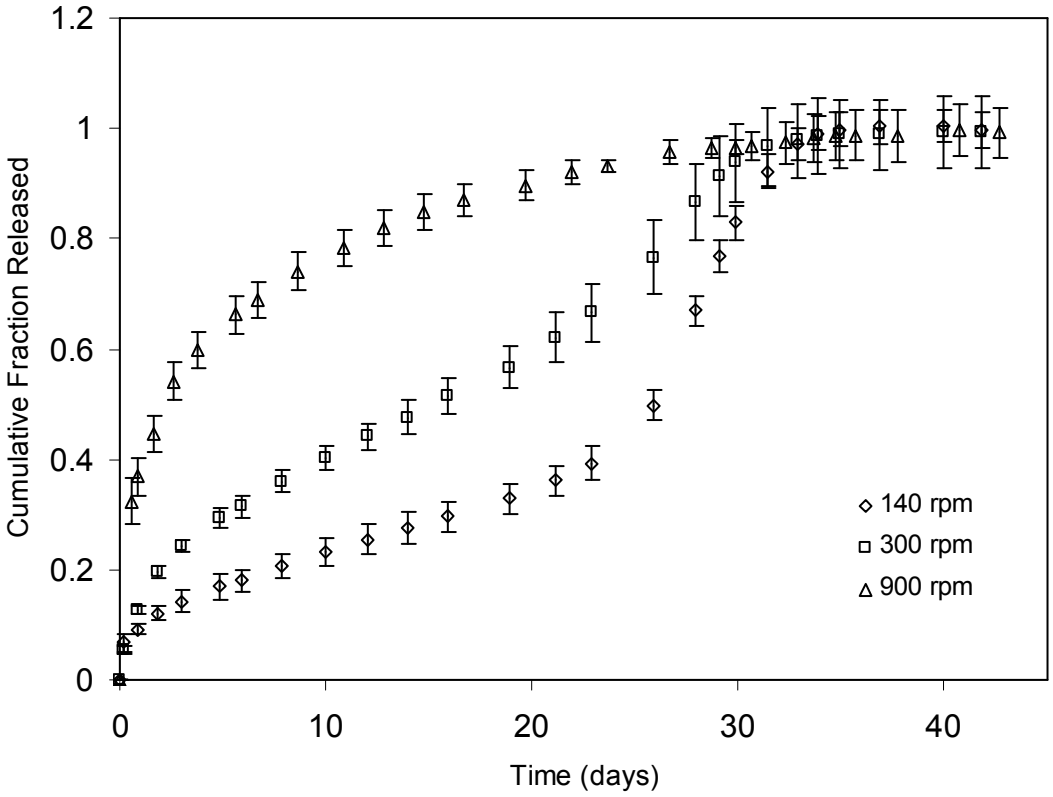

Figure 3.8 Effect of microsphere size on piroxicam release for raw microspheres.

3.4.3. Model Results

A Matlab program was written to solve the derived cumulative release equations (Equations (3.8) and (3.11)), with a time dependent diffusivity and two fitting parameters (D_0 and k_{deg}), to predict the release of piroxicam from PLG microspheres having different mean diameters and size distributions. Dependence of diffusivity on molecular weight was modeled using Equation (3.9). To account for the initial burst release, an initial diffusivity (D_0) is used as a fitting parameter. D_0 is used until the time dependent diffusivity $D(M_w)$ is larger than D_0.

Since the molecular weight of PLG polymer varies with time, it was modeled using Equation (3.10). The rate of polymer degradation, represented by the degradation constant (k_{deg}), is dependent on the hydrolysis mechanism taking place. PLG degradation has been widely investigated [24,79,88-91], and reported values for k_{deg} range from 0.0638 d^{-1} to 0.104 d^{-1}. Here k_{deg} is used as a fitting parameter, and the obtained values are compared with the reported data in the literature.

Size distribution of the microspheres was represented in the mathematical model in two different approaches to investigate the use of the population size distribution model, and the alternative mean diameter model. For accurate modeling of the drug release profile, the size distribution of the populations was incorporated into the model, and Equation (3.11) was solved. Alternatively, Equation (3.8) was solved which utilizes the volume moment mean diameter to represent the size distribution of the population. As mentioned previously, the volume moment mean diameter is the center of gravity of the volume fraction size distribution. The aim was to investigate the effect of polydispersity

on drug release rate. Figure 3.9 and Figure 3.10 show the release profiles generated by the model compared with the experimental drug release data for sieved and raw microsphere populations respectively. The solid lines represent modeling results based on size distribution, while dashed lines represent modeling results based on mean diameter. It is evident from Figure 3.9 and Figure 3.10 that the model based on size distribution is in good agreement with all the experimental results, and that the deviation of the mean diameter based model from experimental results increases as the polydispersity of the population increases. Here we use the value of the parameter *b* (Table 3.1), obtained by curve fitting the cumulative Rosin-Rammler function to the experimental cumulative volume fraction distributions, to represent the degree of polydispersity of the populations. For populations having a value of *b* close to or less than 3.0 (0.2 -20 μm, 300, and 900 rpm in Table 3.1), the deviation is considerable (Figure 3.9 (d), Figure 3.10 (b),(c)), $R^2 < 0.974$). Alternatively, populations that have a value of *b* equal to 3.78 and above (20 – 40, 40 – 63 and 63 – 90 μm, 140 rpm, in Table 3.1), the deviation is negligible (Figure 3.9 (a-c) Figure 3.10 (a), $R^2 > 0.994$). Thus, for populations having a value of *b* value ~ 3, the effect of polydispersity on drug release is significant, and as a result incorporating the size distribution of the population into the model is necessary to provide an adequate fit for practical use. Consequently, it is recommended that the size distribution be incorporated into the model, when working with populations which have a value of *b* equal to or less than 3.

From Figure 3.9 and Figure 3.10, it can be observed that the degradation constant (k_{deg}), obtained by curve fitting, increased from 0.07 d^{-1} for the microsphere population

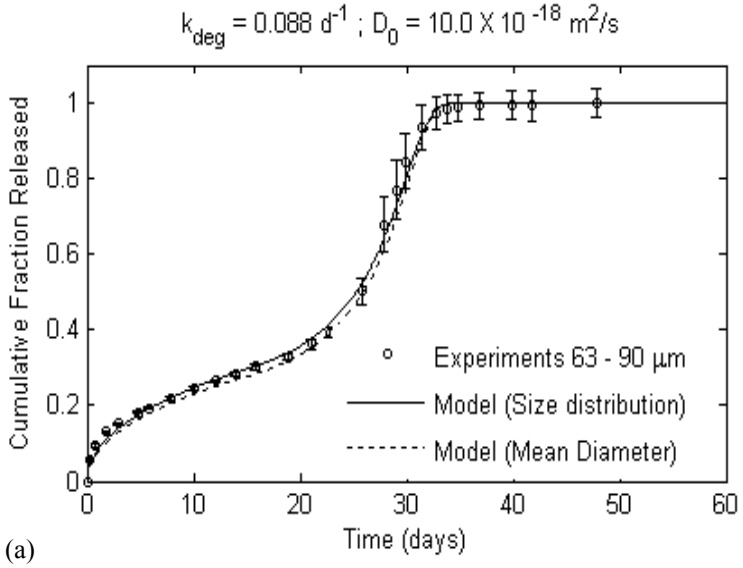

(a)

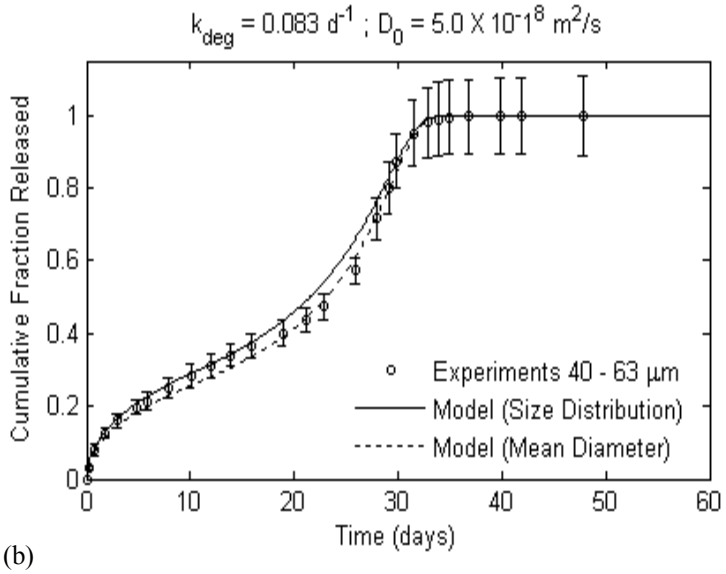

(b)

Figure 3.9 Comparison of model profiles to experimental results of sieved piroxicam loaded PLG microspheres: (a) 63 – 90 µm, (b) 40 – 63 µm, (c) 20 – 40 µm, and (d) 0.2 – 20 µm.

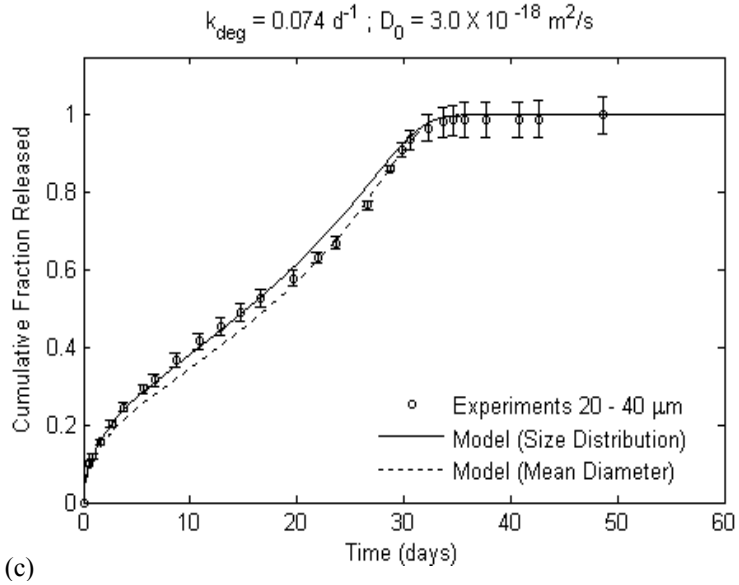

(c)

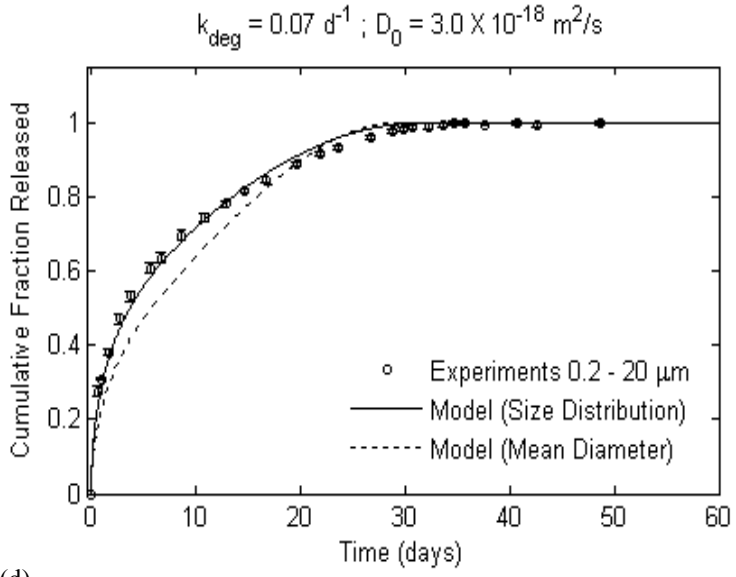

(d)

Figure 3.9 Continued

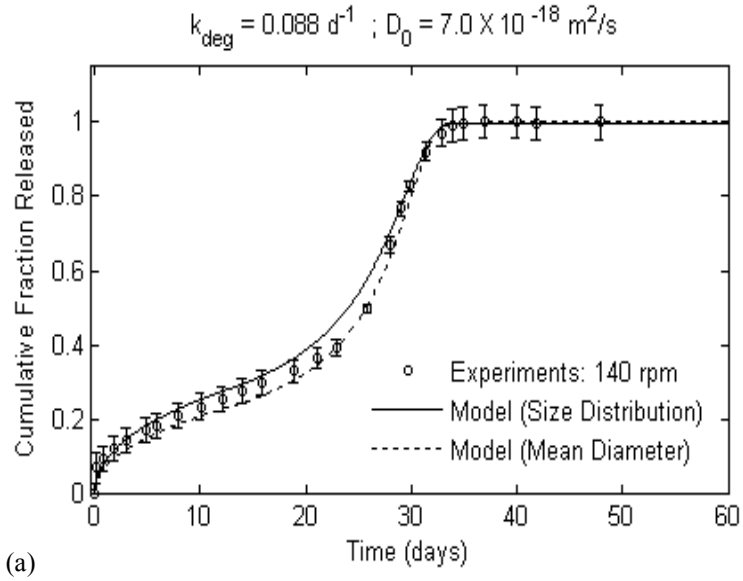

(a)

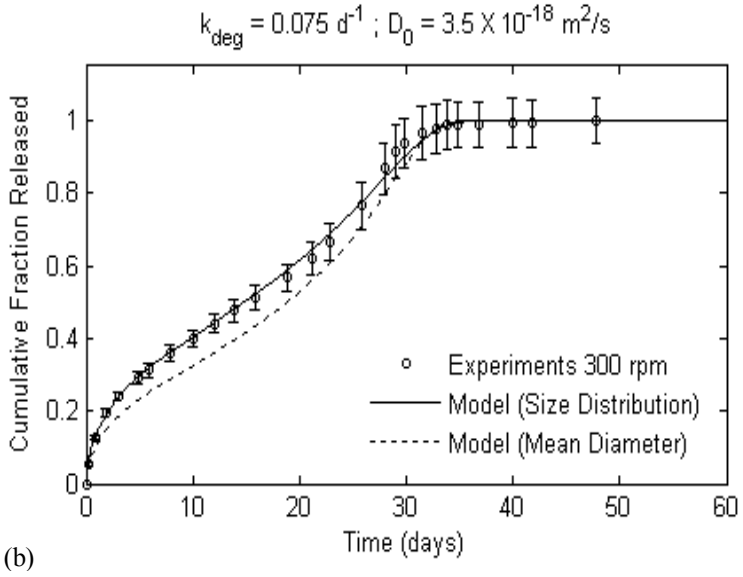

(b)

Figure 3.10 Comparison of model profiles to experimental results of raw piroxicam loaded PLG microspheres: (a) *N* = 140 rpm, (b) *N* = 300 rpm, and (c) *N* = 900 rpm.

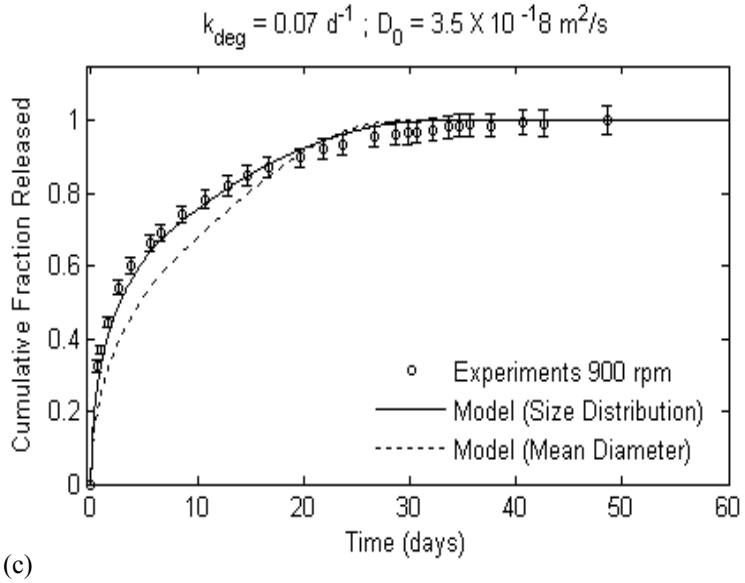

(c)

Figure 3.10 Continued

having a mean diameter of 13.5 μm (900 rpm population, Figure 3.10 (c)) to 0.088 d^{-1} for the microsphere population having a mean diameter of 81.2 μm (63 – 90 μm population, Figure 3.9 (a)). This is consistent with published work which report that large microspheres degrade faster than small microspheres because of an increased buildup of acidic byproducts [78]. In addition, the values for k_{deg} obtained in this work are in good agreement with data reported in the literature which range between 0.0638 d^{-1} and 0.104 d^{-1} [24,79,88-91].

It has been previously mentioned that an initial diffusivity (D_0) is used in this work to account for the initial drug burst release. Although this burst release is well documented in the literature, the underlying mechanism is not clearly understood [87]. It has been hypothesized that polydispersity is one of the main causes for the initial drug burst release, due to the presence of small microspheres which encapsulate sufficient amount of drug that is released more rapidly [78]. Here we investigate this hypothesis by considering the release from the 63-90 μm sieved population (Figure 3.9 (a)). This population has a value of b equal to 9.7 (Table 3.1), which indicates negligible polydispersity effect on drug release. However, by inspecting Figure 3.9 (a), it is observed that this population has high initial rate of drug release with an initial diffusivity (D_0, obtained by curve fitting the size distribution based mathematical model to the experimental results) equal to 10.0×10^{-18} m^2/sec. This value is significantly higher than the time dependent diffusivity, $D(M_w)$, at time $t = 0$ ($D(M_w(0)) = 1.7 \times 10^{-18}$ m^2/sec), which indicates that the diffusion model does not account for this initial burst release. Thus although this population has negligible polydispersity effect, it exhibits an

initial drug burst release that cannot be merely explained by the diffusion model. This leads us to the conclusion that polydispersity is not the main cause for this initial burst release. The same conclusion can be made from recent work published by Raman et al. [79], which investigated drug release rates from monodisperse PLG microspheres. Despite the uniformity of the microsphere populations, a high initial rate of drug release was observed which also cannot be explained by the diffusion model [79]. One potential explanation for the burst effect is that some drug becomes trapped on the surface of the polymer matrix during the manufacturing process [87].

3.5. Conclusions

Piroxicam loaded PLG microspheres have been prepared using an emulsion technique. The effect of microsphere mean diameter, polydispersity, and polymer degradation on drug release rate from the microspheres was investigated. A mathematical model is reported that predicts drug release from polydisperse PLG microspheres. The model accounts for the effects of diffusion, polymer degradation and microsphere size distribution. It was shown that drug initial release rate decreased with an increase in microsphere size. Also, the release profile changed from first order to concave-upward as the microsphere size was increased. Polydispersity did not have a significant effect on drug release rate for populations having a polydispersity parameter (*b)* larger than 3. Alternatively, for distributions having a value of *b* close to or below 3, incorporating the size distribution of the population into the model provided a better fit to the experimental results. In addition it was shown that polydispersity was not the main

cause for the initial “burst” release. The model results were in good agreement with experimental results, and thus can be used to predict drug release from polydisperse populations of microspheres.

4. DESIGNING DRUG RELEASE PROFILES

4.1. Background

Rapid development in the field of molecular biology and biotechnology resulted in generation of numerous new drugs that treat a wide range of indications. The therapeutic potential of these compounds lies in our ability to design and achieve an effective and stable delivery system. The ideal drug release profile is one that initiates the optimum response in a patient such as zero-order release and pulsatile release [5,49-54]. Zero-order release [49-51] is desired for a wide range of drugs because it maintains a constant level of drug concentration well within the therapeutic window for extended time periods. Pulsatile release [5,52-54] is attractive for vaccine delivery, as the drug release formulation can be designed to deliver distinct pulses which solves the need for booster shots. Difficulty in achieving the desired drug release rates (simple zero-order profile or more complex pulsatile release profile), remains to be one of the major challenges in controlled drug delivery. Different parameters have been employed to control the release rate from biodegradable PLG microspheres [10,23,24,79]. In addition to microsphere size [23,24], PLG molecular weight [79] and lactide glycolide ratio [10] play a significant role in controlling drug release kinetics. To gain further control over release rates, some researchers have combined individual microsphere preparations having different release profiles to achieve desired release kinetics [23,49]. Narayani and Rao [49] successfully obtained near constant release of anticancer drugs 5-fluorouracil (5-Fu), and methotrexate (MTX) for 6 to 10 days by mixing drug loaded gelatin

microspheres of different size ranges. Similarly, Berkland et al. [23] mixed known ratios of rhodamine and piroxicam containing PLG microsphere populations having different mean diameters and drug loadings to attain zero-order release [23]. The ratios of the individual populations were determined by trial and error where multiple linear combinations were examined computationally to identify a combination resulting in linear drug release. It was found that the release profile from a mix of microsphere populations corresponded to mass-weighted linear combination of the individual release profiles, and constant release of rhodamine and piroxicam for 8 days and 13 days respectively was achieved [23].

In this Section, PLG microspheres having 2 different M_w and three different size fractions are prepared using the solvent extraction emulsion technique. The effect of microspheres mean diameter and polymer molecular weight, on drug release rate from poly(lactide-co-glycolide) (PLG) microspheres is investigated experimentally. The mathematical theory developed in the previous Section is used to model the effect of polymer molecular weight on drug release. A numerical optimization technique based on the least squares method is developed to achieve desired release profiles by combining appropriate proportions of individual microsphere populations.

4.2. Materials and Methods

4.2.1. Materials

Poly(D,L-lactide-co-glycolide) (PLG) polymer having a co-polymer composition of 50:50, and two different M_w (18 kDa: inherent viscosity 0.41 dl/g, and 55 kDa: inherent viscosity 0.87 dl/g; inherent viscosity measured in hexaflouroisopropanol) was purchased from Birmingham Polymers. The Poly (vinyl-alcohol) (PVA) was 87%-89% hydrolyzed, with a Mw of 13 – 23 kDa. In addition to PVA, Piroxicam (Mw 331.3), and HPLC grade Dichloromethane (DCM) were purchased from Sigma. Sodium hydroxide was purchased from EM Science. All chemicals were used as provided.

4.2.2. Microsphere Preparation

PLG microspheres were prepared using a previously described method (Section 2.2.2, Figure 2.1). Briefly, Piroxicam was co-dissolved with PLG (10% w/v) in dichloromethane (DCM) at 10% of the PLG mass (10% theoretical loading (w/w)). PVA solution (8% w/v) was stirred at the desired stirring speed for 5 minutes in a 400 ml Pyrex beaker with a Caframo ultra high torque stirrer (model BDC1850) having a speed range of 0 -1800 rpm. The PLG solution was slowly added to the beaker and stirring was continued for 60 minutes. Afterwards, the resulting emulsion was added to 1L of double distilled water, and stirring was continued for an additional 90 minutes at a speed of 1200 rpm. Microspheres were then collected by filtration, where the filter size used was 0.2 μm to prevent any loss of microspheres.

PLG microspheres having two different polymer molecular weights (18 kDa. and 55 kDa) were prepared at different impeller speeds (Table 4.1). The correlation developed by Berchane et al. [80], which relates PLG microsphere population mean diameter to impeller speed, was utilized to determine the impeller speeds that would result in the desired microsphere sizes. Each microsphere preparation was then sieved separately using the appropriate sieve sizes (Table 4.1) to obtain three different size fractions for each polymer molecular weight: 0.2 - 20, 20 - 40, and 63 - 90 μm (average pore sizes of the sieves: 20, 40, 63, and 90 μm; Keison Products, United Kingdom). Once sieved, the microspheres were lyophilized and stored at -20˚C.

4.2.3. Determination of Piroxicam Loading

The experimental loading of piroxicam was determined by dissolving 2 mg of microspheres in 1 ml of 0.25 M sodium hydroxide. Piroxicam free microspheres having the same molecular weight were treated similarly. Drug concentration was determined by measuring the absorbance of the piroxicam containing solution in a quartz cuvette at 276 nm (Gilford Response Spectrophotometer) and subtracting the absorbance of the piroxicam free solution.

4.2.4. *In Vitro* Release

Drug release was determined by suspending 5 mg of piroxicam loaded microspheres in 1.3 ml of phosphate buffered saline (PBS, pH 7.4). The suspension was continuously

Table 4.1 Characterization of piroxicam-loaded PLG microspheres

M_w (kDa)	Impeller Speed (rpm)	Sieve Fraction (μm)	Mean Diameter[a] d_{43} (μm)	Encapsulation Efficiency (%)
18.0	150	0.2-20	14.9 ± 0.3	28.0
18.0	300	20-40	31.2 ± 0.3	23.6
18.0	900	63-90	76.2 ± 0.7	33.3
55.0	200	0.2-20	12.8 ± 0.2	26.0
55.0	400	20-40	32.3 ± 0.3	24.7
55.0	1200	40-63	83.2 ± 0.7	24.6

[a]Mean diameter ± standard error

agitated by shaking (Glas-Col, Terre Haute, USA) at 100 strokes per minute in a 37 ºC incubator. At predetermined intervals, the samples were centrifuged, and 1 ml of the supernatant was extracted, and replaced by fresh buffer. The microspheres were then vortexed and put back into the incubator. The piroxicam concentration in the supernatant was determined by measuring the absorbance at 276 nm in a spectrophotometer (Gilford Response Spectrophotometer). Piroxicam-free microspheres were treated similarly, and the absorbance from their supernatant was subtracted from all measurements.

4.2.5. Microsphere Characterization

Imaging of microspheres was performed with a LEO-VP1530 field emission scanning electron microscope. The mean diameter was quantitatively determined by measuring ~1000 microspheres from the SEM micrographs using the Scion Image Analysis software. The pixel to distance ratio for each micrograph was entered into the software, and the edges of the spheres were specified by hand. The number of microspheres (~1000) measured for each population was sufficient to provide an accurate mean diameter (Table 4.1).

4.3. Mathematical Model

The theoretical model developed in Section 3.3 accounts for microsphere size and polymer molecular weight, and is used in this Section to predict drug release profiles from PLG microspheres having different size distribution and polymer molecular

weight. A brief description of the model is included in this Section for completeness; however, more details are included in Section 3.3.

The PLG microspheres were prepared by co-dissolving the polymer and the drug in DCM which results in a monolithic solution. Desorption of the drug from monolithic systems was first described by Crank in 1956 [84]. Solving the one-dimensional mass diffusion equation for a sphere (Equation (3.6)), with the appropriate boundary conditions, gives the cumulative release equation for the total amount of diffusing drug leaving a sphere (Equation (3.8)) [84].

The drug diffusion coefficient in the cumulative release equation ($D(t)$) is time dependent due to bulk degradation of the polymer matrix. As the polymer molecular weight (M_w) decreases, the drug has more available space to diffuse through the polymer chains, and so the diffusion coefficient increases. The dependence of diffusion coefficient of piroxicam on PLG molecular weight was investigated by Raman et al. [79], and is expressed in Equation (3.9). To account for the initial burst release, an initial diffusivity (D_0) is used as a fitting parameter. D_0 is used until the time dependent diffusivity $D(M_w)$ is larger than D_0.

Hydrolysis, which causes bulk degradation of PLG polymer, starts with water uptake. The degradation process, which results in a decrease in the polymer molecular weight caused by random ester cleavage, is expressed in Equation (3.10) [13]. In this Section we investigate drug release from microspheres having different initial polymer molecular weights. This is implemented into the mathematical model by changing the value of polymer molecular weight at time $t = 0$ ($M_w(0)$) in Equation (3.10).

The microsphere populations prepared in this work has a non-uniform size distribution. In this Section, the size distribution of the microsphere populations is represented by the mass/volume moment mean diameter (d_{43}), also known as De Brouckere mean diameter, which is the center of gravity of the mass/volume fraction size distribution.

4.4. Numerical Optimization Technique

A numerical optimization technique is developed, based on the least squares method, to compute the optimum proportions at which individual microsphere populations can be combined to attain desired release kinetics. An optimization problem can be formulated mathematically as follows [93-97]:

$$\begin{aligned} &Minimize: E(f) \\ &\text{Subject to } f \in S \end{aligned} \qquad \textbf{(4.1)}$$

where *E(f)* is the objective function to be minimized, and *f* is an *n* x 1 vector of design parameters whose values are to be determined. For a solution to be feasible, it must belong to the constraint set *S*, which is a subset of the space *n* x 1 column vectors R^{n}. When $S = R^n$, then the problem is an unconstrained optimization. In general, the constraint set is a collection of equality and inequality constraints on *f*. Few of the optimization techniques are available for finding the global minimum of a function. Instead, it is typical to search for a local minimum.

Here the objective function is the cumulative error between the target release profile and a linear combination of the available profiles:

$$E(f) = \sum_{i=1}^{m} (f_1 M_{1,i} + f_2 M_{2,i} + ... + f_n M_{n,i} - T_i)^2 \quad \textbf{(4.2)}$$

where m is the total number of points at which the profiles are evaluated, n is the total number of profiles to be combined, $M_1 ... M_n$ are the individual profiles to be combined, $f_1 ... f_n$ are the mass fractions of the individual populations to be combined, and T is the target profile.

4.4.1. Steepest Descent Method

The steepest descent method [93-95] is used in this work to solve the optimization problem. Starting with an initial guess, f^0, we determine a search direction, d^0, and perform a line search along that direction. The result of the line search is taken as an updated estimate, and the process is repeated. The search direction is determined by evaluating the gradient vector of partial derivatives of E with respect to the components of f [93]:

$$\nabla E_k(f) = \frac{\partial E(f)}{\partial f_k} \quad 1 \le k \le n \quad \textbf{(4.3)}$$

where $\nabla E(f)$ is the direction of steepest ascent, and $d^0 = -\nabla E(f)$ is the direction of steepest descent. If α^j denotes the optimal step length resulting from searching along the direction d^j, starting from the point f^j, then the values of *f* are updated as follows:

$$f_k^{\,j+1} = f_k^{\,j} - \alpha^j \nabla E_k^{\,j}(f); \quad 1 \le k \le n \tag{4.4}$$

where *j* denotes the iteration number. The iterative process is repeated until the components of the direction vector d^j fall below a user-specified error tolerance, ε.

4.5. Results and Discussion

4.5.1. *In Vitro* Drug Release Kinetics

Figure 4.1 shows experimentally measured *in vitro* release from PLG microspheres having different size distribution and polymer molecular weight. The release profiles shown in the figure are normalized to the total amount of drug release at the end of the study, which was within 10% of the experimental loading shown in Table 4.1. The mean diameters (d_{43}) of the microspheres range from 12.8 μm to 83.2 μm, and the M_w ranges between 18 kDa and 55 kDa (Table 4.1). Inspection of Figure 4.1 reveals that microsphere size is a major determinant of the release profile, and drug initial release rate decreased with increase in microsphere size, which confirms the results obtained in Section 3.4.2. This is also consistent with Fick's law of diffusion which attributes this decrease in drug release rate to an increase of diffusion pathways (reduced surface area

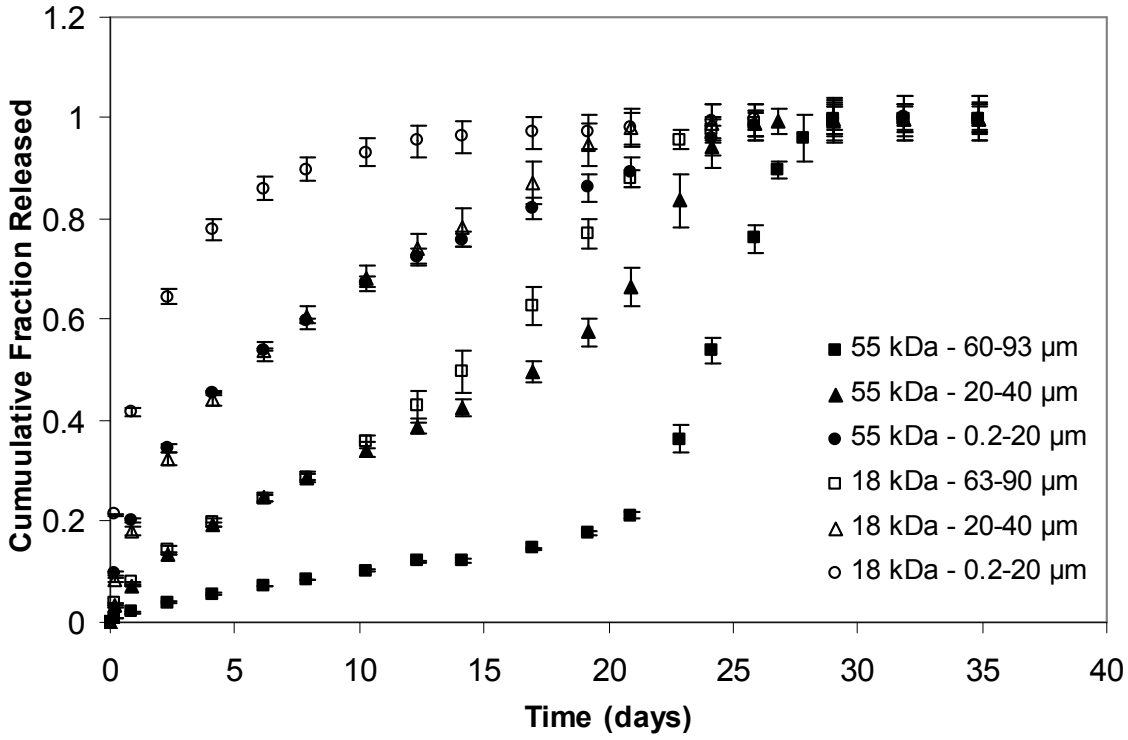

Figure 4.1 Effect of microsphere size and polymer molecular weight on piroxicam release from PLG microspheres.

to volume ratio for large spheres). In addition, inspection of Figure 4.1 reveals that polymer molecular weight is also a major determinant of the release profile, and drug initial release rate decreased with increasing polymer molecular weight. As the polymer molecular weight is increased, the drug has less available space to diffuse through the polymer chains, and the diffusion coefficient decreases, which results in reduced initial drug release rates. The combined effect of varying the microsphere size and polymer molecular weight resulted in release profiles having different durations (10 to 28 days) and shapes (first-order, near zero-order, and sigmoidal).

4.5.2. Model Results

The Matlab program developed in the previous Section was used to solve the cumulative release equation (Equation (3.8)), and predict the release of piroxicam from PLG microspheres having different mean diameters and polymer molecular weights. Dependence of diffusivity on molecular weight was modeled using Equation (3.9). To account for the initial burst release, an initial diffusivity (D_0) is used as a fitting parameter. D_0 is used until the time dependent diffusivity $D(M_w)$ is larger than D_0. Since the molecular weight of PLG polymer varies with time, it was modeled using Equation (3.10). Size distribution of the microspheres was represented in the mathematical model by the volume moment mean diameter. As mentioned previously, the volume moment mean diameter is the center of gravity of the volume fraction size distribution. It is evident from Figure 4.2 that the release profiles generated by the model are in good

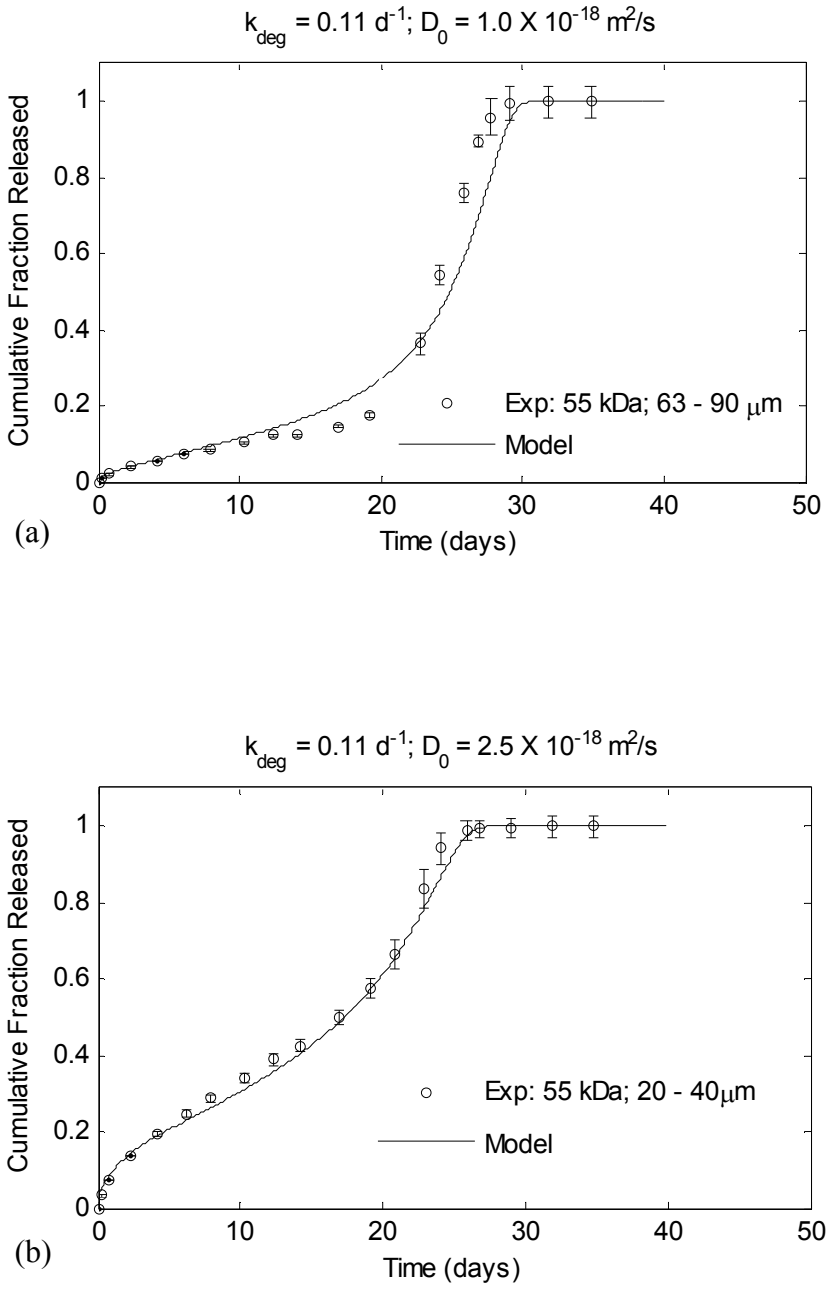

Figure 4.2 Comparison of model profiles to experimental results of piroxicam loaded PLG microspheres: (a) 55 kDa, 63 – 90 µm; (b) 55 kDa, 20 – 40 µm; (c) 55 kDa, 0.2 – 20 µm; (d) 18 kDa, 63 – 90 µm; (e) 18 kDa, 20 – 40 µm; and (f) 18 kDa, 0.2-20 µm.

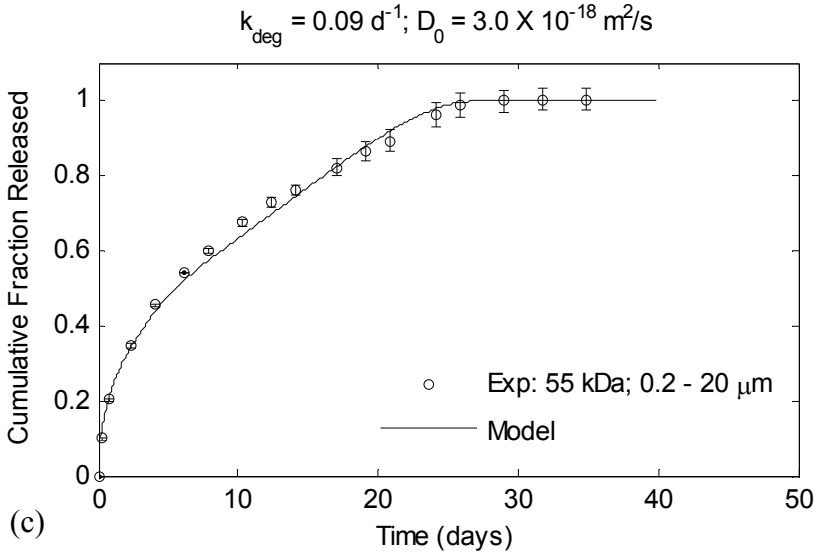

(c)

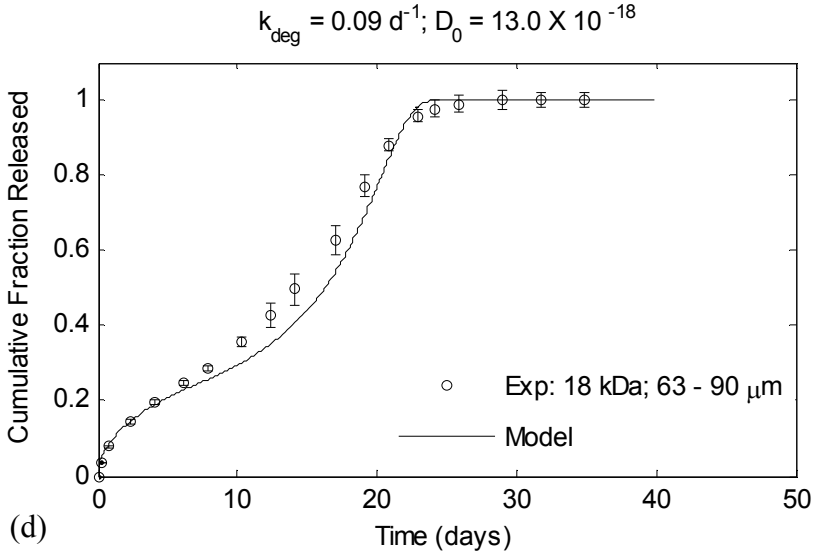

(d)

Figure 4.2 Continued

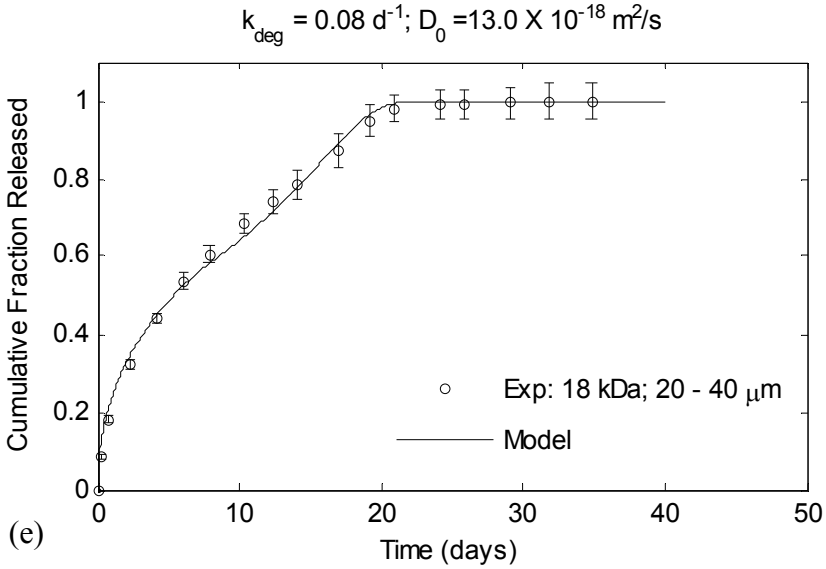

(e)

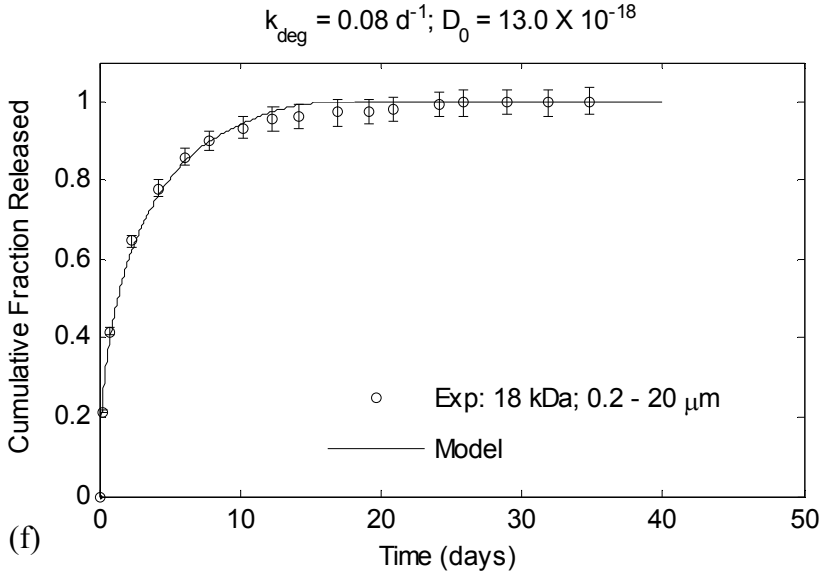

(f)

Figure 4.2 Continued

agreement with the experimental drug release data for the different microsphere populations.

4.5.3. Release from Mixtures of Individual Microsphere Populations

Based on the different shapes of the individual release profiles depicted in Figure 4.1, it might be possible to achieve desired release rates by mixing appropriate proportions of two or more individual microsphere populations. To this end, a numerical optimization technique was developed, based on the least squares method, that computes the optimum proportions at which individual microsphere populations can be combined to attain desired release kinetics.

To test this hypothesis, we constructed several desired release profiles (Figure 4.3), in particular, pulsatile, zero-order, and near zero-order release profiles. The ideal desired drug release profile is one that initiates the optimum response in a patient. Pulsatile release [5,52-54] is attractive for vaccine delivery, as the drug release formulation can be designed to deliver distinct pulses which solves the need for booster shots. Zero-order release [49-51] is desired for a wide range of drugs because it maintains a constant level of drug concentration well within the therapeutic window for extended time periods. In addition, it is sometimes desirable to have a near-zero order release profile where a small amount of drug is released in a burst, followed by constant release over extended period. After the desired release profiles were constructed, the numerical optimization technique was utilized to identify the best candidates to be combined and their optimum proportions. The initial goal was to achieve the desired profiles by combining two

individual populations. In Figure 4.3, the dashed line is the target profile, while the solid line is the predicted optimum release. To validate the predicted release, *in vitro* release experiments of a mixture of the individual populations at the determined proportions were performed.

In Figure 4.3 (a) the desired release has a pulsatile profile that delivers its first pulse (~ 45% of the total drug load) in the first 3 days, and then delivers its second pulse (~ 40% of the total drug load) from day 22 to day 28. Using the numerical optimization technique, it was determined that the optimum release can be achieved by mixing the 63-90 μm / 55 kDa microsphere population and the 0.2-20 μm / 18 kDa microsphere population at mass fractions of 0.47 and 0.53 respectively. From inspection of Figure 4.3 (a), it is evident that the predicted optimum release profile is in good agreement with the desired release ($R^2 = 0.988$), and that the pulsatile release was successfully achieved by combining microsphere populations.

The desired release in Figure 4.3 (b) has a zero-order profile that delivers its drug load at constant rate for 28 days (3.57% of total drug load delivered per day). Using the numerical optimization technique, it was determined that the optimum release can be achieved by mixing the 63-90 μm / 55 kDa microsphere population and the 20-40 μm / 18 kDa microsphere population at mass fractions of 0.43 and 0.57 respectively. Inspection of Figure 4.3 (b) shows that designing a truly zero-order release by mixing two individual populations had a limited success ($R^2 = 0.965$).

The desired release in both Figure 4.3 (c) and Figure 4.3 (d) has a near zero-order profile that starts with a high initial drug release rate for two (2) days and then shifts to a

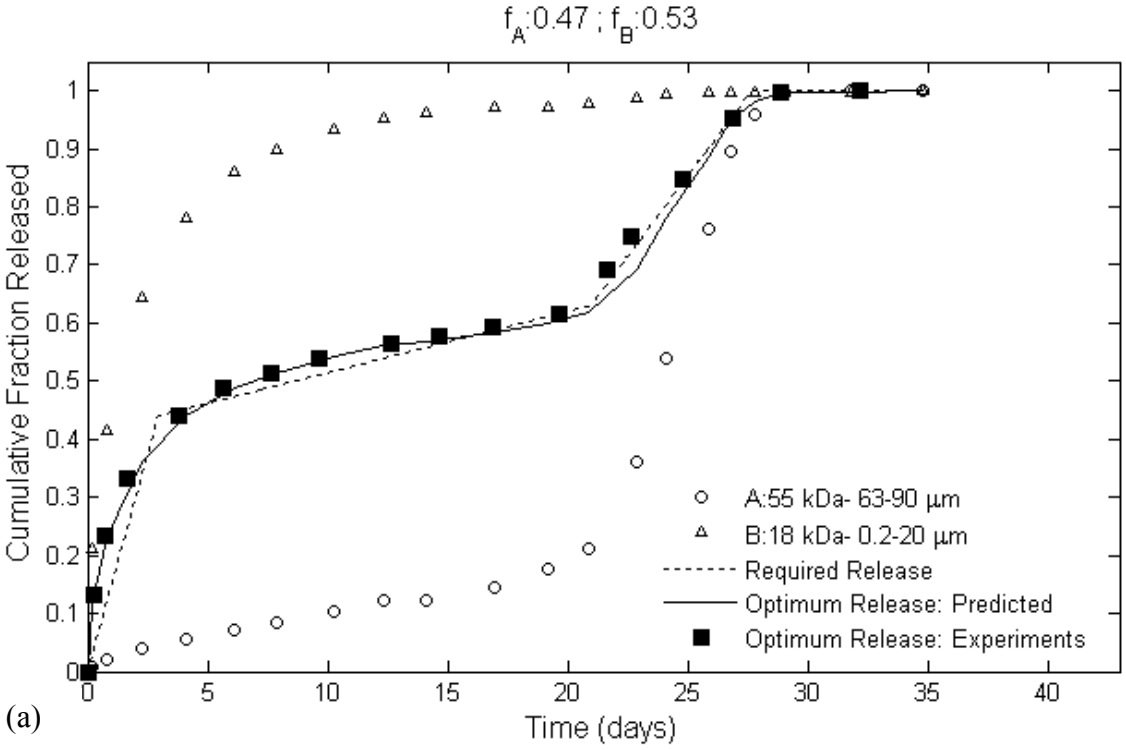

Figure 4.3 Combining appropriate proportions of two individual PLG microsphere populations to achieve desired drug release profiles: a) pulasatile, b) zero-order, c) near zero-order, and d) near zero-order.

(b)

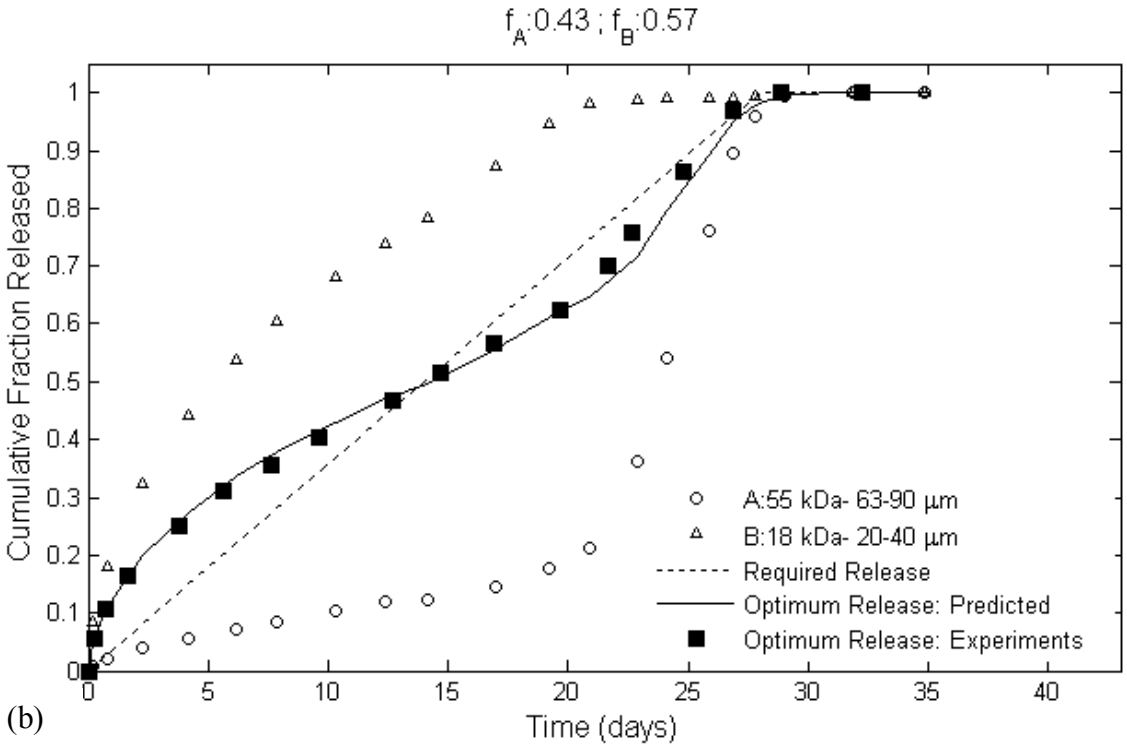

Figure 4.3 Continued

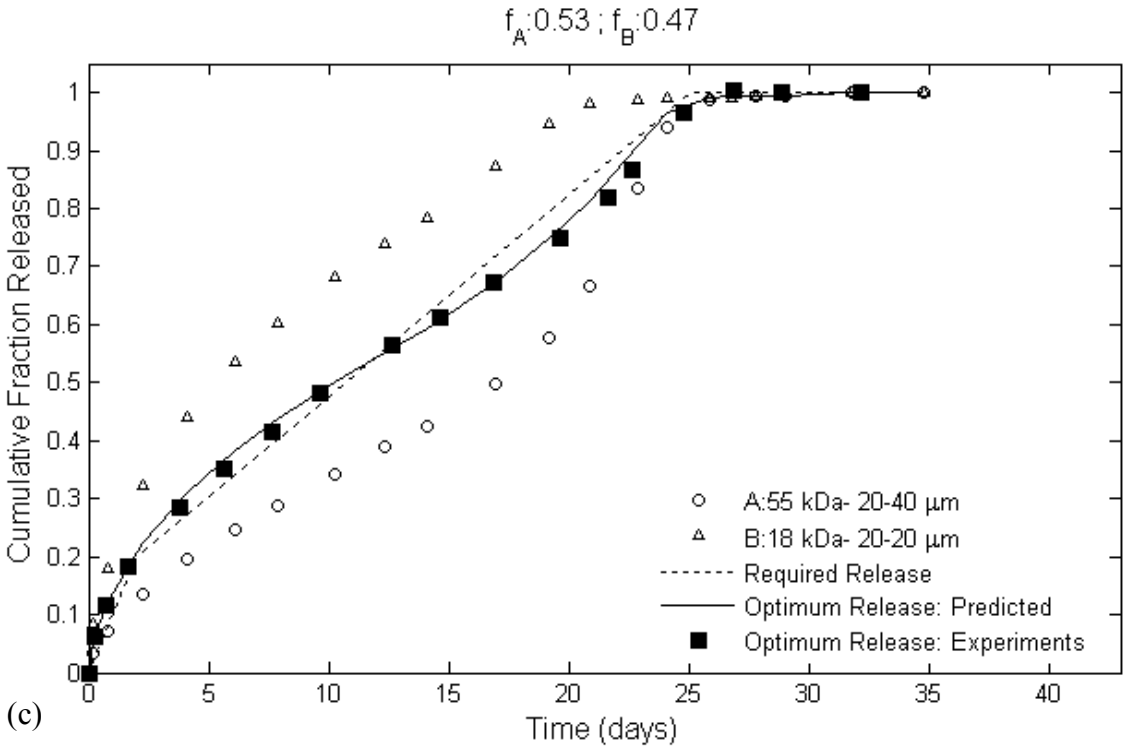

(c)

Figure 4.3 Continued

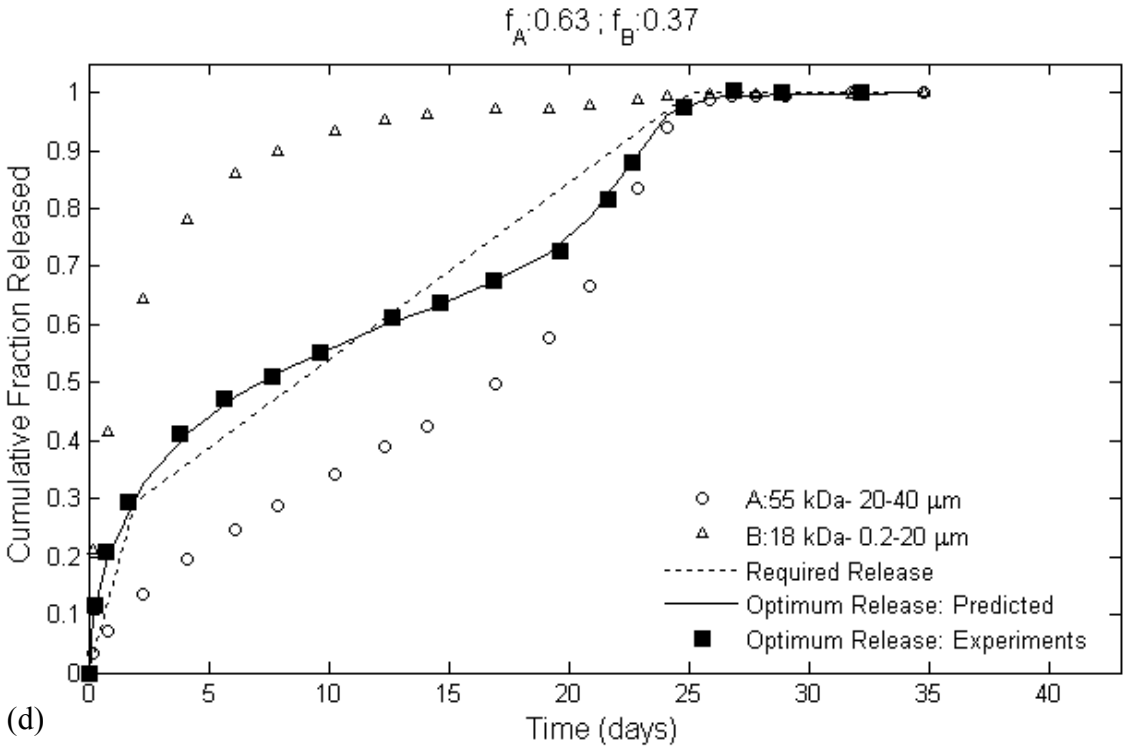

(d)

Figure 4.3 Continued

lower release rate for the additional 23 days. In Figure 4.3 (c) the desired release delivers 20% of the total drug load in the first two (2) days, while the desired release in Figure 4.3 (d) delivers 30% of the total drug load in that same time period. The optimum release in Figure 4.3 (c) was achieved by mixing the 20-40 μm / 55 kDa microsphere population and the 20-40 μm / 18 kDa microsphere population at mass fractions of 0.53 and 0.47 respectively. It is evident from Figure 4.3 (c) that the predicted optimum release profile is in good agreement with the desired release ($R^2 = 0.994$). Alternatively, the optimum release in Figure 4.3 (d) was achieved by mixing the 20-40 μm / 55kDa microsphere population and the 0.2-20 μm / 18 kDa microsphere population at mass fractions of 0.63 and 0.37 respectively. From inspection of Figure 4.3 (d), it is evident that the predicted optimum release profile is in fair agreement with the desired release ($R^2 = 0.981$).

In addition, Figure 4.3 (a-d) shows that the experimental optimum release profiles are all in good agreement with the predicted optimum release profiles. This validates the predicted release profiles, and shows that the measured release from a combination of microsphere populations corresponds to a mass-weighted linear combination of the individual profiles.

Given the agreement between the predicted release profiles and the experimental data, the optimization technique was then utilized to achieve the desired release kinetics by combining multiple release profiles. The numerical algorithm was developed to automatically consider the different combinations of microsphere populations and report the optimum proportions and the cumulative error associated with each combination.

The number of combinations (N) for selecting q profiles from a total of p available profiles (p is equal to six in this work) can be expressed as follows [98]:

$$N = \frac{p!}{q!(p-q)!} \tag{4.5}$$

For example, to achieve a desired release, there are 15 different combinations for selecting two profiles out of a total of six profiles, and 20 different combinations for selecting three profiles, and so forth. The total number of combinations (N_{tot}) is equal to 57 and can be expressed as follows:

$$N_{tot} = \sum_{q=2}^{q=6} \frac{p!}{q!(p-q)!} \tag{4.6}$$

In Figure 4.4 the desired release profiles, previously described in Figure 4.3, are achieved by combining three individual populations. Combining more than three profiles to achieve the desired release kinetics did not provide any improvement in the optimum release. Comparison of Figure 4.4 (a) with Figure 4.3 (a) reveals that combining three individual profiles provides a marginally improved fit ($R^2 = 0.992$) to the desired release profile than combining two profiles ($R^2 = 0.988$). The same conclusion can be made by comparing Figure 4.4 (c) ($R^2 = 0.998$) with Figure 4.3 (c) ($R^2 = 0.994$). This slight improvement in the optimum release should be weighed against the additional effort

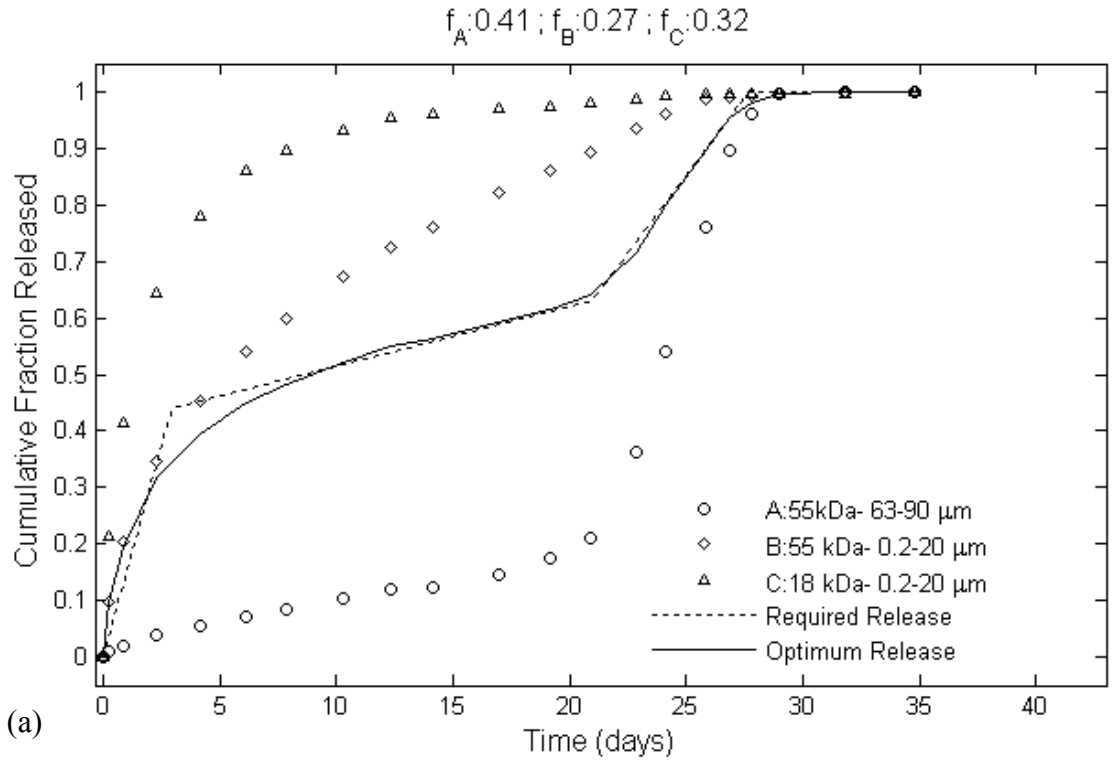

(a)

Figure 4.4 Combining appropriate proportions of multiple individual PLG microsphere populations to achieve desired drug release profiles: a) pulasatile, b) zero-order, c) near zero-order, and d) near zero-order.

(b)

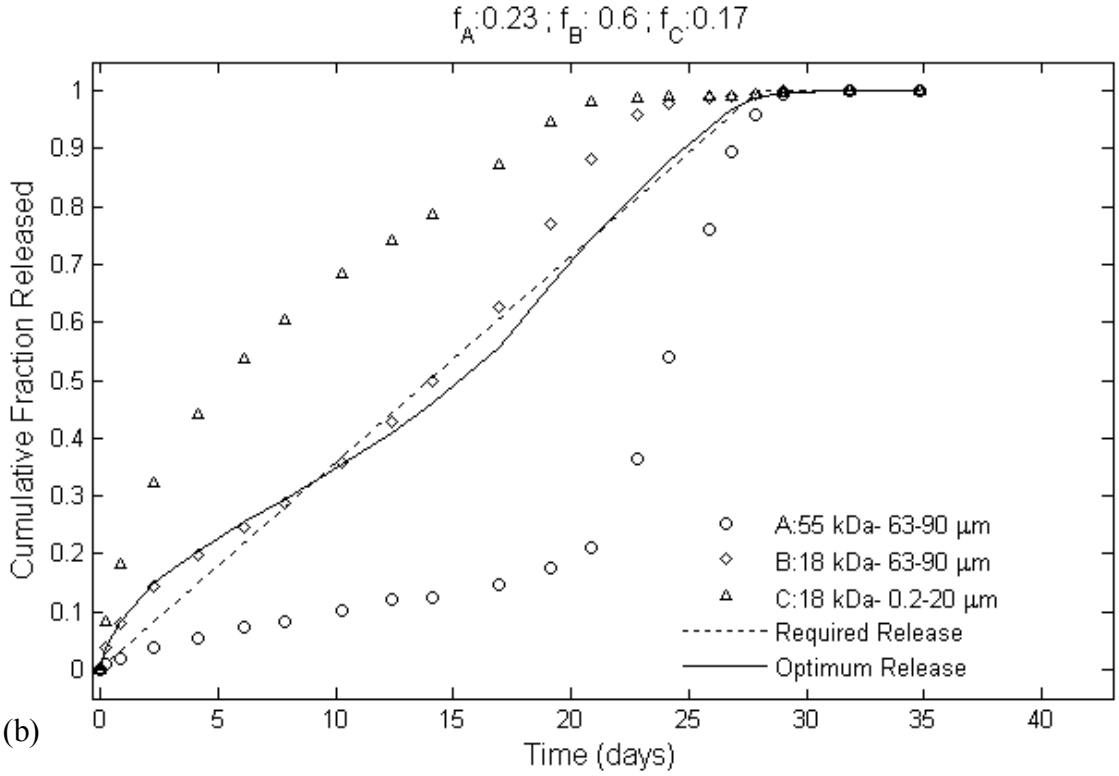

Figure 4.4 Continued

(c)

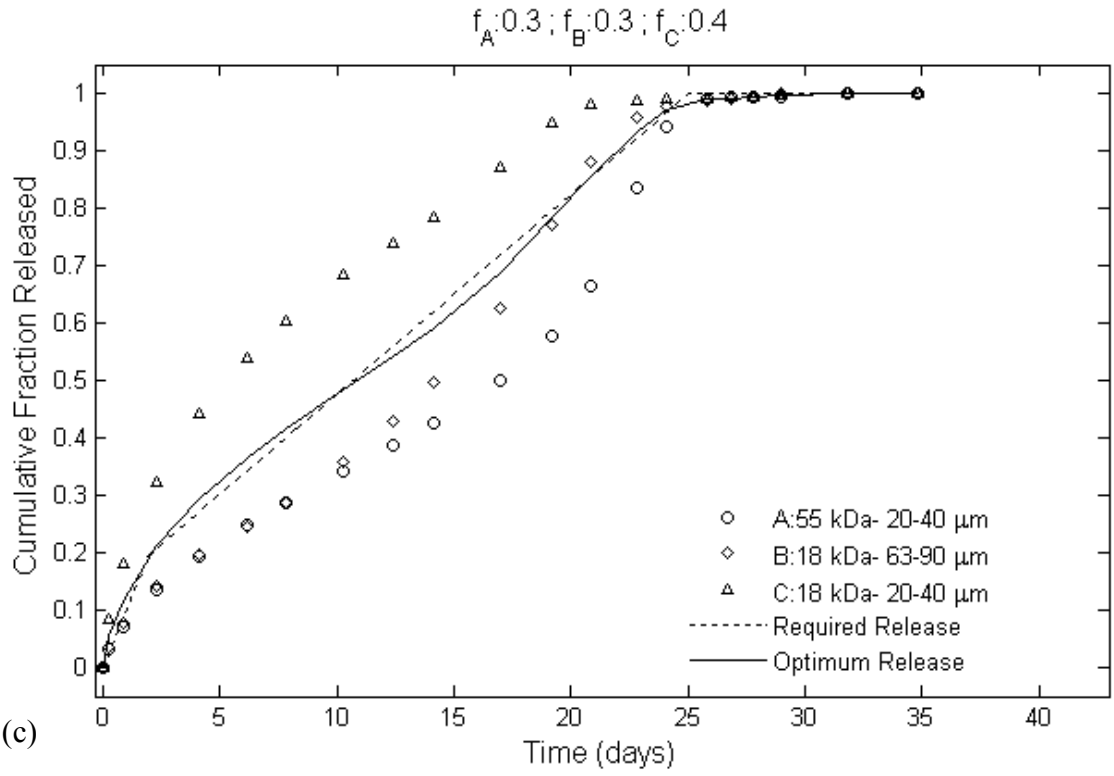

Figure 4.4 Continued

(d)

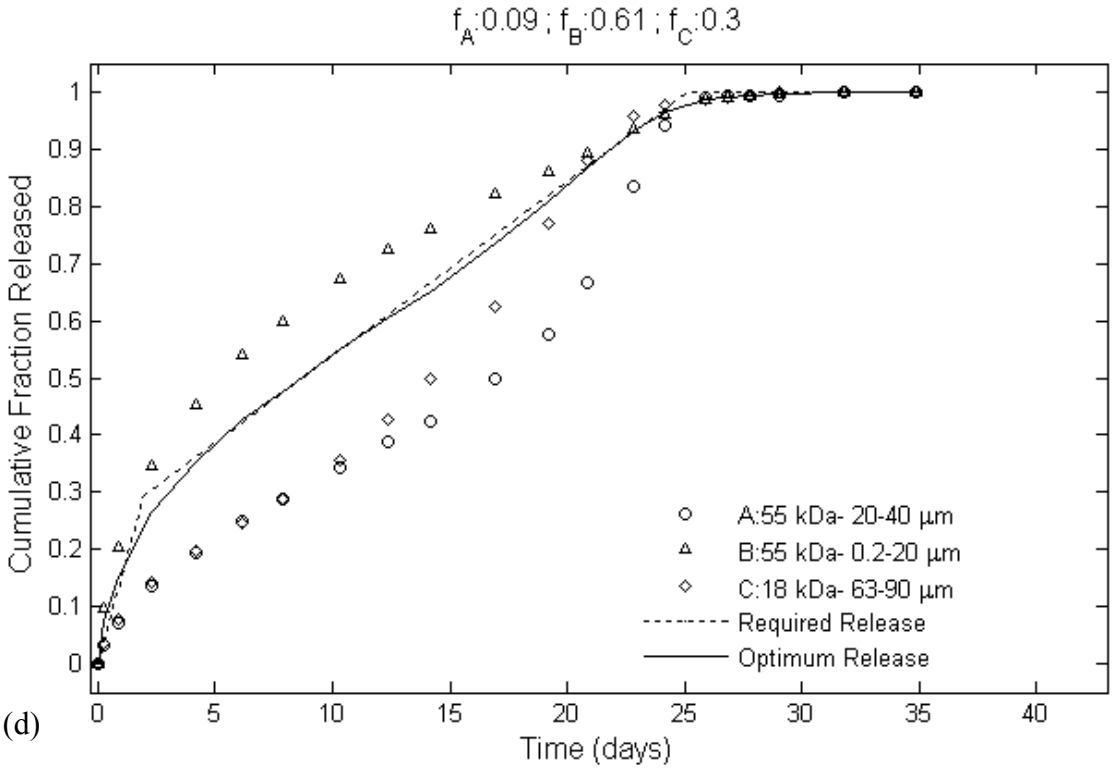

Figure 4.4 Continued

required to prepare and combine three microsphere populations versus two microsphere populations.

Alternatively, inspection of Figure 4.4 (b) shows that the optimum release obtained by combining three individual profiles provides a considerably better fit ($R^2 = 0.993$) to the desired release, than was achieved by combining two profiles ($R^2 = 0.965$; Figure 4.3 (b)). The same conclusion can be made by comparing the optimum release in Figure 4.4 (d) ($R^2 = 0.998$) with the optimum release in Figure 4.3 (d) ($R^2 = 0.98$).

More complex drug release profiles can be achieved by mixing individual PLG microsphere populations having a wider range of sizes and polymer molecular weights. In addition, other key parameters such as polymer composition in general and lactide/glycolide ratio in particular, can be utilized to prepare PLG microspheres having a wide variation of drug release profiles. In Appendix A, a drug release profile having three distinct pulses is achieved by combining the predicted release from a PLG microsphere population having a mean diameter of 160 μm, and a polymer molecular weight of 220 kDa, with the 63-90 μm / 55 kDa and the 0.2-20 μm / 18 kDa microsphere populations. The numerical optimization technique was used to determine the optimum proportions at which the individual microsphere populations need to be combined.

4.6. Conclusions

Piroxicam loaded PLG microspheres have been prepared using the oil-in-water (o-w) emulsion technique. The effect of microsphere mean diameter, and polymer molecular weight on drug release rate from the microspheres was investigated. The mathematical

model developed in the previous Section was used to predict drug release from PLG microspheres having different size and polymer molecular weight. A numerical optimization technique was developed to tailor desired drug release profiles by combining individual microsphere populations at appropriate proportions. It was shown that the initial drug release rate decreased with an increase in polymer molecular weight. The combined effect of varying the microsphere size and polymer molecular weight resulted in release profiles having different durations (10 to 28 days) and shapes (first-order, zero-order, sigmoidal). The model results were in good agreement with the experimental results. It was also shown that the mixture release profiles corresponded to a mass weighted linear combination of the individual profiles. Using the numerical optimization technique, it was possible to determine the appropriate proportions of individual microspheres that generate the desired release profiles, in particular, zero-order, and pulsatile.

5. CONCLUSIONS AND RECOMMENDATIONS

This work has investigated the effect of various parameters on small molecule release from PLG microspheres prepared using an emulsion technique. Due to the importance of microsphere size on release kinetics, a quantitative study has been performed on the microsphere size distributions and a fluid mechanics based mathematical correlation was developed to predict the mean diameter of the microspheres prepared. The correlation was validated by comparison with experimental results for a wide range of We_m. This correlation is valid for non-coalescing dispersions, with the dispersed phase having low viscosity, and volume fraction. The size distribution of PLG microspheres prepared using the emulsion technique was described by the Rosin-Rammler distribution function. The effect of microsphere mean diameter, polydispersity, polymer initial molecular weight, and polymer degradation on therapeutic drug release rate from the microspheres was investigated experimentally. Based on the experimental results, a mathematical model that predicts drug release from polydisperse PLG microspheres was developed. The model accounts for the effects of diffusion, polymer initial molecular weight, polymer degradation, and microsphere size distribution. Finally, a numerical optimization technique was developed to tailor desired therapeutic drug release profiles by combining individual microsphere populations at appropriate proportions. The significant conclusions of this work are summarized below.

- The derived fluid mechanics based mathematical correlation provided a good estimate to the microsphere populations mean diameter over a wide range of We_m
- The Rosin-Rammler distribution function provided a good description of the size distribution of the PLG microspheres prepared using the solvent extraction technique.
- Microsphere size had a significant effect on the drug release kinetics, and the initial drug release rate decreased with increase in microsphere size. Also, the release profile changed from first order to concave upward as microsphere size was increased.
- Polymer initial molecular weight had a significant effect on release kinetics, and it was shown that the initial drug release rate decreased with an increase in polymer molecular weight.
- Polydispersity did not have a significant effect on drug release rate for populations having a polydispersity parameter (b) larger than 3. Alternatively, for distributions having a value of b close to or below 3, incorporating the size distribution of the population into the model provided a better fit to the experimental results. Also polydispersity was not believed to be the main cause for the initial "burst" release
- The model results were in good agreement with experimental results, and thus can be used to predict therapeutic drug release from polydisperse populations of microspheres.

- The combined effect of varying the microsphere size and polymer molecular weight resulted in release profiles having different durations (10 to 28 days) and shapes (first-order, zero-order, and sigmoidal).
- It was shown that the mixture release profiles corresponded to a mass weighted linear combination of the individual profiles.
- Using the numerical optimization technique, it was possible to determine the appropriate proportions of individual microspheres that generate the desired release profiles, in particular, zero-order, and pulsatile.

The following recommendations are proposed for future work:

- Expand the current study to investigate additional key parameters that can be utilized to control the release rate of pharmaceuticals from microspheres, in particular polymer composition (polymer chemistry and copolymer ratio).
- Rapid developments in the field of molecular biology and biotechnology resulted in generation of many macromolecular therapeutic drugs including peptides, proteins, polysaccharides and nucleic acids. The methodology developed in this work for small molecule release can be applied to tailor drug release kinetics of macromolecules from polymeric microspheres.
- Determining the mean diameter of the microsphere populations by measuring microspheres from SEM micrographs using the Scion Image Analysis software was time consuming. Laser diffraction and electrozone sensing techniques can be

used instead to provide faster and more accurate measurements for the mean diameter.

- The conventional microsphere preparation impeller set-up used in this work produces microsphere populations of non-uniform size distribution. New manufacturing techniques are being developed to produce monodisperse microsphere populations, which eliminates the need for sieving.

REFERENCES

1. R.W. Baker, Controlled Release of Biologically Active Agents, John Wiley and Sons, NY, 1987.
2. S.D. Bruck, Controlled drug delivery, Volume I Basic Concepts, CRC Press Inc., Boca Raton, FL, 2000.
3. G.W. Creasy, M.E. Jaffe, Endocrin/reproductive pulsatile delivery systems, Adv. Drug Deliv. Rev. 6 (1991) 51-56.
4. G.M. Zenter, G.S. Rork, K.J., Himmelstein, The controlled porosity osmotic pump, J. Control. Release 1 (1985) 269-282.
5. A.C. Richards Grayson, I.S. Choi, B.M. Tyler, P.P. Wang, H. Brem, M.J. Cima, R. Langer, Multi-pulse drug delivery from a resorbable polymeric microchip device, Nat. Mater. 2 (2003) 767-772.
6. B.I. Dahiyat, M. Richards, K.W. Leong, Controlled release from poly(phosphoester) matrices, J. Control. Release 33 (1995) 13-21.
7. A. Gopferich, Bioerodible implants with programmable drug release, J. Control. Release 44 (1997) 271-281.
8. J. Heller, Controlled drug release from poly(ortho esters) – a surface eroding polymer, J. Control. Release 2 (1985) 167-177.
9. M.N.V. Ravi Kumar, Nano and microparticles as controlled drug delivery devices, J. Pharm. Pharm. Sci. 3 (2000) 234-258.

10. D.E. Cutright, E. Perez, J.D. Beasley, W.J. Larson, W.R. Posey, Degradation rates of polymers and co-polymers of polylactic and polyglycolic acids, Oral Surg. Oral Med. Oral Pathol. 37 (1974) 142-152.
11. C.G. Pitt, F.I. Chasalow, Y.M. Hibionada, D.M. Klimas, A. Schindler, Aliphatic Polyesters. I. The degradation of poly(ϵ-caprolactone) in vivo, J. Appl. Polym. Sci. 26 (1981) 3779-3787.
12. C.G. Pitt, M.M. Gratzl, G.L. Kimmel, J. Surles, A. Schindler, Aliphatic Polyesters. II. The degradation of poly(DL-lactide), poly(ϵ-caprolactone) and their copolymers in vivo, Biomaterials 2 (1981) 215-220.
13. C.G. Pitt, and Z. Gu, Modification of the rates of chain cleavage of poly(ϵ-caprolactone) and related polyesters in the solid state, J. Control. Release, 4 (1987) 283-292.
14. S. Li, Hydrolytic degradation characteristics of aliphatic polyesters derived from lactic and glycolic acids, J. Biomed. Mater. Res. (Appl. Biomater.) 48 (1999) 342-353.
15. A. Sodergard, M. Stolt, Properties of lactic acid based polymers and their correlation with composition, Prog. Polym. Sci. 27 (2002) 1123-1163.
16. J. Fu, J. Fiegel, E. Krauland, J. Hanes, New polymeric carriers for controlled release drug delivery following inhalation and injection, Biomaterials 23 (2002) 4425-4433.
17. M.E. El-Baseir, I.W. Kellaway, Poly(L-lactic acid) microspheres for pulmonary drug delivery: release kinetics and aerosolization studies, Int. J. Pharmaceut. 175 (1998) 135-145.

18. P. Wu, Y. Huang, J. Chang, M. Tsai, Y. Tsai, Design and evaluation of sustained release microspheres of potassium chloride prepared by Eudragit, Pharm. Sci. 19 (2003) 115-122.

19. A. Khan, M. Benboubetra, P.Z. Sayyed, K.W. Ng, S. Fox, G. Beck, I.F. Benter, S. Akhtar, Sustained polymeric delivery of gene silencing antisense ODNs, siRNA, DNAzymes and Ribozymes: in vitro and in vivo studies, J. Drug Target. 12 (2004) 393-404.

20. K. Cifti, H.S. Kas, A.A. Hincal, T.M. Ercan, O. Guven, S. Ruacan, In vitro and in vivo evaluation of PLGA (50/50) microspheres containing 5-fluorouracil prepared by solvent evaporation method, Int. J. Pharmaceut. 131 (1996) 73-82.

21. P.A. Dickinson, I.W. Kellaway, G. Taylor, D. Mohr, K. Nagels, H. Wolff, In vitro and in vivo release of estradiol from intra-muscular microsphere formulation, Int. J. Pharmaceut. 148 (1997) 55-61.

22. J.M. Bezemer, R. Radersma, D.W. Grijpma, P.J. Dijkstra, C.A. van Blitterswijk, J. Feijen, Microspheres for protein delivery prepared from amphiphilic multiblock copolymers 2. Modulation of release rate. J. Control. Release 67 (2000) 249-260.

23. C. Berkland, M. King, A. Cox, K.K. Kyekyoon, and D.W. Pack, Precise control of PLG microspheres size provides enhanced control of drug release rate. J. Control. Release, 82 (2002) 137-147.

24. J. Siepmann, N. Faisant, J. Akiki, J. Richard, and J.P. Benoit, Effect of the size of biodegradable microparticles on drug release: experiment and theory, J. of Control. Release, 96 (2004) 123-134.

25. R. Herrero-Vanrell, L. Ramirez, A. Fernandez-Carballido, M.F. Refojo, Biodegradable PLGA microspheres loaded with Ganciclovir for intraocular administration. Encapsulation technique, in vitro release profiles, and sterilization process, Pharm. Res. 17 (2000) 1323-1328.
26. J.K. Lalla, and K. Sapna, Biodegradable microspheres of poly(DL-lactic acid) containing piroxicam as a model drug for controlled release via the parenteral route, J. Microencapsul. 10 (1993) 449-460.
27. S. Bozdag, S. Calis, H.S. Kas, M.T. Ercan, I. Peksoy, A.A. Hincal, In vitro evaluation and intra-articular administration of biodegradable microspheres containing naproxen sodium, J. Microencapsul. 18 (2001) 443-456.
28. A. Messaritaki, S.J. Black, C.F. van der Walle, S.P. Rigby, NMR and confocal microscopy studies of the mechanisms of burst release from PLGA microspheres, J. Control. Release, 108 (2005) 271-281.
29. J. Braunecker, M. Baba, G.E. Milroy, R.E. Cameron, The effects of molecular weight and porosity on the degradation and drug release from polyglycolide, Int. J. Pharm. 282 (2004) 19-34.
30. D.R. Cowsar, T.R. Tice, R.M. Gilley, and J.P. English, Poly(lactide-co-glycolide) microcapsules for controlled release of steroids, Methods Enzymol. 112 (1985) 101-116.
31. B. Bittner, T. Kissel, Ultrasonic atomization for spraydrying: a versatile technique for the preparation of protein loaded biodegradable microspheres, J. Microencapsul. 16 (1999) 325-341.

32. M. Sandor, D. Enscore, P. Wetson, E. Mathiowitz, Effect of molecular weight on release from micron-sized PLGA microspheres, J. Control. Release, 76 (2001) 297-311.

33. M. Shi, Y. Yang, C. Chaw, S. Goh, S.M. Moochhala, S. Ng, J. Heller, Double walled POE/PLGA microspheres, encapsulation of water-soluble and water-insoluble proteins and their release properties, J. Control. Release 89 (2003) 167-177.

34. Y. Yang, T. Chung, N.P. Ng, Morphology, drug distribution, and in vitro release profiles of biodegradable polymeric microspheres containing protein fabricated by double-emulsion solvent extraction/evaporation method, Biomaterials, 22 (2001) 231-241.

35. G. Jiang, W. Qiu, P. DeLuca, Preparation and in vitro/in vivo evaluation of insulin-loaded poly(acryloyl-hydroxyethyl starch)- PLGA composite microspheres, Pharm. Res. 20 (2003) 452-459.

36. D. M. Ciombor, A. Jaklenec, A.Z. Liu, C. Thanos, N. Rahman, P. Weston, R. Aaron, E. Mathiowitz, Encapsulation of BSA using modified W/O/O emulsion solvent removal method, J. Microencapsul. 23 (2006) 183-194.

37. T.G. Park, W. Lu, G. Crotts, Importance of in vitro experimental conditions on protein release kinetics, stability and polymer degradation in protein encapsulated poly(D,L-lactic acid-co-glycolic acid) microspheres, J. Control. Release 33 (1995) 211-222.

38. J.E. Vandegaer, Microencapsulation: Processes and applications, Plenum Press, New York, NY, 1974.

39. R.A. Jain, The manufacturing techniques of various drug loaded biodegradable poly(lactide-co-glycolide) (PLGA) devices, Biomaterials 21 (2000) 2475-2490.
40. S. Freitas, H.P. Merkle, B. Gander, Microencapsulation by solvent extraction/evaporation: reviewing the state of the art of microsphere preparation process technology, J. Control. Release 102 (2005) 313-332.
41. C. Thomasin, H. P. Merkle, B. Gander, Drug microencapsulation by PLA/PLGA coacervation in the light of thermodynamics. 2. Parameters determining microsphere formation, J. Pharm. Sci. 87 (1998) 269-275.
42. B.W. Wagenaar, B.W. Muller, Piroxicam release from spray-dried biodegradable microspheres, Biomaterials 15 (1994) 49-54.
43. L.R. Beck, D.R. Cowsar, D.H. Lewis, R.J. Cosgrove, C.T. Riddle, S.L. Lowry, T. Epperly, A new long-acting injectable microcapsule system for the administration of progesterone, Fertil. Steril. 31 (1979) 545-551.
44. H. Jeffery., S.S. Davis, D.T. O'Hagan, The preparation and characterisation of poly(lactide-co-glycolide) microparticles. I: oil-in-water emulsion solvent evaporation, Int. J. Pharm. 77 (1991) 169-175.
45. H. Jeffery, S.S. Davis, D.T. O'Hagan, The preparation and characterization of poly(lactide-co-glycolide) microparticles. II. The entrapment of a model protein using a (water-in-oil)-in-water emulsion solvent evaporation technique, Pharm. Res. 10 (1993) 362-368.

46. Y. Ogawa, M. Yamamoto, H. Okada, T. Yashiki, T. Shimamoto, A new technique to efficiently entrap Leuprolide Acetate into microcapsules of polylactic acid or copoly(lactic/glycolic acid), Chem. Pharm. Bull., 36 (1988) 1095-1103.

47. R.H. Parikh, J.R. Parikh, R.R. Dubey, H.N. Soni, K.N. Kapadia, Poly(D,L-lactide-co-glycolide) microspheres containing 5-Fluorouracil: optimization of process parameters, AAPS PharmSciTech 4 (2003), Article 13.

48. A. Porjazoska, K. Goracinova, K. Mladenovska, M. Glavas, M. Simonovska, E.I. Janjevic, and M. Cvetkovska, Poly(lactide-co-glycolide) microparticles as systems for controlled release of proteins- preparation and characterization, Acta Pharm., 54 (2004) 215-229.

49. R. Narayani, K. P. Rao, Gelatin microsphere cocktails of different sizes for the controlled release of anticancer drugs, Int. J. Pharm. 143 (1996) 255-258.

50. B.H. Woo, J.W. Kostanski, S. Gebrekidan, B.A. Dani, B.C. Tahanoo, P.P. Deluca, Preparation, characterization and in vivo evaluation of 120-day poly(DL-lactide) leuprolide microspheres, J. Control. Release 75 (2001) 307-315.

51. D.L. Wise, D.J. Trantolo, R.T. Marino, J.P. Kitchell, Opportunities and Challenges in the design of implantable biodegradable polymeric systems for the delivery of anti-microbial agents and vaccines, Adv. Drug Deliv. Rev. 1 (1987) 19-39.

52. D.M. Schachter, J. Kohn, A synthetic polymer matrix for the delayed release or pulsatile release of water-soluble peptides, J. Control. Release, 78 (2002) 143-153.

53. D.R. Mathews, D.A. Lang, M.A. Burnett, R.C. Turner, Control of pulsatile insulin secretion in man, Diabetologia, 24 (1983) 231-237.

54. J.T.Jr Santini, A.C. Richards, R. Scheidt, M.J. Cima, R. Langer, Microchips as controlled drug-delivery devices, Angew. Chem. Int. Edn 39 (2000) 2396-2407.

55. S.S., D'Souza, F. Selmin, S.B. Murty, W. Qui, B.C. Thanoo, P.P. Deluca, Assesment of fertility in male rats after extended chemical castration with GnRH antagonist, AAPS PharmSci. 6 (2004) Article 10.

56. M. Chaubal, Polylactide/Glycolide – Excipients for injectable drug delivery and beyond, Drug Deliv. Technol. 2 (2002) 34-35.

57. H. Okada, One and three-month release injectable microspheres of the LH-RH superagonist leuprorelin acetate, Adv. Drug Deliv. Rev. 28 (1997) 43-70.

58. S.S. D'Souza, J.A.Faraj, and P.P. Deluca, A model-dependent approach to correlate accelerated with real-time release from biodegradable microspheres, AAPS PharmSciTech 6 (2005) Article 70.

59. B.H. Woo, K-H. Na, B.A. Dany, G. Jiang, B.C. Thanoo, P.P. Deluca, In vitro characterization and in vivo testosterone suppression of 6 month release poly(D,L-lactide) leuprolide microspheres, Pharm. Res. 19 (2002) 546-550.

60. J.M. Kane, M. Eerdekens, J-P. Lindenmayer, S.J. Keith, M. Lesem, K. Karcher, Long-acting injectible risperidone: efficacy and safety of the first long-acting atypical antipsychotic, Am. J. Psychiatry 160 (2003) 1125-1132.

61. J.L. Cleland, O.L. Johnson, S. Putney, A.J.S. Jones, Recombinant human growth hormone poly(lactide-co-glycolide) microsphere formulation development, Adv. Drug Deliv. Rev. 28 (1997) 71-84.

62. H. Okada, M. Yamamoto, T. Heya, Y. Inoue, S. Kamei, Y. Ogawa, H. Toguchi, J. Control. Release, 28 (1994) 121-129.

63. G.. Spenlehauer, M. Vert, J.P. Benoit, A. Boddaert, In vitro and in vivo degradation of poly(D,L lactide/glycolide) type microspheres made by solvent evaporation method, Biomaterials 10 (1989) 557-563.

64. H.T. Wang, E. Schmitt, D.R. Flanagan, and R.J. Linhardt, Influence of formulation methods on the in vitro controlled release of protein from poly(ester) microspheres, J. Control. Release 17 (1991) 23-32.

65. M.T. Aguado, P.H. Lambert, Controlled - release vaccines - biodegradable polylactide/ploy glycolide (PL/PG) microspheres as antigen vehicles, Immunobiol. 184 (1992) 113-125.

66. A. Giletto, Biodegradable bioadherent microcapsules for orally administered sustained release vaccines, Lynntech Inc., College Station TX, 77840, December 1998.

67. C. Berkland, K. Kim, D.W. Pack, Fabrication of PLG microspheres with precisely controlled and monodisperse size distributions, J. Control. Release 73 (2001) 59-74.

68. P. Bahukudumbi, K.H. Carson, A.C. Rice-Ficht, M.J. Andrews, On the diameter and size distributions of Bovine Serum Albumin (BSA)-based microspheres, J. Microencapsul. 21 (2004) 787–803.

69. J.O. Hinze, Fundamentals of the hydrodynamic mechanism of splitting in dispersion processes, A.I.Ch.E. Journal 1 (1955) 289-295.

70. G. Zhou, and S. M. Kresta, Correlation of mean drop size and minimum drop size with the turbulence energy dissipation and the flow in an agitated tank. Chem. Eng. Sci., 53 (1998) 2063-2079.

71. S.B. Pope, Turbulent flows, Cambridge University press, Cambridge, 2000.

72. J. Baldyga, J. R. Bourne, A.W. Pacek, A. Amanullah, A.W. Nienow, Effects of agitation and scale-up on drop size in turbulent dispersions: allowance for intermittency, Chem. Eng. Sci. 56 (2001) 3377-3385.

73. A.W. Pacek, C. C. Man, A.W. Nienow, On the sauter mean diameter and size distributions in turbulent liquid/liquid dispersions in a stirred vessel, Chem. Eng. Sci., 53 (1998) 2005-2011.

74. A.H. Lefebvre. Atomization and Sprays, Hemisphere Publishing Corporation, Washington D.C., 1989.

75. J.M.G. Lankveld, J. Lyklema, Adsorption of polyvinyl alcohol on the paraffin-water interface 1.interfacial tension as a function of time and concentration. J. Colloid Interface Sci. 41 (1972) 454-465.

76. F. Boury, E. Olivier, J.E. Proust, J.P. Benoit, Interactions of poly (α-hydroxy Acid)s with poly (vinyl alcohol) at the air/water and at the dichloromethane/water interfaces J. Colloid Interface Sci., 163 (1994) 37-48.

77. F. Boury, Tz. Ivanova, L. Panaiotov, J.E. Proust, A. Bois, J. Richou, Dynamic properties of poly (DL-lactide) and polyvinyl alcohol monolayers at the air/water and dichloromethane/water interfaces, J. Colloid Interface Sci., 169 (1995) 380-392.

78. C. Berkland, K. Kim, and D.W. Pack, PLG microsphere size controls drug release rate through several competing factors, Pharm. Res. 20 (2003) 1055-1062.

79. C. Raman, C. Berkland, K.K. Kyekyoon, D.W. Pack, Modeling small-molecule release from PLG microspheres: effects of polymer degradation and nonuniform drug distribution, J. Control. Release 103 (2005) 149-158.

80. N.S. Berchane, F.J. Farzaneh, K.H. Karson, A.C. Rice-Ficht, M.J. Andrews, About mean diameter and size distributions of poly(lactide-co-glycolide) (PLG) microspheres, J. Microencapsul. 23 (2006) 539-552.

81. S. d'Arpino, V. Corbrion-Archer, J.P. Marty, L. Lantieri, C.M. Vincint, A. Astier, M. Paul, Influence of vehicles on the in vitro percutaneous absorption of piroxicam to optimize the formulation of patch tests in dermatology, Drug. Develop. Res. 58 (2003) 283-290.

82. R. Ficarra, A. Villari, N. Micali, S. Tommasini, M.L. Calabro, M.R. Di Bella, S. Melardi, M.F. Agresta, S. Coppolino, R. Stancanelli, Stability study of piroxicam and cinnoxican in solid pharmaceuticals, J. Pharmaceut. Biomed. 20 (1999) 283-288.

83. M. Gibaldi, and S. Feldman, Establishment of sink conditions in dissolution rate determinations, J. Pharm. Sci. 56 (1967) 1238-1242.

84. J. Crank, The Mathematics of Diffusion, Oxford University Press, London, 1956.

85. A. Fick, Ann. Phys. Lpz. 170 (1855), 59.

86. J.B. Fourier, Theorie analytique de la chaleur, Oeuvres de Fourier (1822).

87. X. Huang, C.S. Brazel, On the importance and mechanisms of burst release in matrix controlled drug delivery systems, J. Control. Release 73 (2001) 121-136.

88. N. Faisant, J. Siepmann, and J.P. Benoit, PLGA-based microparticles: elucidation of mechanisms and a new, simple mathematical model quantifying drug release, Eur. J. Pharm. Sci., 15 (2002) 355-366.

89. L.K. Chui, W.J. Chui, Y.L. Cheng, Effects of polymer degradation on drug release- a mechanistic study of morphology and transport properties in 50:50 poly(*dl*-lactide-co-glycolide), Int. J. Pharm. 126 (1995) 169-178.

90. R.A. Kenley, M.O. Lee, T.R. Mahoney, L.M. Sanders, Poly(lactide-co-glycolide) decomposition kinetics in vivo and in vitro, Macromolecules 20 (1987) 2398-2403.

91. D.H. Lewis, in: M. Chasin, R. Langer (Eds.), Biodegradable Polymers as Drug Delivery Systems, Maecel Dekker, NY, 1990.

92. R.E Larson, R.P. Hostetler, Calculus with analytic geometry, D.C. Health and Company, Lexington, MA / Toronto, 1986.

93. R.J. Schilling, and S.L. Harris, 2000. Applied Numerical Methods for Engineers Using Matlab and C, Brooks/Cole Publishing Company, Pacific Grove, CA, 2000.

94. W.H. Press, B.P. Flannery, S.A. Teukolsky, and W.T. Vetterling, 1992, Numerical recipes in Fortran: the art of scientific computing, Cambridge University Press, Cambridge.

95. W. Cheney, and D. Kincaid, Numerical Mathematics and Computing, Third Edition, Brooks/Cole Publishing Company, Pacific Grove, CA, 1994.

96. D.G. Luenberger, Introduction to linear and nonlinear programming, Addison-Wesley, MA, 1965.

97. W.I. Zangwill, Nonlinear programming: A unified approach, Prentice Hall, NJ, 1969.

98. R.L Ott, and M. Longnecker, Statistical Methods and Data Analysis, Fifth edition, Duxbury, CA, 2001.

APPENDIX A

DRUG RELEASE PROFILE HAVING THREE DISTINCT PULSES

Here we design a three pulse drug release profile using the mathematical model developed in Section 3, and the numerical optimization technique developed in Section 4. In Figure A.1, the dashed line is the target profile, while the solid line is the predicted optimum release. The target release has a pulsatile profile that delivers its first pulse (~ 25% of the total drug load) in the first 3 days, and then delivers its second pulse (~ 29% of total drug load) from day 22 to day 28, and finally delivers its third pulse (~ 28 % of total drug load) from day 38 to day 44. The mathematical model developed in Section 3, was used to predict drug release from PLG microspheres having a mean diameter of 160 μm and a molecular weight of 220 kDa (population A in figure A.1). Then using the numerical optimization technique, it was determined that the optimum release can be achieved by mixing the 160 μm / 220 kDa microsphere population, the 63-90 μm / 55 kDa micosphere population, and the 0.2-20 μm /18 kDa microsphere population at mass fractions of 0.38, 0.35, and 0.27 respectively. From inspection of Figure A.1, it is evident that the predicted optimum release is in good agreement with the desired release (R^2 = 0.998), which shows that drug release having three distinct pulses can be achieved by combining individual microsphere populations.

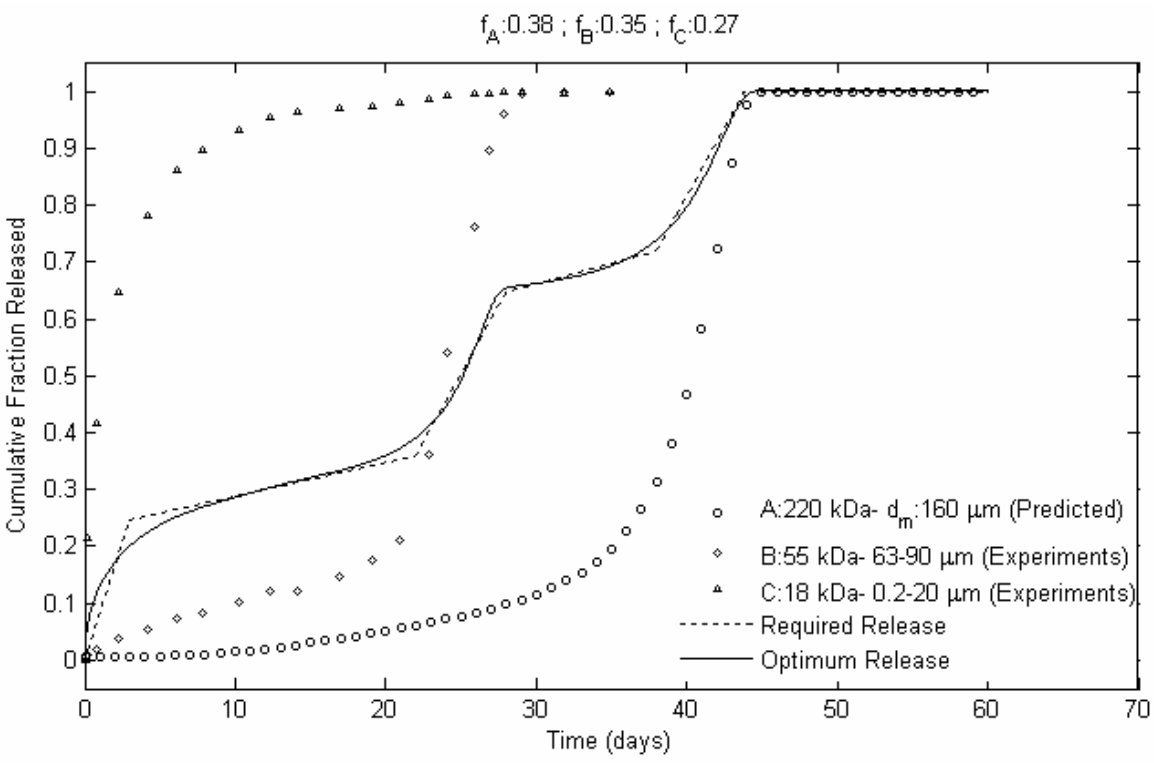

Figure A.1 Designing a drug release profile having three distinct pulses.

VITA

Nader Samir Berchane is the son of Samir Berchane and Nadia Berchane. He was born on December 23, 1979 in Beirut and has two brothers, George and Merhij, and one sister, Rima. He attended Evangelical School and St. Joseph High School in Metin, Lebanon. He received the Bachelor of Engineering degree in Mechanical Engineering from the American University of Beirut, Beirut, Lebanon, in 2001. He attended graduate school at Texas A&M University, College Station, Texas, in the Department of Mechanical Engineering. He received the Master of Science degree in 2003 and the Doctor of Philosophy degree in 2007. His permanent mailing address is:

Permanent Address
Samir Berchane
Tripoli Street 67
Bourje Hammoud
Beirut, Lebanon